Alma Mater Studiorum – Università di Bologna

DOTTORATO DI RICERCA IN
BIOLOGIA CELLULARE E MOLECOLARE

Ciclo 33

Settore Concorsuale: 05/D1 - FISIOLOGIA

Settore Scientifico Disciplinare: BIO/09 - FISIOLOGIA

ALTERED TRANSCRIPTIONAL AND EPIGENETIC REGULATION AFFECTS BRAIN CELLS PROLIFERATION AND DIFFERENTIATION IN THE ULTRA-RARE GENETIC DEMYELINATING DISEASE AGC1 DEFICIENCY: A STUDY ON IN VITRO MODELS

Presentata da: Eleonora Poeta

Coordinatore Dottorato

Vincenzo Scarlato

Supervisore

Barbara Monti

Co-supervisore

Sabrina Petralla

Esame finale anno 2021

INDEX

ABSTRACT

AGC1 deficiency is a rare demyelinating disease caused by mutations in the SLC25A12 gene, which encodes for the mitochondrial glutamate-aspartate carrier 1 (AGC1/Alarar), highly expressed in the central nervous system. In neurons, impairment in AGC1 activity leads to reduction in N-acetyl-aspartate, the main lipid precursor for myelin synthesis (Profilo *et al.,* 2017); in oligodendrocytes progenitors cells, AGC1 down regulation has been related to early arrest proliferation and premature differentiation (Petralla *et al.*, 2019). Additionally, *in vivo* AGC1 deficiency models *i.e.,* heterozygous mice for AGC1 knock-out and neurospheres from their subventricular zone, respectively, showed a global decrease in cells proliferation and a switch in neural stem cells (NSCs) commitment, with specific reduction in OPCs number and increase in neural and astrocytic pools (Petralla *et al.,* 2019). Therefore, the present study aims to investigate the transcriptional and epigenetic regulation underlying the alterations observed in OPCs and NSCs biological mechanisms, in either AGC1 deficiency models of Oli-neu cells (murine immortalized oligodendrocytes precursors cells), partially silenced by a shRNA for SLC25A12 gene, and SVZ-derived neurospheres from AGC1$^{+/-}$ mice. Western blot and immunofluorescence analysis revealed significant variations in the expression of transcription factors involved in brain cells' proliferation and differentiation, in association with altered histone post-translational modifications, as well as histone acetylases (HATs) and deacetylases (HDACs) activity/expression, suggesting an improper transcriptional and epigenetic regulation affecting both AGC1 deficiency *in vitro* models. Furthermore, given the large role of acetylation in controlling in specific time-windows OPC maturation (Hernandez and Casaccia; 2015), pharmacological HATs/HDACs inhibitions were performed, confirming the involvement of chromatin remodelling enzymes in the altered proliferation and early differentiation observed in the AGC1 deficiency models of siAGC1 Oli-neu cells and AGC1$^{+/-}$ mice-derived neurospheres.
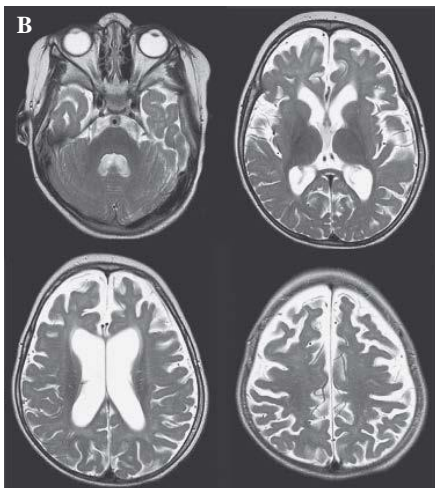
1.

INTRODUCTION

1.1 AGC1 deficiency

AGC1 deficiency is a rare genetic and demyelinating disease caused by recessive autosomal mutations of SLC25A12 gene, which encodes for the mitochondrial Aspartate Glutamate Carrier 1 (AGC1)/Aralar. The first human case was reported by Wibom *et al.* (2009), due to a c.1769A → G transition in exon17 and, consequently, a Q590R substitution (a highly conserved residue of the binding site), leading to a non-functional AGC1 protein. To this day, few more AGC1 deficiency cases are known, although not all yet reported in literature: in 2014, a whole exosome sequencing showed a novel a c.1058G → A transition in exon11 in two siblings, causing a R353Q switch and an 85% reduction of carrier's functionality (Falk *et al.* 2014); in 2019, in a 21-month-old child, it was reported that a T444I mutation in the SLC25A12 gene, is responsible for structural alterations in the mitochondrial transporter (Pfeiffer *et al.*, 2019). However, despite the variety of mutations, all AGC1 dysfunctions lead to common symptoms in the early stages of infancy. Children show profound developmental delay, severe muscular hypotonia, epilepsy, with general impairment of basic psychomotor activities (*i.e.,* standing or grabbing objects) within three years of age. Furthermore, magnetic resonance images (MRI) of AGC1 deficiency patients, revealed an age-correlated hypomyelination and a progressive reduction in brain volume, with parallel appearance of cortical sulci and ventricle enlargement at 8 and 16-months of age; however, no effects were observed in cerebellum and brainstem (Fig.1.1). Subsequently, through magnetic resonance spectroscopy, was detected a decrease in NAA level and increase in blood lactate content, indicating a mitochondrial defect in AGC1 deficiency patients as expected (Falk *et al.*, 2014).
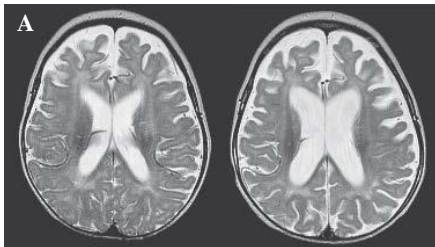
Fig. 1.1: AGC1 deficiency patient MRI. A) 8-month and 16-month MRI brain images. B) patient's MRI image at 2 years and 9 months of age. A high signal in white matter persists in frontal, occipital and temporal lobes, indicating ongoing hypomyelination; normal myelination was observed in cerebellum and brainstem whereas pale globe and putamen show a slight decrease in volume. Both panels show progressive reduction in brain volume and formation of prominent cortical sulci and ventricle enlargement (Wibom *et al.*, 2009).

One of the first murine model for studying AGC1 deficiency was reported by Jail and colleagues in 2005. Homozygous SLC25A12/Aralar$^{-/-}$ mice expressing a truncated AGC1 protein with one aspartate catalytic site (Solcar-1), and therefore a residual activity, were obtained through gene trapping by inserting a premature stop codon at exons 13-14 of SLC25A12 gene (Jail *et al.*, 2005). Similarly, in 2010 Sakurai and colleagues obtained SLC25A12 KO mice expressing a fully inactive protein with no AGC1 catalytic sites, through insertion of a stop codon in exon 1 (Sakurai *et al.*, 2010). Phenotypically, both models showed normal embryogenic development (according to the postnatal onset of AGC1 deficiency symptoms), but growth delays, smaller size, and lower lifespan (22-23 days) than AGC1$^{+/+}$ and AGC1$^{+/-}$ mice after few days of birth. Tremors and motor-coordination problems due to an arrest in neuromuscular development appeared around 13-15 postnatal days, and no AGC1 KO mice survived over 4 weeks. Moreover, hypothalamus, thalamus and striatum resulted dramatically reduced, with global lack of myelination in all brain structures. The hypomyelination state affecting KO mice was then confirmed by quantification of MBP, MOBP and PLP - positive fibres, which, together with myelin-specific lipids (Galactocerebroside and NAA), turned out to be lower if compared to wild-type. In addition, the aspartate-glutamate shuttle activity (MAS) was found to be inhibited in neurons mitochondrial extracts, suggesting that alterations in neuronal metabolism could be responsible, together with hypomyelination, for neurodegeneration and impairment in neuronal differentiation (Jalil *et al.*, 2005; Sakurai *et al.*, 2010). Therefore, oligodendrocytes cultures from SLC25A12/Aralar$^{-/-}$ mice showed up to be able to mature similarly to wild type-derived cultures when supplemented with fatty acids and metabolites. This evidence, leaded to consider as pathogenic mechanism of AGC1 deficiency the neurons defective metabolism and the inability to provide NAA to oligodendrocytes, with subsequent reduced Galactocerebroside synthesis (the main myelin precursor) and demyelination, rather than an oligodendrocyte-specific defect (Jalil *et al.*, 2005; Ramos *et al.*, 2008; Satrustegui *et al.*, 2007). Additionally, Dahlin *et al.* (2015) reported a clear improvement in psychomotor development and recovery in myelination in a 6 years old AGC1 deficiency patient, when submitted to a ketogenic diet based on carbohydrate restriction and high-fat and protein rate (Fig. 1.2).

Fig. 1.2. MRI investigations in AGC1 deficiency patient before and 6 months after treatment. (A, B) Axial and (D, E) coronal imaging before Ketogenic diet showed lack of myelination and progressive reduction in cerebral volume. (C) Axial and (F) coronal imaging after 6 months of treatment. The previous signal corresponding to white matter is lower, and ventricles less prominent, indicating reversal of volume loss. Tx: duration of treatment with ketogenic diet (Dahiln *et. al*., 2005).
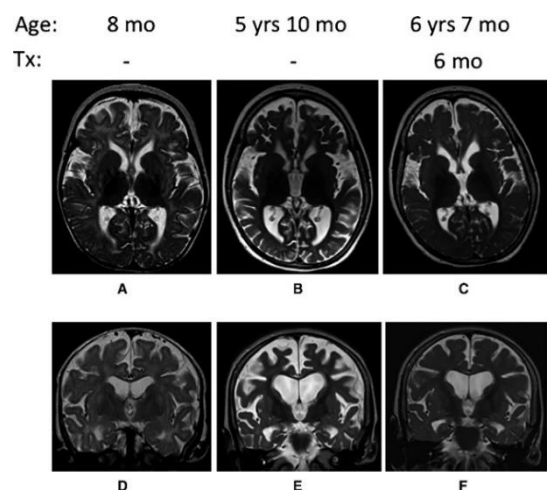
The reduced glycolysis prevents accumulation of NADH reducing equivalents in cytoplasm and the subsequent increase in NADH/NAD+ *ratio*, compensating the metabolic defect in AGC1 deficiency, without affecting oxidative phosphorylation. The inversion of the malate-aspartate shuttle (MAS), thanks to low levels of NADH in cytoplasm, results then in cytosolic aspartate synthesis (substrate for N-acetylaspartate (NAA) by aspartate-N-acetyltransferase), and allows secondary remyelination in AGC1 deficiency patients (Fig. 1.3) (Dahiln *et al.*, 2015). Furthermore, oxidation of fatty acids supplies ketone bodies, a direct source of acetyl-CoA, and consequently acetyl-groups for energetic and biosynthetic processes. As discussed, the pathogenesis of AGC1 deficiency is therefore complex, and includes both neuronal energy deficiency and lack of secondary myelination due to reduced levels of NAA in the brain.
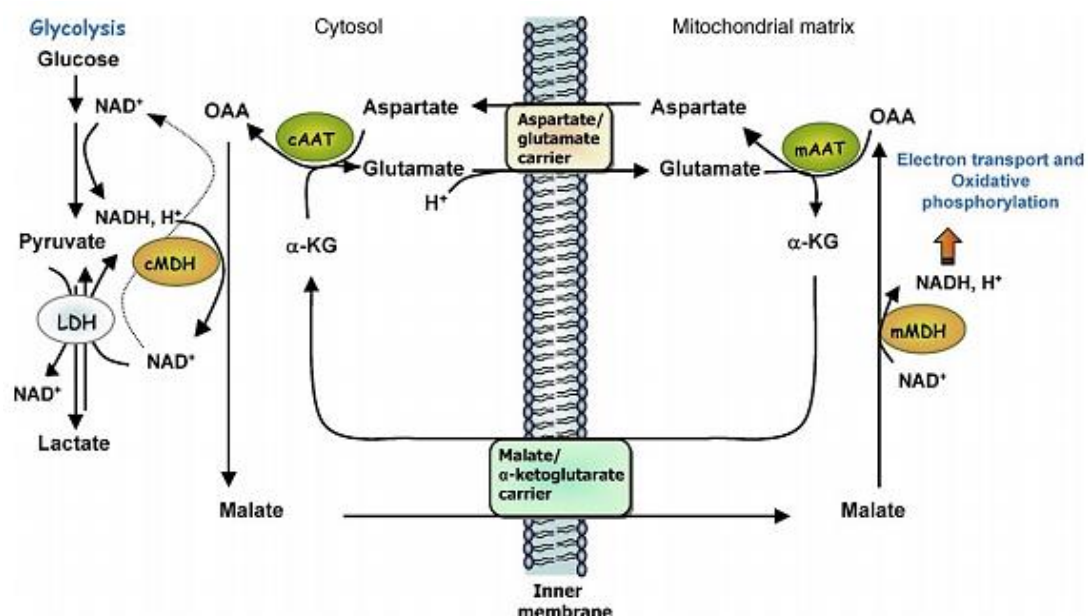
Fig 1.3: The malate-aspartate shuttle (MAS). MAS is composed by two enzymatic functions (AAT and MDH) both present in cytosol and mitochondria, and two transporters (AGC and OGC) in the inner mitochondrial membrane. In CNS, MAS translocates electrons produced through glycolysis in mitochondria for oxidative phosphorylation. MDH function to reduce oxaloacetate into malate is regulated by NADH/NAD+ ratio. Once in mitochondria, NADH is then regenerated from malate and provides electrons to the respiratory chain for ATP synthesis. Oxaloacetate is finally converted into aspartate, which is translocated into cytosol by AGC to guarantee redox balance. In addition, AGC1 in neurons has important metabolic functions to supply aspartate for myelin synthesis (McKenna *et al.*, 2006).

1.2 AGC1 and its role in the Central Nervous System

The aspartate-glutamate carriers (AGCs), together with the ATP-Mg/Pi transporters, are members of the Calcium-binding Mitochondrial Carriers family (CaMCs), commonly characterized by three repeated domains containing each two hydrophobic α-helices into the phospholipidic bilayer.

As calcium-regulated transporters, AGCs' secondary structure is composed by four calcium-binding EF-hand motifs at the N-terminal domain located in the intermembrane space, in addition to a 300aa MC homologous region at the C-terminal domain (Pebay-Peyroula and Brandolin, 2004) (Fig. 1.4).
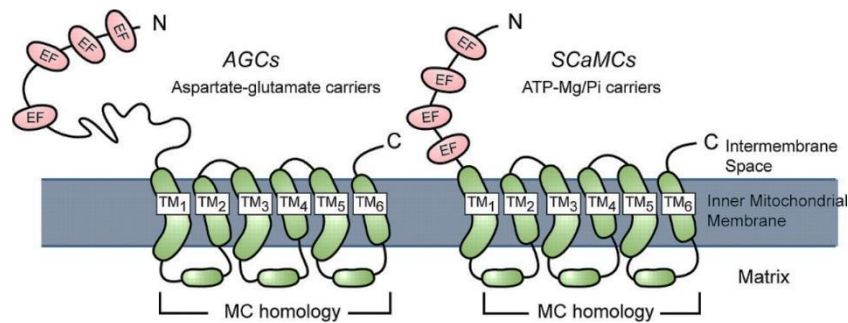
Fig. 1.4: CaMCs secondary structure. The mitochondrial carrier homology region at the C-terminal domain is characterized by 6 transmembrane helices (TM1-6) and located at the C-terminal domain. The N-terminal domain contains the Ca^{2+}-binding EF-hand motifs in the intermembrane space (Pebay-Peyroula and Brandolin, 2004).

Currently, two AGCs isoform with 77.8% of sequence homology have been identified, depending on the different expression and tissue localization: Aralar/AGC1, only expressed in excitable tissues *i.e.*, central nervous system and skeletal muscle, and Citrin/AGC2, mainly located in heart, liver, and kidney (Del Arco *et al.*, 1998; Palmieri *et al.*, 2001; Amoedo *et al.,* 2016), encoded by genes on chromosomes 2q31 and 7q21, respectively (Sanz R *et al.*, 2000; Sinasac DS *et al.*, 1999). Mutations in the SLC25A12 gene are responsible for the demyelinating disease AGC1 deficiency, whereas mutations in SLC25A13 lead to the neonatal intrahepatic cholestasis (NiCCD) and the adult-onset type 2 citrullinemia (CTLN2) (Amoedo *et al.*, 2016). Besides these, AGCs homologues have also been reported in other organisms: Agc1p in yeast, with mitochondrial localization, but no calcium binding domains (Cavero *et al.*, 2003), and OSCP1 in Drosophila, a similar mitochondrial carrier with nuclear localization too (Huu *et al.*, 2014). About their role, AGCs catalyze a 1:1 antiport reaction by transferring aspartate from the mitochondrial matrix to the intermembrane space in exchange for glutamate and a proton (Palmieri *et al.*, 2001). In addition, they are component of the malate-aspartate shuttle (MAS) by carrying NAD-reducing equivalents (NADH) produced by glycolysis from cytosol into mitochondria, allowing oxidative phosphorylation and ATP synthesis. The isoform 1 is the largest aspartate-glutamate carrier expressed in the CNS, especially in neurons-rich area and undetectable in white matter, where plays a crucial role in myelin synthesis. Neuronal aspartate, once in the cytosol thanks to AGC1 activity, is converted into N-acetylaspartate (NAA) by aspartate-N-acetyltransferase (Asp-NAT) and transferred to oligodendrocytes trough transaxonal transport, where it supplies acetyl groups for synthesis of myelin lipids (Urenjak *et al.*, 1993; Wiame *et al.*, 2003). NAA is then introduced by Na^+-dependent high-affinity dicarboxylate transporter

(NADC3) into oligodendrocyte cytoplasm and converted by aspatrocyclase (ASPA) into fatty acids and steroids for myelin synthesis (Fig. 1.5). Summing up, genetic variations and consequently Aralar/AGC1 different expression or insertion into the mitochondrial membrane, can lead to MAS disfunction, an altered neuronal aspartate synthesis or N-acetylaspartate production, resulting in the onset of CNS diseases.
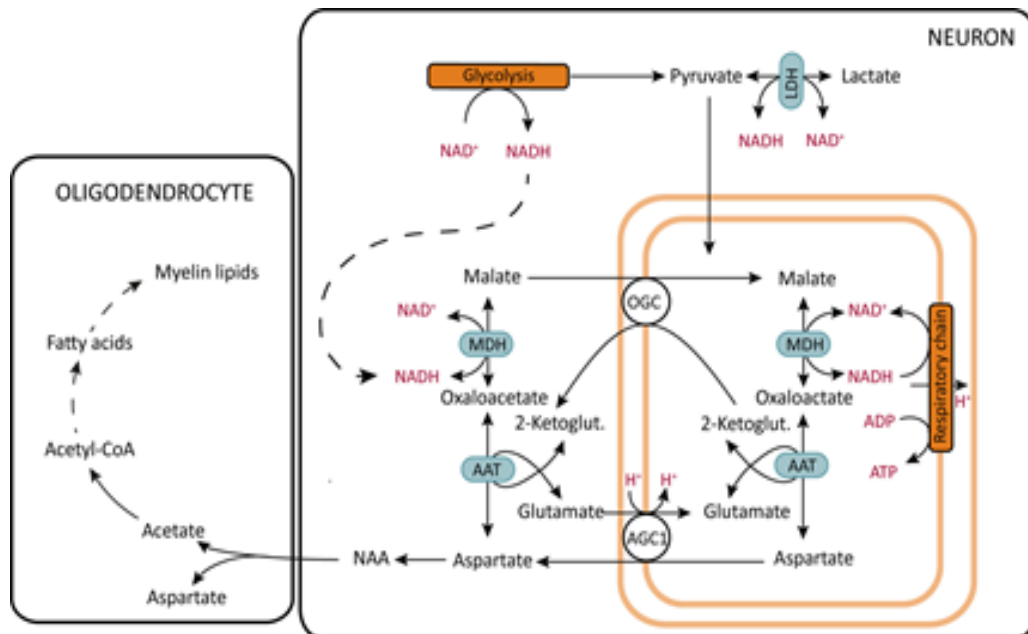
Fig. 1.5: AGC1 function in the Central Nervous System. In neuron, the aspartate-glutamate carrier 1 is a component of MAS and transports NAD-reducing equivalents produced by glycolysis from cytosol to mitochondria allowing oxidative phosphorylation and ATP production. Therefore, it plays a crucial role for myelination processes transferring aspartate into the intermembrane space, which is then converted in NAA and carried to oligodendrocytes for synthesis of myelin lipid (Dahiln *et al.*, 2015).

1.3 Neuronal metabolism and AGC1 deficiency

Given the high energy demand of the brain, neurological disorders are often correlated with mitochondrial dysfunction, and cells' energetic metabolism proves to be fundamental for the proper operation and development of the central nervous system. Glucose oxidation derived from glycolysis and tricarboxylic acid cycle (TCA) represents the main energy-source in neurons, and enhanced glycolysis and respiration are required to sustain the biosynthetic needs requested for neuronal differentiation. Therefore, being MAS the main redox shuttle system in neurons, AGC1 activity turned out to be essential to support the specific energetic demand (Mergenthaler *et al.*, 2013). In 2016, Agostini and colleagues reported an increase in mitochondrial activity and glycolytic enzymes expression in neuronal primary culture following *in vitro* maturation (Agostini *et al.*, 2016). In addition, a peak of AGC1 expression has been registered in neurons once differentiated in culture. An adaptive mechanism has been then proposed to be implemented subsequently AGC1

downregulation (Ramos *et al.*, 2003; Profilo *et al.*, 2017). In fact, mouse neuroblastoma cells (N2A cells) showed higher lactate synthesis and unbalanced redox state with parallel increase in glutamine oxidation following AGC1 silencing. Furthermore, cells cultured in glutamine-deprived medium decreased oxygen consumption and proliferation rates, suggesting their capability to survive only in presence of glutamine sources. *In vivo*, glutamine is provided by astrocytes, through the glutamate-glutamine cycle. In this pathway, glutamate released from glutamatergic synapses enters astrocytes where is converted into glutamine by glutamine-synthase enzyme. Glutamine is then delivered back to neurons and derived-glutamate is finally turned to α-KG, which enters the TCA cycle as an auxiliary energetic substrate in addition to the one imported by AGCs activity (Erecinska *et al.*, 1990; Fiermonte *et al.*, 2002). Since in astrocytes aerobic glycolysis and aspartate translocation are necessary for the synthesis of glutamate and TCA cycle intermediates (Hertz, 2011), astrocytic AGC1 defects contribute to alter the correct neuronal maturation. Additionally, MAS impairment in neurons inhibits pyruvate oxidation, the main source of acetyl-CoA, which, together with aspartate, represent the substrate of the Asp-NAT enzyme for NAA synthesis, causing increase in NADH/NAD$^+$ *ratio* and lactate production (McKenna *et al.*, 2006). The considerable reduction in NAA observed in AGC1 silenced N2A cells due to low availability of aspartate and acetyl-CoA, could lead to failure in myelin lipids synthesis and consequently myelination (Profilo *et al.*, 2017). As previously describe, the positive results obtained from the ketogenic diet (Dahlin *et al.*, 2015) of symptoms improvement and recovery of myelination indicates AGC1 deficiency as strictly correlated to an inborn error of neuronal metabolism, with subsequent impairment in energetic and biosynthetic processes and consequences in proper CNS development.

1.4 Embryonic and adult neurogenesis

During gastrulation in the embryo, the release by mesodermal cells of neuronal inducers, which arrest the epidermal differentiation pathway and promote neural genes expression, leads to morphological changes of the surrounding dorsal ectoderm, giving rise to neuroectoderm and neural progenitors that constitute the neural plate. Then, throughout neurulation, in response to stimuli by notochord and the overlying ectoderm, the crests of the neural plate turn inwards and fuse to form the neural tube: the caudal part will give rise to the spinal cord, while the anterior portion will origin the three primaries brain vesicles from, which will develop the mature CNS. At this stage, the pseudostratified neuroepithelium, which form the wall of the neural tube takes the name of ventricular zone (VZ), represents the primary neurogenic niche in the embryo. Except microglia, which arises from erythromyeloid precursors that migrates into the developing CNS during neurogenesis (Ginhoux and Prinz, 2015), cells composing the ventricular zone are multipotent stem cells, known as neural stem

cells (NSCs), able to differentiate in all the cell types of the central nervous system: neurons, oligodendrocytes, astrocytes, and ependymal cells. During the CNS development, NSCs proliferate and go through a gradual restriction of their cell-fate. Initially, they divide both symmetrically, to guarantee the self-renewal of the stem pool, and asymmetrically (Merkle and Alvarez-Buylla, 2006; Kriegstein and Alvarez-Buylla, 2009); some of these NSCs acquire an astrocytic-like phenotype induced by signals released by meninges (*i.e.,* FGF10 and retinoic acid; Siegenthaler *et al.*, 2009), and express astrocytes-specific markers, as GFAP, GLAST and BLBP, taking the name of radial glial cells (RGCs) (Campbell and Gotz, 2002). RGCs present an apical-basal polarity, which is essential for the proper development of cortical architectures: their cell body is located into the VZ, whereas cytoplasmatic processes span the developing neocortex contacting both ventricular and pial surfaces. Furthermore, depending on which phase of the cell cycle RG cells are, nuclei move along the cell body becoming exposed to different signals in a phenomenon known as nucleokinesis (Del Bene *et al.*, 2008). Through asymmetric divisions, RGCs origin a new RG cell and an intermediate progenitor cell (IPC) expressing pro-neural genes, as Neurog2 and Pax6, characterized by restricted potential and committed to a neuronal differentiation, or an immature neuron directly (Scardigli *et al.*, 2003; Kriegstein and Alvarez-Buylla, 2009). Neo-formed cells then migrate radially along RG processes above the VZ, giving rise to another high neurogenic niche called subventricular zone (SVZ) (Noctor *et al.*, 2004). Depending on the time of the development and the subregion where they came from, due to the different exposition to morphogens, RG cells can origin to several types of neurons (Shen *et al.*, 2006; Hochstim *et al.*, 2008). Migration and proliferation of neuron precursors (NPs) lead to the generation of a six-layered cortex, whose deeper layers are constituted by the earlier migrating neurons (Sanes *et al.*, 2013). At the end of cortical development, most RG cells detach from VZ and migrate by soma translocation to the cortex and subcortical region, acquiring a multipolar morphology and differentiating into astrocytes, while remained RGCs persist and proliferate in the adult central nervous system (Fig. 1.6) (Noctor *et al.*, 2008).
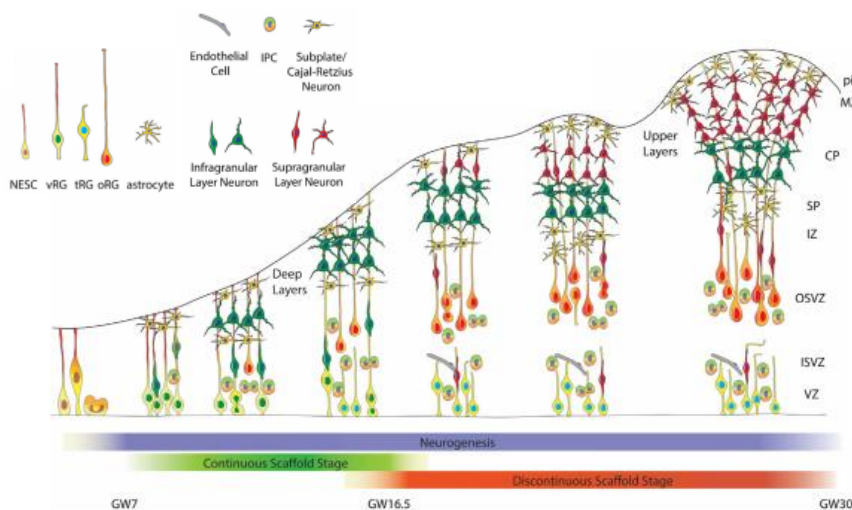
Fig. 1.6: Schematic cortical development. During neurogenesis radial glia processes contact both VZ and the pial surface. Newborn neurons migrate along ventricular as well as intermediate progenitors giving rise the 6-layered cortex. VZ, ventricular zone; NESC, neuroepithelial stem cell; ISVZ, inner subventricular zone; OSVZ, outer subventricular zone; IZ, intermediate zone; SP, subplate; CP, cortical plate; MZ, marginal zone; IPC, intermediate progenitor cell; vRG, ventricular radial glia; tRG, truncated radial glia; oRG, outer radial glia.
(Nowakowski J. T., 2016).

Although restricted to few cerebral areas, neurogenesis has also been reported in adult CNS especially in two major neurogenic niches: the subventricular zone (SVZ) and the hippocampal dentate gyrus (DG), both characterized by different cell types, precise cell-cell contacts and specific extracellular environments (Batiz *et al.*, 2015). In SVZ, adult NSCs are known as type B1 cells and express astrocytes-specific markers, such as GFAP, Nestin, GLAST and BLBP, like embryonic RG. They are located along the lateral ventricle within ependymal cells and show an apical-basal polarity keeping contact with cerebrospinal fluid and vessels with their end-feet. Once properly induced, B1 cells go through asymmetric divisions to allow self-renewal and type C cells production (transit amplifying progenitors); C cells then divide symmetrically and give rise to type A cells, new neuroblasts which migrate through the rostral migratory stream (RMS) towards olfactory bulbs before differentiating in various types of interneurons depending on the area of origin (dorsal, medial or ventral SVZ) (Fig.1.6) (Lim and Alvarez-Buylla, 2016).

Fig. 1.6: Cellular composition of SVZ.
(Lim and Alvarez-Buylla, 2016).

Additionally, B1 cells in the SVZ can also give rise to oligodendrocytes and nonneurogenic astrocytes: Reynolds and Weiss (1996) observed *in vitro* generation of oligodendrocytes precursors (OPCs) from neurospheres derived from adult mice SVZ; Menn and colleagues (2006) reported a rise in both neurons and oligodendrocytes derived from adult SVZ type B cells when co-cultured with cortical astrocytes, in addition to the *in vivo* capability of SVZ newly-generated OPCs to migrate through corpus callosum and striatum and differentiate into myelinating and non-myelinating oligodendrocytes. Furthermore, an increase in oligodendrocytes generation from SVZ B1 cells has been observed following demyelinating injury, suggesting even the ability of these cells to respond to demyelination (Nait-Oumesmar *et al.,* 1999; Picard-Riera *et al.*, 2002).

1.4.1 An *In vitro* model to study neurogenesis: neurospheres

Neurospheres are floating cultures of neural stem cells and neuronal, astrocytic and oligodendrocytic progenitors at different stages of maturation isolated from adult or foetal brain (Tropepe *et al.*, 2001). Although the hippocampal dentate gyrus is known to contain adult neural precursors, SVZ derived stem cells have the best capability to proliferate and create neurospheres *in vitro* (Fig. 1.7). They are considered a near-perfect system to provide a consistent and self-renewable source of CNS undifferentiated precursors and are widely
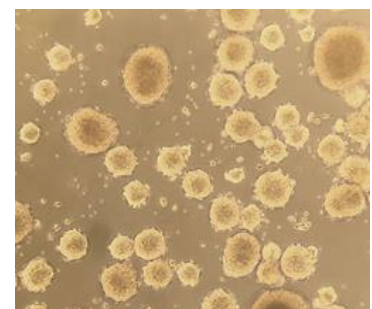
Fig. 1.7: Neurospheres from SVZ.
Image acquired by optical microscopy. 40X objective

use in *in vitro* studies of NSCs analysis/characterization. Cells stemness is maintained by adding mitogens to culture medium, whereas by plating on adhesive substrates (laminin or fibronectin matrixes), neurospheres are able to differentiate in the three types of neural cells acquiring the form of a cell monolayer (Bez *et al.*, 2003). Through this approach, it is then possible to perform proliferation assays or studying spontaneous differentiation of NSCs under specific treatments or culture conditions (Gil-Perotìn *et al.*, 2013; Walker and Kempermann, 2014).

1.5 Oligodendrogenesis

To allow the correct transmission of nerve impulses and consequently neuronal survival, myelination by oligodendrocytes is required in CNS throughout development and adult life. During neurogenesis, specification of oligodendrocytes progenitor cells (OPCs) from RG cells occurs early in the neural tube, following expression of Olig2 transcription factor, in a restricted area of the ventral VZ called pMN domain (Timsit *et al.*, 1995). Despite that, oligodendrocytes originate lastly in developing brain and the majority of oligodendrogenesis takes place postnatally. At E12.5 in mice, morphogen Shh induces in the ventral region of the neural tube a switch to OPCs production, whereas Wnt and BMP signalling suppress in parallel the oligodendrocytic fate in the dorsal area (Dessaud *et al.*, 2010). OPCs occur dorsally at E15.5 and after birth following induction by FGF, to then migrate towards all CNS structures and differentiate into mature oligodendrocytes to myelinate nerve fibres (Kessaris *et al.*, 2006) (Fig. 1.8).
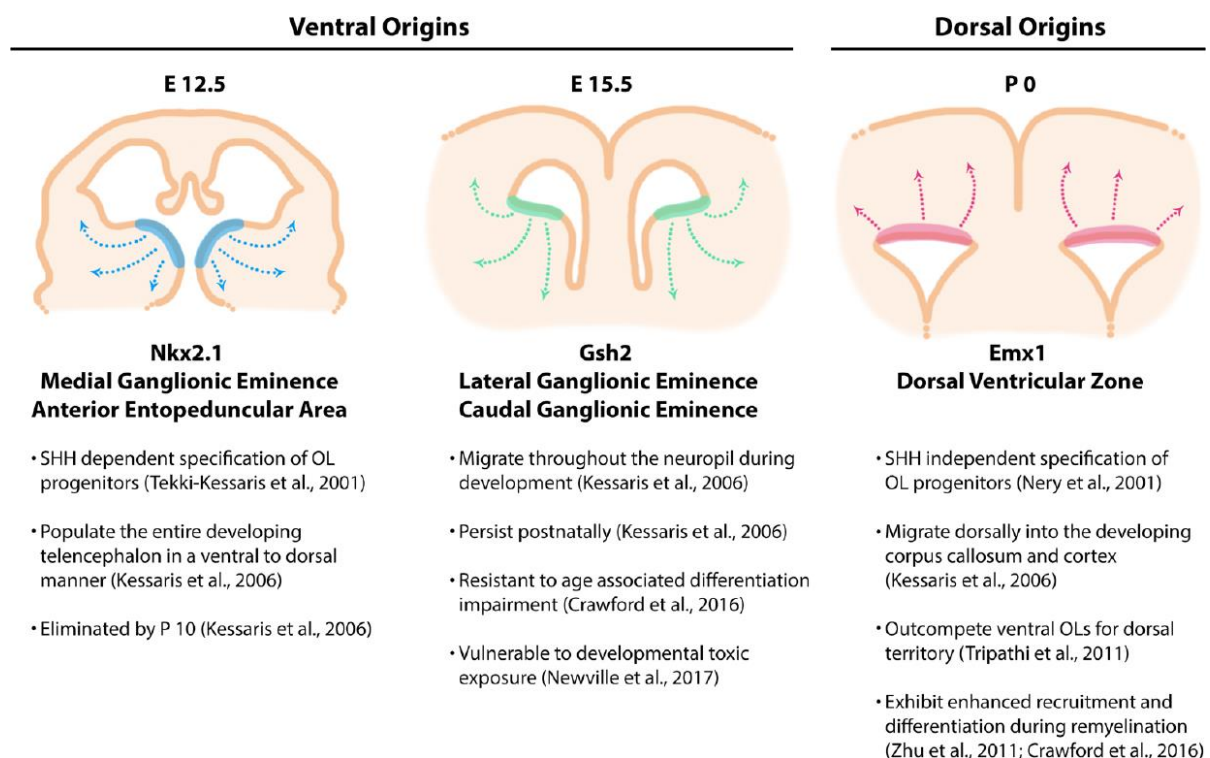
Fig. 1.8. OPCs specification during neural tube development (Steve A. *et al.,* 2015).

Quiescent OPCs persist, however, also in the adult brain representing about 5% of the total cell population of the CNS (Levine *et al.*, 2001), and are identified by specific markers *i.e*., NG2, PDGFRα, O4 antigen, Olig1, Olig2 and Nkx2.2 (Fancy *et al.*, 2004). Since continuous myelin renewal is required to ensure insulation to axons and proper nerve conduction, constant OPCs' proliferation and differentiation is fundamental to allow remyelination in the brain. Therefore, their proliferation-differentiation *ratio* is carefully regulated by specific signals and transcription factors combinations, either autocrine or paracrine (derived from neuronal axons to be myelinated), to regulate myelin gene expression and to guarantee the proper availability of myelinating cells when biologically needed (Fig.1.9).
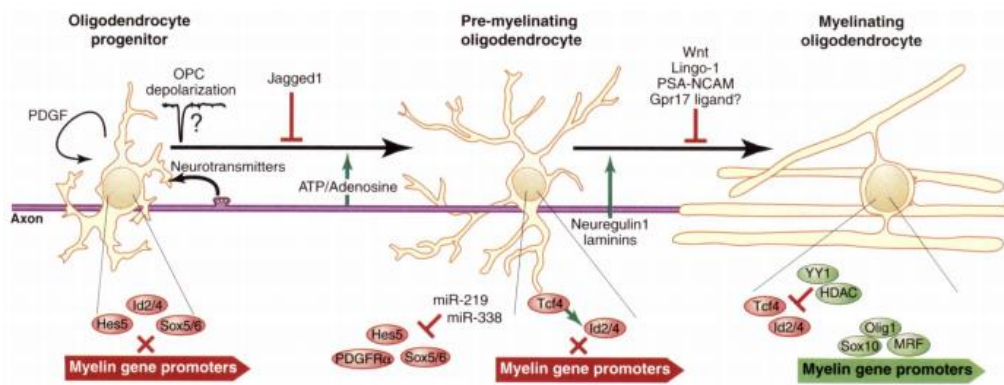
Fig. 1.9: Transcription factors involved in OPCs differentiation. The transition from OPC to pre-myelinating and myelinating oligodendrocyte requires different transcriptional activators and repressors which act together to regulate specific gene expression (Emery *et al.*, 2010).

Initially, OPCs are maintained in an undifferentiated state due to the activity of several transcription factors, as Id2/4, Hes5 and Sox6, which act at the promoters of myelin genes and prevent their expression. In parallel, platelet-derived growth factor (PDGFα) and fibroblast growth factor (FGF-2) through their tyrosine-kinase receptors on the plasma membrane (PDGFRα and FGFR, respectively), trigger a phosphorylation cascade and activate p42/44MAPK, p38MAPK and pp70S6 kinase, resulting in stimulation of the cell cycle and creating an autocrine loop that maintain OPCs in proliferation (Baron *et al.*, 2000; Emery *et al.*, 2010). Maturation is also prevented by Wnt signalling, which block myelin genes trough the β-catenin/Tcf4 activated complex and promotes expression of those ones involved in proliferation *i.e.,* c-Myc (Fancy *et al.*, 2009; Jeong *et al.*, 2018). At this stage, expression of microRNAs miR-219 and miR-338 determine the transition from undifferentiated OPCs to pre-myelinating oligodendrocyte by downregulation of these repressor factors (Dugas *et al.*, 2010). Cell cycle exit is firstly induced by transforming growth factor (TGFβ) signalling, which

repress c-Myc transcription and stimulate expression of cyclin-dependent kinase inhibitors p15, p21 and p27; TGFβ factor binds and phosphorylates its receptors (TGFβR1/2), causing a consequent activation of intracellular effectors SMAD2/3/4, Sp1 and FoxO1 (Siegel *et al.*, 2003; Palazuelos *et al.*, 2014). Complete maturation is then achieved thanks to Olig1, Sox10 and MRF transcription factors, which bind promoters and allow myelin gene expression (Wegner, 2007). Differentiated oligodendrocytes now contact and wrap neuronal axons to produce myelin sheets, thus expressing high levels of mature-specific oligodendrocytes markers: myelin basic protein (MBP), myelin associated glycoprotein (MAG), glycoprotein (MOG), proteolipid protein (PLP) and CNPase (Barateiro and Fernandes, 2014).

1.5.1   Transcription factors involved in OPCs proliferation and differentiation

The oligodendrocytic commitment and the subsequent OPCs maturation into myelinating oligodendrocytes is strictly related to the activity and interactions of high number of different transcription factors. During neural tube development, the pMN domain in the ventral region is the main embryonic oligodendrogenic site, marked by expression of the basic helix-loop-helix Olig2, which induces expression of OPCs-specific markers, such as PDGFRα, Nkx2.2 and Sox10, and therefore its activity is necessary for oligodendrocytes precursors specification. Another transcription factor implicated in controlling oligodendroglial and neuronal differentiation is the cAMP response element binding protein (CREB), which is activated by phosphorylation on serine 133, following PKA activation by cAMP signalling. It is characterized by a leucine-zipper domain for dimerization and a C-terminal basic DNA-binding domain through which it binds to CRE promoter sequences and regulates gene expression. Its transcriptional activity is enhanced by interaction with CBP (CREB binding protein), a histone acetyltransferase, which acetylates lysine residues at the protruding N-terminal tail of nucleosome histone-core and allows chromatin relaxation. *In vitro*, OPCs induced to differentiate into mature oligodendrocytes through cAMP treatment, showed higher levels of CREB phosphorylation (pCREB); indeed, it is reported that CREB expression increases at the onset of myelination to promote myelin gene expression, and then drops down in myelinating oligodendrocytes (McMorris 1983, Sato and DeVries, 1996). Its activation is also required to promote neurons' proliferation and survival, enabling long-term memory establishment and synaptic remodelling (Lonze and Ginty, 2002; Siddiq and Hannila, 2015). Genes expression in also regulated by the zinc-finger transcriptional repressor REST (RE1 silencing transcription factor), which binds the 21-bp RE1 sequence and repress, by recruitment of two histone deacetylase complexes, neuronal genes expression in glia cells (Belyaev *et al.*, 2004). Together with its co-repressor (CoREST), REST is also implicated in controlling expression of genes involved in oligodendrocyte lineage specification

and maturation, which are usually little expressed in OPCS and need to be further repressed to allow subsequent differentiation. Therefore, REST increase is crucial for complete oligodendrocytes maturation (Abrajano *et al.*, 2009; Dewald *et al.*, 2011). Lastly, the proto-oncogene C-Myc, besides acting as transcription activator or repressor based on what factor it dimerizes, it is also known to be involved in chromatin remodelling and histone acetylation. High expression of c-Myc stimulates cell cycle and sustains proliferation, whereas its inhibition is needed to start differentiation. *In vitro,* following T3 (thyroid hormone) treatment, differentiated OPCs showed remarkable c-Myc downregulation and decreased in DNA binding. In addition, ChIP experiments confirmed c-Myc interaction with promoters of gene encoding for chromatin remodellers and cell cycle modulators (Magri *et al.*, 2014).

1.5.2 Epigenetic modifications in OPCs maturation

Epigenetic modifications are persistent and heritable DNA changes, which regulate genes expression without affecting the nucleotide sequence itself. They include DNA methylation, chromatin remodelling and histone modification, and microRNA expression/regulation. Given oligodendrocytes complex biology, many different epigenetic modifications are required for OPCs maturation to temporally regulate gene expression and repress cell cycle. Lysine acetylation on histones N-terminal tails by histone acetyl transferases (HAT) results in chromatin relaxation and euchromatin formation that increases DNA sequences exposure and favours gene expression. Conversely, acetyl group removal, thanks to histone deacetylases (HDAC) activity, induces heterochromatin organization and inhibits RNA transcription (Kouzarides *et al.*, 2007). Undifferentiated OPCs are generally characterized by widely loose chromatin structure; an active proliferate state is guarantee by mitogens and cell cycle promoting genes, whereas transcriptional inhibitor complexes impede myelin genes expression. Throughout differentiation, OPCs then undergo progressive heterochromatin formation; oligodendrocyte maturation needs downregulation of these transcriptional inhibitors, with subsequent enhancement of activators and myelin genes expression (Liu *et al.*, 2006; Shen *et al.*, 2008). It is known that histone deacetylases play controversial roles during oligodendrocytes development. In undifferentiated OPCs, Liu and colleagues (2010) pointed out that until the myelinating state, HDACs repress myelin genes through deacetylation of respective promoters (Liu *et al.*, 2010). Castelo-Branco and co-workers also reported that HDACs inhibition leads to myelin gene expression in NPCs treated with thyroid hormone. Subsequently, HDACs activity is decisive to allow OPCs differentiation. Adult multipotent NPCs (neural progenitor cells) showed a decrease in oligodendroglial commitment, when treated with HDAC inhibitors valproic acid (VA), trichostatin A or sodium butyrate (Hsieh *et al.*, 2004). Cultured OPCs proved to be unable to differentiate into mature oligodendrocyte if previously

treated with same inhibitors (Conway *et al.*, 2012). Furthermore, an increase in HDAC1 expression has been reported in mice during remyelination, following induction of demyelinating lesions (Shen *et al.*, 2008). Therefore, at the beginning of OPCs differentiation HDACs activity is crucial to promote oligodendrocytes maturation pathway, confirming the controversial role of histone deacetylases throughout oligodendrocytes development. HDAC1/2 complexes deacetylate Id2/4 and Hes5 promoters and block their expression allowing de-repression on myelin genes (Shen *et al.*, 2008), whereas its deletion leads to nuclear stabilization of β-catenin/Tcf4 complex and consequent Olig2 inhibition (Liu and Casaccia, 2010). Hence, HDACs initially act to arrest maturation in proliferating OPCs and their inhibition is required to unlock myelin gene expression; conversely, at the onset of differentiation, their activity is needed to allow OPCs maturation and myelinating oligodendrocytes development. Hernandez and Casaccia (2015) identified selective temporal windows in OPCs differentiation that require differential HDACs and HATs activity. In the first stages, undifferentiated OPCs present abundant euchromatin and high acetylation level on promoters of both cell cycle and transcriptional inhibitors; histone deacetylase enzymes can be recruited by these repressors and act on promoters of myelin genes or of their positive regulators; otherwise, they can sequester transcriptional activators of differentiation genes through protein-protein interaction. At the onset of differentiation HDACs then change their function, deacetylate cell cycle and inhibitors promoters, allowing expression of transcriptional activators *i.e*., MYRF and Sox10 which act by recruiting HATs on late myelin genes (Fig. 1.8).
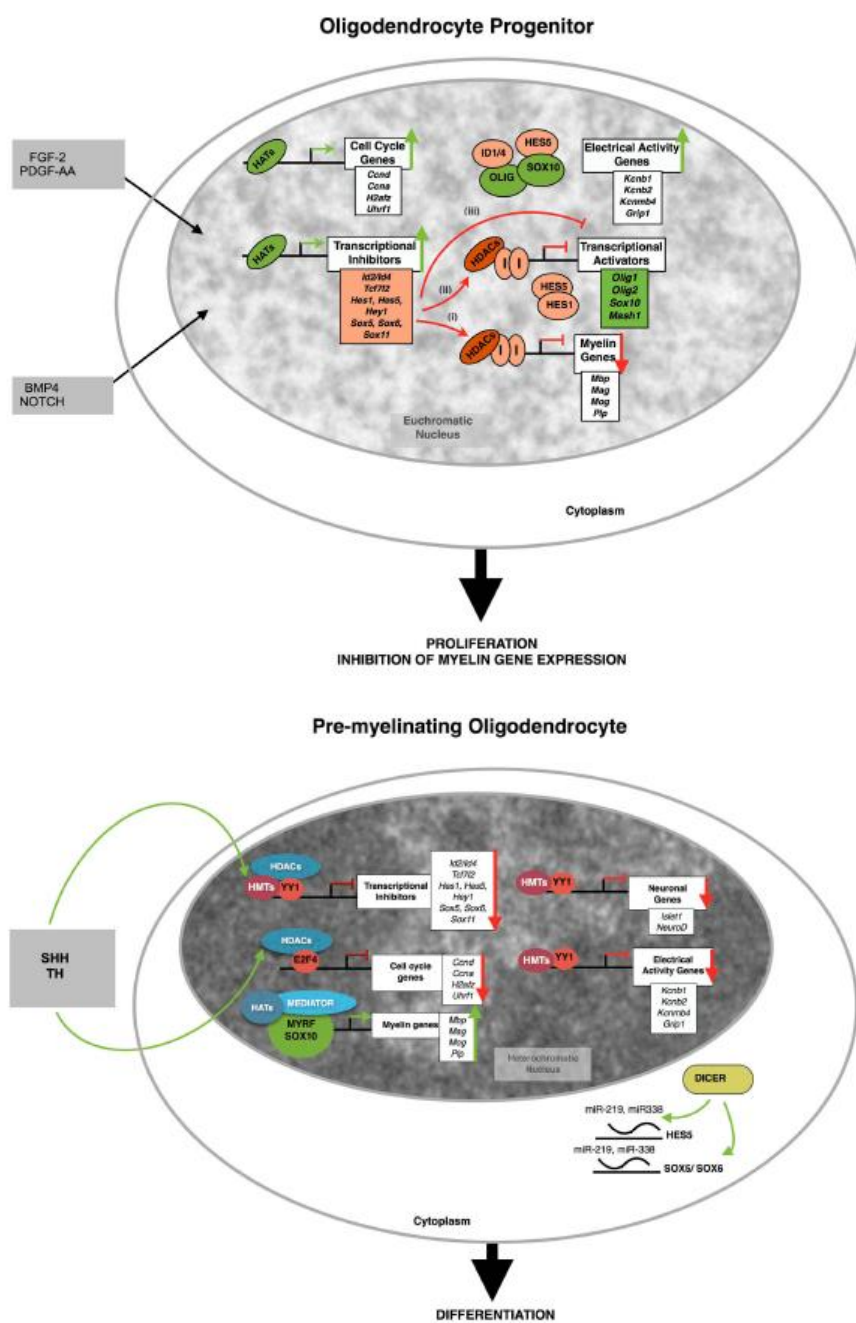
Fig. 1.8: Role of HATs and HDACs in regulating gene expression in OPCs maturation. (Hernandez and Casaccia, 2015).

Methylation on histones is also involved in oligodendrocytes specification and maturation. Oligodendroglial fate acquirement strictly depends on inhibition of neuronal genes expression; H3K27me3 on genes related to cell cycle and neuronal linage seems to be required from OPCs generation from NSCs, whereas differentiation into myelinating oligodendrocytes is regulated by H3K9me3 modification (Sher *et al.*, 2008; Liu *et al.*, 2015). Additionally, during stem cells differentiation methylation leads to loss of pluripotency and heterochromatin formation.

2.

AIM OF THE THESIS

The demyelinating disease AGC1 deficiency, is caused by recessive mutations in the SLC25A12 gene, which encodes for the mitochondrial aspartate-glutammate carrier 1 (AGC1/Aralar). AGC1 is a member of MAS (malate-aspartate shuttle), where it carries aspartate in cytosol in exchange to glutamate into the mitochondrial matrix. Main features of the disease are CNS hypomyelination, cerebral atrophy, and general arrest of psychomotor development (Wibom *et al.,* 2009; Falk *et al.,* 2014); all symptoms associated with significant reduction in NAA, substrate required for myelin synthesis, due to neuronal impairment in AGC1 activity (Jalil *et al.,* 2005; Sakurai *et al.,* 2010). Studies conducted by our group, reported proliferation defects and early differentiation in a stable clone of immortalized murine oligodendrocytes precursors (Oli-neu cells), transfected with a shRNA for SLC25A12 gene, which leaded to 30-40% reduction in AGC1 activity. Same observations were made on brain sections of heterozygous mice for AGC1 knock-out (AGC1$^{+/-}$ C57BL6/N background) and neural stem cells derived from their subventricular zone (SVZ), where a global decrease in cells proliferation and a consistent reduction in oligodendrocytes progenitors was observed. In addition, all AGC1 deficiency models showed alterations in signalling pathways involved in OPCs proliferation and differentiation, such as reduced expression of growth factor PDGFα (which promotes OPCs proliferation) and concomitant increase in TGFβ1/2 (required for OPCs maturation) (Petralla *et al*., 2019). Taken together, the results obtained led to consider the failure in myelin synthesis, and the subsequent hypomyelination, a consequence of the unbalanced OPCs proliferation and differentiation characterizing AGC1 deficiency. Therefore, the present study aims to understand the transcriptional and epigenetic regulation underlying the differences observed in brain cells biological mechanisms, in both AGC1 deficiency models of Oli-neu cells and SVZ-derived neurospheres. For this purpose, transcription factors known to be involved in proliferation and differentiation processes (c-Myc, Olig2, REST, serine133-phosphorylated CREB) were analyzed on AGC1 partially silenced Oli-neu cells and AGC1$^{+/-}$ mice-derived neurospheres, showing significant variations, in accordance with the alterations in brain cells proliferation and maturation previously reported. Subsequently, given the large functional role of histone acetyltransferases (HATs) and histone deacetylases (HDACs) in oligodendrocyte lineage development, the hypothesis that the premature OPCs differentiation and transcriptional dysregulation affecting our AGC1 deficiency models could be consequence of an improper epigenetic regulation, has been investigated. In this

sense, analysis were performed to study the major post-translational histone modifications (acetylation and methylation), and HATs and HDACs expression, activity, and sub-cellular localization, in both Oli-neu cells and neurospheres, revealing an altered epigenetic profile characterizing both oligodendrocytes and neuronal progenitors cells. Furthermore, given the wide role of acetylation in regulating OPCs specification, cell-cycle progression, and maturation (Hernandez and Casaccia; 2015), to better clarify HATs and HDACs implication in the unbalance regulation of brain cells biological processes, Oli-neu cells and neurospheres were treated with specific HAT or HDACs inhibitors (curcumin and SAHA respectively). Analysis of morphology (filaments number and length), Western blot, and immunostainings, showed worsening of siAGC1 Oli-neu phenotype following both HAT and HDACs inhibition, with effects of reduced proliferation and increased differentiation. Similarly, curcumin and SAHA treatments on AGC1$^{+/-}$ neuropheres, leaded to a further reduction in proliferation rate and alterations in neural progenitors commitment, confirming the implication of HAT and HDAC enzymes in the improper regulation of proliferation and differentiation observed in AGC1 deficiency models. Subsequently, to investigate the relation between transcription factors and epigenetic modulators, co-immunoprecipitations were performed, in order to observe whether their interactions, and thus alteration, could play a role in AGC1 deficiency. Starting from recent observations that identify c-Myc as one of the transcription factors mainly involved in promoting OPCs in a proliferative active and undifferentiated state (Magri *et al.,* 2014 b), immunoprecipitation experiments were conducted to understand if its interaction with other factors or epigenetic modulators could play a role in Oli-neu cells following AGC1 knocking down. Lastly, given the unexpected interplay between AGC1 and c-Myc, further chromatin immunoprecipitations (ChIP) will be performed on Oli-Neu cells to verify c-Myc binding, by itself or through multi-protein complexes, to promoter regions of genes involved in OPCs proliferation/differentiation.

3.

MATERIALS AND METHODS

3.1 Cell cultures: Oli-neu cells

To generate stable cellular models with a partial silencing of SLC25A12 gene (A36 for control and siAGC1 for silenced cells), immortalized mouse oligodendrocyte precursor cells (Oli-Neu, kind gift from Dr. Jacqueline Trotter, University of Mainz, Germany) were transfected using Lipofectamine 2000 reagent (Thermo Fisher) and a pLKO1-pure DNA plasmid (Sigma-Aldrich) containing a scrambled control sequence or an AGC1 targeting sequence as previously published (Petralla *et al*., 2019). AGC1 expression was tested by western blotting, and a specific clone with a reduction up to 40% of carrier's activity (like AGC1 deficiency patients) was selected for subsequent studies. For experiments, cells were let grown on poly-L-lysine (Sigma-Aldrich, St Louis, MO, USA) coated Petri dishes at $37^{o}C$ and 5% CO_2 in SATO medium (DMEM medium, 2mM glutamine, 10µg/ml insulin, 5.5µg/ml transferrin, 38.72nM sodium selenite, 100µM putrescine, 520nM L-thyroxine, 500nM triiodo-L-thyronine (T3), 200nM progesterone, 25µg/ml gentamycin; all from Sigma-Aldrich, except for insulin-transferrin-sodium selenite 100X supplement, Thermo Fisher Scientific, Waltham, Massachusetts, USA), supplemented with 1% heat-inactivated Horse Serum (HS; Sigma-Aldrich), and 1µg/ml puromycin (Sigma-Aldrich) to maintain transfected clones (Trotter J., *et al*., 1989). Once confluent, cells were washed with PBS (0.9% NaCl in 50mM phosphate buffer pH 7.4) and detached with 0.01% trypsin - 0.02% EDTA-HBSS (Sigma-Aldrich) for 3-4 minutes at $37^{o}C$. Trypsin reaction was then stopped by adding an equal volume of DMEM basal medium supplemented with 10% Horse Serum, and cells collected and centrifugated at 300g for 5 min. Lastly, Oli-neu cells were counted and plated in complete culture medium SATO 1% HS + puromycin (1µg/ml) at different growth densities depending on the experiment.

3.1.1 Sub-cellular fractionation

Cytosolic, mitochondrial, and nucleic extracts were obtained from a modified Grove BD and Bruckey protocol. Oli-neu cells were collected in 100µl/10cm Petri dish of isotonic buffer (10mM Hepes, 200mM mannitol, 70mM sucrose, 1mM EDTA pH 7.6, 1X protease and phosphatase inhibitor cocktails; all from Sigma-Aldrich) in 1.5ml Eppendorf tube and left 30 minutes on ice. Then, cells were lysed with a Potter homogenizer (B.Braun, Melsungen AG) at 1000rpm/30 strokes, and 1/6 of the volume was collected as total extract for future WB analysis. After centrifugation at 800g for 10

min at 4°C, the supernatant (cytoplasmic fraction; CF) was transferred into a new 1.5ml Eppendorf tube, whereas pellet (nucleic fraction) was resuspended with 100µl/10cm Petri dish of isotonic buffer and centrifuged at 800g for 10 min at 4°C. The supernatant was then discarded and nuclei were washed two times: *i*) with 300µl/tube of buffer A (2 mM Hepes pH 7.9, 10mM NaCl, 3mM $MgCl_2$, 0.1% NP40, 10% glycerol, 0.2mM EDTA, 1mM DTT, 1X protease and phosphatase inhibitor cocktails), left on ice for 10min and centrifuged at 800g for 10 min at 4°C; *ii*) in 1ml/tube buffer B (20mM Hepes pH 7.9, 0.2mM EDTA, 200mM glycerol, 1mM DTT, 1X protease and phosphatase inhibitor cocktails) and centrifuged at 800g for 10 minutes at 4°C to remove detergent NP-40; the supernatant was discarded every time after centrifugation. In parallel, to isolate cytosolic and mitochondrial extracts, the cytoplasmic supernatant fraction (CF) was centrifuged 800g for 10min at 4°C, pellet removed and supernatant centrifugated again 14,000g for 20 min. Supernatant was transferred into a new 1.5ml Eppendorf whereas pellet (mitochondria) was resuspended in 500µl/tube of isotonic buffer (10mM Hepes, 200mM mannitol, 70mM sucrose, 1mM EDTA pH 7.6, 10µl/ml protease and phosphatase inhibitor cocktails); both centrifuged at 14,000g for 20 min. Lastly, to quantify the total protein extraction, the Lowry quantification method was used (Lowry *et al.*, 1951). Nuclei were resuspended in 30µl/10cm Petri dish of extraction buffer with salt (20mM Hepes, pH 7.9, 400mM NaCl, 2% SDS, 0.2mM EDTA, 200mM glycerol, 1mM DTT, 1X protease and phosphatase inhibitor cocktails), whereas mitochondria resuspended in 50µl/10cm Petri dish of mitochondrial lysis buffer (50mM Tris, 1% SDS, 1mM EDTA, pH 7.4). All samples were sonicated for 3 pulses of 2 seconds each (waiting for 5 seconds between each pulse) with a Branson 250 digital sonifier before quantification, and stored at -80°C until used.

3.1.2 Extraction, isolation, and analysis of histones

Histone component of Oli-Neu nuclei was isolated and purified by using the acid extraction protocol of Schechter *et al.* 2007. Once at confluence, cells were washed with PBS, detached with 0.01% trypsin -EDTA-HBSS 0.02%, diluted with an equal volume of 10% DMEM-HS and centrifuged at 300g for 5 min. The pellet obtained was then resuspended in 1% HS SATO medium and cells counted with the Neubauer chamber. $5x10^6$ cells were transferred to a new tube, centrifuged at 300g for 5 min and the resulting pellet washed in 10ml of PBS. After centrifugation at 300g for 5 min, cells were lysed in 1ml of hypotonic lysis buffer (10Mm Tris-Cl pH 8.0, 1mM KCl, 1.5mM $MgCl_2$, 1mM DTT, 1X protease and phosphatase inhibitor cocktails; all from Sigma-Aldrich) and transferred into a new 1.5ml Eppendorf tube. To favor hypotonic swelling and lysis, cells were then incubated for 30 min at 4°C in mild shaking. Intact nuclei were pelleted 10,000g for 10 min at 4°C, supernatant discarded, pellet carefully resuspended in 400µl of 0.4N H_2SO_4 and incubated 30 min in rotation. After

centrifugation at 16,000g for 10 min at 4°C to remove nuclear debris, supernatant containing histones was then transferred into a new 1.5ml Eppendorf and 132µl of TCA 100% (Trichloroacetic acid; Sigma-Aldrich) were added dropwise, taking care to invert several times to mix the solution. Histones were let precipitate overnight at 4°C. The following day, the solution was centrifugated at 16,000g for 10 min at 4°C, supernatant was discarded, and pellet washed in glacial acetone to remove acids from the histone component. Lastly, after two washes in glacial acetone each of which followed by centrifugation at 16.000g for 5 min at 4°C, supernatant was removed, and pellet allowed to dry for 20 min at RT. Histones were then resuspended in 100µl of PBS + 10µl/ml protease and phosphatase inhibitor cocktails. All samples were sonicated with a Branson 250 digital sonifier and stored at -80°C until use.

3.2 Cell cultures: Neurospheres

Neurospheres used in this work were acquired from the sub-ventricular zone (SVZ) of 8-months-old C57BL/6N wild-type and heterozygous SLC25A12 male mice (*Mus musculus*), generated through gene-trapping technique by the Texas A & M Institute for Genomic Medicine (Houston, Texas, USA). AGC1$^{+/-}$ mice were obtained through homologous recombination, where an inactive protein no able to bind substrates was produced due to an insertion of a premature stop-codon between exon 2 and 3 of AGC1 mRNA. The heterozygous mutation revealed a reduction up to 50% of carrier activity in AGC1$^{+/-}$ mice, whereas the homozygous one resulted lethal in embryonic age (Petralla *et al.*, 2019). During the study, animals were bred with *ad libitum* access to food and water, in 12/12-hour light-dark cycle at 20 °C ± 2 °C and set humidity; appropriate environmental enrichments were placed to guarantee their well-being. Mice health and physical state was periodically controlled by veterinarians from the University of Bologna, and experiments were conducted in agreement with European Community laws and Italian legislation and approved by an Ethical committee for Animal Experimentation at the University of Bologna (Protocol No 17-72-1212).

To perform SVZ microdissection, AGC1$^{+/+}$ and AGC1$^{+/-}$ mice where anesthetized through an intraperitoneal injection of 10mg/kg xylazine followed by cervical dislocation. Once collected in PBS, brains were cut above the optic chiasm, and the rostral part containing the lateral ventricles and the respective anterior periventricular regions was used for SVZ dissection. Tissues were mechanically dissociated in Hank's Balanced Salt Solution (HBSS; 3.9mg/ml HEPES, 0.5mg/ml NaHCO$_3$, 0.9mg/ml glucose, 0.5% penicillin/streptomycin), transferred in 15ml tube and centrifuged at 1000rpm for 5 min. The supernatant was discarded, and pellet resuspended in papain solution (0.2mg/ml EDTA, 0.66mg/ml Papain, 0.2mg/ml cysteine in HBSS) to promote stem cell release, and placed at 37°C for 20 min taking care to shake every 5 min. For further dissociation, tissues were

resuspended again in HBSS and let other 10 min at 37°C. Papain reaction was then inhibited by adding DMEM F-12 (Gibco Life Technologies, Waltham, MA, USA), and samples were centrifuged at 1000rpm for 5 min. Cells were finally plated in 35mm dishes in complete culture medium: DMEM-F12 supplemented with 2mM glutamine, 10µg/ml insulin, 20ng/ml Epidermal Growth Factor (EGF; PeproTech EC, London, UK), 20ng/ml Fibroblast Growth Factor-2 (FGF2; PeproTech), 1% N2 (ThermoFisher Scientific, Waltham, MA, USA), 1% B27 (ThermoFisher), 10units/ml penicillin and 10µg streptomycin. Neo-formed neurospheres were passed every week (5/7 days of growth). Cells were collected and centrifugated at 1000rpm for 5 min, washed in PBS and centrifugated again 5 min at 1000rpm. Spheres were then dissociated as single cells through incubation in Accutase (Aurogene Srl, Roma, Italy) 5 min at 37°C, and basal DMEM F-12 was added to stop the reaction. After the last 5 min centrifuge at 1000rpm, supernatant was then discarded, and pellet resuspended in complete culture medium to then proceed with cell count. Depending on concentration, specific volumes were plated to obtain a final cell density of $5x10^3$ cells/cm^2.

3.3 SAHA and Curcumin treatments

To evaluate the role of HDACs or HATs on AGC-1 *in vitro* models' proliferation and differentiation, Oli-neu cells and neurospheres were treated with different concentrations of specific inhibitors, respectively. To reduce histone deacetylase activity, the general HDAC inhibitor Suberanilohydroxamic acid (SAHA; Zhou *et al.,* 2011), approved by FDA for cancer therapy, was used; in parallel, to act on histone acetyltransferase enzymes, cells were treated with the natural compound Curcumin, a specific HAT p-300 activity inhibitor (Sunagawa *et al.,* 2018).

For Western Blot or microscopy analysis on Oli-neu cells proliferation and differentiation, $2x10^5$cells/well were plated in 6-well plates or 24mm diameter glass coverslips, both previously treated with poly-L-lysine (10µg/mL), respectively. After 2h, complete SATO medium was replaced with fresh medium containing SAHA (0.5µM; 1µM) or curcumin (10µM; 20µM) based on MTT assay (not shown), and cells were incubated 24h or 48h at 37°C and 5% CO_2. The same DMSO volume, in which molecules are dissolved, was used as control. To perform immunostainings, cells on glass coverslips were then fixed with 4% PFA for 30 min, washed with PBS and stored at 4°C in PBS. For Western Blot analysis, Oli-neu on dishes were collected with lysis buffer (50mM Tris, 1% SDS, 1mM EDTA, pH 7.4) and kept at -80°C until used. In parallel, to study the effect of HDAC and HAT inhibition on neurospheres proliferation, spheres were plated as single stem cells in 96-well plates ($5x10^3$cells/well) in presence of SAHA (0.5µM; 1µM) or curcumin (10µM; 20µM), based on MTT assay (not shown), in complete DMEM F-12 culture medium; same volumes of DMSO were used as control. SAHA-treated neurospheres were let 5 days in culture (because of inhibitor's toxicity

after long-time in culture), and 7 days curcumin-treated ones. By contrast, to evaluate differentiation, 75 or 30 neurospheres were plated on 35mm Petri dishes or 13mm glass coverslips in complete DMEM F-12 medium plus DMSO (control) or inhibitors, depending on Western Blot or immunofluorescence analysis, respectively. To allow stem cells adhesion and consequently differentiation, both dishes and coverslips were previously treated with poly-L-lysine (10µg/mL) and incubated with fibronectin (1µg/ml) at 37°C at least 3h. After 7 days in culture, differentiated neurospheres were collected in lysis buffer and stored at -80°C for Western Blot, or fixed 30 min with 4% PFA and kept at 4°C in PBS for immunofluorescence studies.

3.4 Oli-neu cells extensions number and length measurement

To analyze Oli-neu cells morphology, five randomly selected fields for each 24mm diameter glass coverslip were acquired (20X objective) with an Eclipse TS100 – Nikon optical microscope. Processes number and length were measured by using Fiji software (ImageJ2, developed by the National Institutes of Health, NIH, USA; RRID:SCR_002285). The "segmented-line function" was used to trace each cell process and the "measure function" (Analyze menu) was used to determine extensions length in micrometers (µM). The number of processes was directly determined from individual processes length measurement.

3.5 Neurospheres proliferation

To assess the effect of HATs and HDACs inhibition on neurospheres proliferation, 5 different image fields/well were acquired by using an eclipse TE 2000-s microscope – Nikon (10X objective). Images were visualized with Fiji ImageJ2 using an automated colony and cell counting method (Choudhry P *et al.*, 2016). Only aggregates bigger than 400µm^2 were considered.

3.6 Western Blot

To perform Western Blot all samples were sonicated with a Branson 250 digital sonifier at 10% power output (3 pulses of 2 seconds each, waiting 5 seconds between each pulse). Total protein content was determined with the Lowry quantification method, and bovine serum albumin (BSA, 1.5mg/ml) was used to obtain the standard calibration curve. All samples were quantified in duplicate: double-distilled water (ddH$_2$O) was added to 2µl of sample to a final volume of 200µl; subsequently, 1ml of solution I (98% solution A; 2% Na$_2$CO$_3$ in 0.1N NaOH; 1% solution B: 0.5% CuSO$_4$; 1% solution C; 1% Na-K tartrate) was added to each sample; after incubation 10min at RT, 100µl of solution II (50% Folin reagent and 50% ddH$_2$O; all reagents were from Sigma-Aldrich) were added, and samples were

mixed and incubated 30 min at RT. Absorbance was read at 700 nm. Equal protein amounts (30µg) from samples were resuspended in 4X Loading buffer (1M Tris-HCl pH 6.8, 20% sodium dodecyl sulfate, 0.4µl/ml glycerol, 2g/l bromophenol blue and 2M dithiothreitol; all from Sigma-Aldrich) and resolved in SDS-PAGE (Sodium Dodecyl Sulphate - PolyAcrylamide Gel Electrophoresis). Proteins were then transferred onto a nitrocellulose membrane (GE Healthcare Life Sciences, Little Chalfont, UK) and non-specific sites were blocked 1h at RT with PBS 0.1% Tween-20 (Sigma-Aldrich) and 5% nonfat dried milk (Bio-Rad). Membranes were then incubated with primary antibody overnight at 4°C. The next day, after 3 washes 10 min each in 0.1% Tween-20/PBS + 5% dried milk, membranes were incubated with the specific HRP-secondary antibody (horseradish peroxidase conjugated) 90 min at RT. Following 3 washes in 0.1% Tween-20/PBS, labeled proteins were visualized by using Clarity™ Western ECL Substrate (Enhanced ChemiLuminescence; Bio-Rad) and detected through Biorad Image Lab software with ChemiDoc™ MP imaging system (Version 6.0.0; RRID:SCR_014210).

Table 1: Primary and secondary antibodies used for Western Blot analysis.

Antibody	Company	Diluition
AGC1/Aralar1 mouse monoclonal IgG	**Santa Cruz Biotechnology;** Cat# sc-271056, RRID: AB_10608837	1/1000
Anti-acetyl-Histone H3 rabbit polyclonal antibody	**Millipore;** Cat# 06-599, RRID:AB_2115283	1/1000
CBP (D6C5) rabbit monoclonal IgG	**Cell Signalling Technology;** Cat# 7389, RRID:AB_2616020	1/1000
CNPase rabbit monoclonal IgG	**Cell Signalling Technology;** Cat# 5664, RRID:AB_10705455	1/1000
CREB (48H2) rabbit monoclonal IgG	**Cell Signalling Technology;** Cat# 9197, RRID:AB_331277	1/1000
c-Myc rabbit polyclonal IgG	**Santa Cruz Biotechnology;** Cat# sc-764, RRID:AB_631276	1/1000
Anti-**Doublecortin** rabbit polyclonal antibody	**Abcam;** Cat# ab18723, RRID:AB_732011	1/1000
GAPDH mouse monoclonal IgG	**Santa Cruz Biotechnology;** Cat# sc-32233, RRID:AB_627679	1/20000
GFAP rabbit immunoglobulins	**Dakopatts;** Cat# sc-33673, RRID:AB_627673	1/1000
Histone Deacetylase 1 (**HDAC1**) Antibody	**Cell Signalling Technology;** Cat# 2062, RRID:AB_2118523	1/1000

HDAC2 (D6S5P) rabbit Antibody	**Cell Signalling Technology**; Cat# 2540, RRID:AB_2116822	1/1000
Histone Deacetylase 3 (**HDAC3**) Antibody	**Cell Signalling Technology**; Cat# 2632, RRID:AB_331545	1/1000
Histone Deacetylase 4 (**HDAC4)** Antibody	**Cell Signalling Technology**; Cat# 2072, RRID:AB_2232915	1/1000
Histone H3 rabbit polyclonal IgG	**Santa Cruz Biotechnology**; Cat# sc-10809, RRID:AB_2115276	1/1000
HSP60 rabbit polyclonal IgG	**Bioss;** Cat# bs-0191R-HRP, RRID:AB_11117391	1/1000
MAX (H-2) mouse monoclonal IgG	**Santa Cruz Biotechnology**; Cat# sc-8011, RRID:AB_627913	1/1000
Anti-**NG2** rabbit polyclonal IgG	**Abcam;** Cat# ab83178, RRID:AB_10672215	1/1000
NRSF (P-18) goat polyclonal IgG	**Santa Cruz Biotechnology;** Cat# sc-15120, RRID:AB_2179628	1/1000
OLIG2 rabbit polyclonal IgG	**Santa Cruz Biotechnology**; Cat# sc-48817, RRID:AB_2157550	1/1000
Pan-Met-H3	**MBL International**; Cat# LS-A4069, RRID:AB_591306	1/1000
PDGFRα (C-20) rabbit polyclonal IgG	**Santa Cruz Biotechnology**; Cat# sc-338, RRID:AB_631064	1/1000
Phospho-CREB (Ser133) rabbit monoclonal antibody	**Cell Signaling Technology;** Cat# 9198, RRID:AB_2561044	1/1000
Goat anti-Rabbit	**Jackson ImmunoResearch Labs**; Cat# 111-035-144, RRID:AB_230739	1/5000
Mouse anti-Goat	**Santa Cruz Biotechnology;** Cat# sc-2354, RRID:AB_628490	1/4000
Goat anti-Mouse	**Jackson ImmunoResearch Labs**; Cat# 115-035-146, RRID:AB_2307392	1/5000

3.7 Immunofluorescence analysis

Double labeling were performed on cells using specific fluorochromes with different emission wavelengths. For the analysis, all samples were previously plated on glass coverslips and fixed with 4% PFA for 30 min, washed with PBS and stored at 4°C until use. To permeabilize the plasma membrane, cells or neurospheres were washed 3 times 10 min each in PBST (PBS + 0.1% Triton) and incubated 1h in Blocking Buffer (PBS-0.1% Triton + 5% normal goat serum) to block non-specific antigenic sites. Primary antibodies diluted in Blocking Buffer (PBST + 2% normal goat serum) were then added, and fixed cells were left overnight at 4°C. The next day, after 3 x 10 min washes in PBST, samples were incubated with specific secondary antibodies for 2h at RT away from light. Then, cells were washed 3 times 10 min each in PBST and once with PBS, and nuclei were stained with Hoechst 33258 (2 µg/ml, Sigma-Aldrich) for 5 min. Glass coverslips were placed in PBS and mounted using Ultracruz Aqueous Mounting Medium with DAPI (Santa Cruz, cat. no. sc-24941) and stored at 4°C in dark.

Table 2: Primary and secondary antibodies used for immunofluorescence analysis.

Antibody	Company	Diluition
AGC1/Aralar1 mouse monoclonal IgG	**Santa Cruz Biotechnology;** Cat# sc-271056, RRID:AB_10608837	1/500
CBP (D6C5) rabbit monoclonal IgG	**Cell Signalling Technology**; Cat# 7389, RRID:AB_2616020	1/500
CNPase rabbit monoclonal IgG	**Cell Signalling Technology**; Cat# 5664, RRID:AB_10705455	1/500
c-Myc rabbit polyclonal IgG	**Santa Cruz Biotechnology**; Cat# sc-764, RRID:AB_631276	1/500
Anti-**Doublecortin** rabbit polyclonal antibody	**Abcam**; Cat# ab18723, RRID:AB_732011	1/500
GFAP rabbit immunoglobulins	**Dakopatts**; Cat# sc-33673, RRID:AB_627673	1/500
HDAC2 (D6S5P) rabbit Antibody	**Cell Signalling Technology**; Cat# 2540, RRID:AB_2116822	1/500
Histone Deacetylase 3 (**HDAC3**) Antibody	**Cell Signalling Technology**; Cat# 2632, RRID:AB_331545	1/500
HSP60 rabbit polyclonal IgG	**Bioss**; Cat# bs-0191R-HRP, RRID:AB_11117391	1/500
MAX (H-2) mouse monoclonal IgG	**Santa Cruz Biotechnology**; Cat# sc-8011, RRID:AB_627913	1/500

anti-Ki67 antibody KO tested	**Abcam;** Cat# ab15580, RRID:AB_443209	1/500
NRSF (P-18) goat policlonal IgG	**Santa Cruz Biotechnology;** Cat# sc-15120, RRID:AB_2179628	1/500
OLIG2 rabbit polyclonal IgG	**Santa Cruz Biotechnology**; Cat# sc-48817, RRID:AB_2157550	1/500
Phospho-CREB (Ser133) rabbit monoclonal antibody	**Cell Signaling Technology;** Cat# 9198, RRID:AB_2561044	1/500
Goat anti-Rabbit IgG Alexafluor 488	**Abcam;** Cat# ab150077, RRID:AB_2630356,	1/1000
Goat anti-Rabbit IgG Alexafluor 555	**Abcam;** Cat# ab150078, RRID: AB_2722519	1/1000
Goat anti-Mouse IgG Alexafluor 488	**Abcam;** Cat# ab150113, RRID:AB_2576208	1/1000
Donkey anti-Mouse IgG Alexafluor 555	**Abcam;** Cat# ab150106, RRID:AB_2857373	1/1000

3.8 Cell counting after immunofluorescence

For stained Oli-neu cells, 3 randomly selected fields for each glass coverslip were acquired with the Nikon EZ-C1 confocal microscope (10X or 100X objective) and analyzed through Fiji software (ImageJ2). Positive cells were manually counted with the counter plugin of Fiji ImageJ2 software. The labeling index was estimated as the ratio of positive/total cells; nuclei were stained with DAPI. For neurospheres, images from 3 different fields/coverslip were obtained by Z-stack acquisition (1μm thickness layers, 40 stacks; 60X objective), and 3D image reconstruction was performed by using Fiji ImageJ2 software - z-project plugin, sum stacks function. Fluorescence intensity index was expressed as markers' positive cells intensity/total cells stained with DAPI.

3.9 Mitotracker Red

To analyze mitochondria morphology, 10^6 control and siAGC1 Oli-neu cells were plated on 24mm glass coverslips previously treated with poly-L-lysine. Following incubation 24h at 37°C and 5% CO_2., Mitotracker Red was added 15min to a final concentration of 10nM. Medium was then replaced with fresh DMEM basal medium -phenol red, and 3 randomly selected fields for each slide were

acquired with the Nikon EZ-C1 confocal microscope (100X objective) and analyzed through Fiji software (ImageJ2).

3.10   Immunoprecipitation

To perform immunoprecipitations, cells were washed 2 times in PBS, collected with 1ml cold RIPA buffer (50Mm Tris-HCl pH 7.4, 150mM NaCl, 1% NP-40, 0.25% Na-deoxycholate, 1mM EDTA, 1mM Na_3VO_4, 1mM NaF, 10µl/ml protease and phosphatase inhibitor cocktails; all from Sigma-Aldrich) in 1.5ml Eppendorf tube, and left 10min on ice in mild shaking. To lysate plasma membrane samples were then resuspended several times with a glass pipette, and centrifugated 10.000rpm 10 min at 4°C to remove cell debris. Supernatants were transferred into new 1.5ml tubes, and 2.5µl of specific control IgG and 20µl of protein A/G PLUS agarose (beads; Santa Cruz) were added to pre-clear cell lysates. Samples were incubated 30 min in mild rotation and subsequently centrifugated 2.5000rpm 20 sec; all carefully performed at 4°C. Pellet was then removed, and the total protein content was determined through the Lowry quantification method. For immunoprecipitation, 300µg of protein were used in a final volume of 1ml in PBS/RIPA buffer; 10µl of a specific primary antibody and 20µl of protein A/G PLUS agarose were added to each 1.5ml tube, and samples were left overnight at 4°C in mild rotation. The next day, after centrifugation 2.5000rpm 30 sec at 4°C, pellets were gently washed 3 times x 10 min in 800µl cold PBS/RIPA buffer, centrifugating every time as previously described. Supernatants were then discarded, and samples were resuspended in 1X Loading buffer and boiled 10 min to be resolve in 12.5% SDS-PAGE (Sodium Dodecyl Sulphate - PolyAcrylamide Gel Electrophoresis).

Table 3: Antibodies used in immunoprecipitation and western blot analysis.

Antibody	Company	Diluition
AGC1/Aralar1 mouse monoclonal IgG	**Santa Cruz Biotechnology;** Cat# sc-271056, RRID: AB_10608837	1/1000
c-Myc rabbit polyclonal IgG (ChIP-grade)	**Santa Cruz Biotechnology**; Cat# sc-764 X, RRID: AB_631276	1/1000
HDAC2 (D6S5P) rabbit Antibody	**Cell Signalling Technology**; Cat# 2540, RRID: AB_2116822	1/1000
MAX (H-2) mouse monoclonal IgG (ChIP-grade)	**Santa Cruz Biotechnology**; Cat# sc-8011 X, RRID: AB_627913	1/1000

Normal Mouse IgG	**Santa Cruz Biotechnology;** Cat# sc-2025, RRID: AB_737182	
Normal Rabbit IgG	**Santa Cruz Biotechnology;** Cat# sc-2027, RRID: AB_737197	
Goat anti-Rabbit	**Jackson ImmunoResearch Labs;** Cat# 111-035-144, RRID: AB_230739	1/5000
Goat anti-Mouse	**Jackson ImmunoResearch Labs;** Cat# 115-035-146, RRID: AB_2307392	1/5000

3.11 Plasmids amplification and purification

In order to induce partial silencing of specific proteins in Oli-neu cells, plasmids containing different shRNAs were transfected by using Lipofectamine 2000 reagent (Thermo Fisher). To amplify and purify plasmids, DH5-alpha (*E. coli*) colonies were let grown in 2ml sterile LB Broth (10ng Bacto-tryptone, 5g yeast extract, 10g NaCl; all from Sigma-Aldrich) overnight at 37°C. The day after, to achieve an optical density (OD_{600}) of 0.3-0.4, 100µl of cultures were incubated in 5ml LB Broth and placed 1h/1.30h at 37°C depending on bacteria growth rate. 1ml of cells was then transferred into 1.5ml Eppendorf tube and pelleted 4000g 10 min at 4°C. To obtain competent cells, supernatant was discarded, pellet resuspended in 1:2 volume of filtered 50mM $CaCl_2$ and centrifuged again 4000g 10 min at 4°C. Lastly, bacteria were resuspended in 1:10 volume 50mM $CaCl_2$ and kept on ice (4°C) until transformation. 100µl of cells were then transformed with 50ng of plasmids and placed 30 min on ice to allow DNA to cross the plasma membrane. Heat shock was performed at exactly 1 min at 42°C and 2 min on 4°C; subsequently, 800µl LB + selection (Ampicillin 10µg/ml) were added, and tubes were placed 1h at 37°C in shaking (250rpm) or rotation. To obtain transformed colonies, 30µl of each mix were spread onto a warmed selection plate and incubate overnight at 37°C. The next day, one bacterial colony for each transformation was selected from the spread plates in order to obtain an unique colony culture, and let grown in 5ml LB + Ampicillin (10µg/ml) in 50ml tube for 8-10h at 37°C. 5ml of amplified cultures were then incubated in 45ml LB + Ampicillin in 500ml flasks and placed on a rocking platform overnight at 37°C. The last day, selected cultures were transferred into new 50ml tubes and pelleted 4000rpm 15 min at 4°C. Supernatants were discarded, and pellet used to purify plasmids trough the QIAGEN Plasmid Midi Kit (QIAGEN, Hilden, Germany), according to manufacturer's instructions. DNA was then quantified by using Nanodorp 2000 (Thermo Scientific™ NanoDrop 2000/2000c).

3.12 Transfections

3×10^5 control and siAGC1 Oli-neu cells were plated on a poly-L-lysine 6-well plate. After incubation 24h at 37°C and 5% CO_2, cells were transfected using Lipofectamine 2000 reagent: 5µl of Lipofectamine 2000 reagent and 2.5µg of psi-LVRU6H DNA plasmid vector (Genecopoeia, Rockville, MD, USA) containing a scrambled control sequence or 3 different targeting sequence against HDAC2, HDAC3 or CBP, respectively, were diluted in 100µl of Opti-MEM medium (Thermo Fisher). After 5 min, DNA was carefully added to each tube of diluted Lipofectamine 2000 (ratio 1:1), gently mixed, and left 20 min at RT. Stable DNA-reagents complexes were then added to cells in fresh SATO 1%HS medium. After 3h of incubation, medium was replaced with fresh SATO 1%HS + puromycin (1µg/ml) and hygromycin (50µg/ml) to select transfected cells and silencing was verified trough Western Blot analysis.

3.13 ChIP (Chromatin immunoprecipitation)

Chromatin immunoprecipitations tests were performed to evaluate the association of proteins with specific DNA regions in Oli-neu cells. 1×10^7 cells were collected in 15ml tube and fixed by adding dropwise directly to the media formaldehyde 37% to a final concentration of 0.75-1%. After incubation 10 min at RT in mild-rotation, glycine 125mM (final concentration) was added to stop cross-linking reaction and cells left with shaking 5 min at RT. Pellet was then washed 3 times in 10ml of cold PBS and centrifugated every time 1000g for 5 min at 4°C, being careful to work on ice to avoid DNA degradation. Supernatant was discarded, and pellet resuspended in 750µl/1×10^7 cells of CHIP Lysis buffer (50mM HEPES-KOH pH 7.5, 140mM NaCl, 1mM EDTA pH8, 1% Triton X-100, 0.1% Sodium Deoxycholate, 0.1% SDS, 1X protease inhibitors) and sonicated 60 min (high intensity) + 20min (low intensity), to shear DNA to 100-300bp fragment size. To verify sonication, after 8000g centrifuge for 10 min at 4°C to pellet cell debris, 50µl of sonicated chromatin was incubated with 70µl of Elution buffer (1% SDS, 100mM $NaHCO_3$), 4.8µl of 5M NaCl and 2µl RNase A (10mg/ml) and left overnight at 65°C. The day after, samples were incubated 1h with 2µl proteinase K (20mg/ml) and DNA was purified by using pheno:chloroform extraction protocol (all reagents were from Sigma-Aldrich). DNA concentration was determined with Nanodorp 2000, and 3µg of purified DNA was then resolved in a 1.5% agarose gel with a 100bp DNA marker to control fragment size.

3.14 HAT and HDAC activity assay

To quantify the enzymatic activity of HAT or HDAC in AGC1 Oli-neu cells, Histone Acetyltransferase Activity Assay Kit (Abcam), and Epigenase HDAC Activity/Inhibition Direct Assay Kit (EpigGenetek, NY, USA) were used respectively, according to manufacturer's instruction. To measure acetyltransferase activity, 50μg of nuclear extract in 40μl water (final volume) were prepared for each assay in a 96-well plate. For background reading, 40μl water instead of sample were used; 10μl of NE (Cell Nuclear Extract) were added to 30μl water as positive control. Plates were incubated at 37°C for 1-4 hours depending on color development and read OD440nm at different times during incubation. For HDAC activity, 5μg of nuclear extracts were diluted in kit specific reagents up to 50µl/well (final volume). Only reagents were used as blank sample and signal was detected at 450nm with a microplate reader after 1-2h of incubation.

3.15 Statistical Analysis

All results were subjected to statistical analysis by using Student′s t-test or one-way ANOVA, followed by Bonferroni post-hoc comparison test, depending on the experiment considered. In drugs treatments, to consider the possible effect of both silencing and inhibition, two-way ANOVA, followed by Dunnett's post-hoc comparison test, was used. Statistical analysis was performed by using the GraphPad Prism 4 software (GraphPad Prism, San Diego, CA, USA; RRID:SCR_002798). $p$values < 0.05 were considered statistically significant.

4.

RESULTS

Previous studies conducted in our lab reported defects in proliferation and early differentiation in a stable clone of immortalized mouse oligodendrocyte precursor cells (Oli-Neu cells) transfected with a shRNA for SLC25A12 gene which leaded to 30-40% reduction in AGC1 activity similarly to patiens (Wibom *et al.,* 2009), or with a scramble shRNA as control. Additionally, *in vivo* AGC1 deficiency model *i.e.,* heterozygous mice for AGC1 knock-out (AGC1$^{+/-}$ C57BL6/N background) and neurospheres from their subventricular zone, respectively, showed a global decrease in cells proliferation and a switch in Neural Stem Cells (NSCs) differentiation commitment, with specific reduction in OPCs number and increase in neural and astrocytic pools; however, no changes in mature oligodendrocytes were detected. The obtained results led to consider the failure in myelin synthesis characterizing AGC1 deficiency a consequence of improper OPCs proliferation and differentiation, leading then to an impairment in remyelination (Petralla *et al.*, 2019). Therefore, the present study aims to understand the transcriptional and epigenetic regulation underlying the differences observed in OPCs biological mechanisms, in both AGC1 deficiency models of Oli-neu cells and SVZ-derived neurospheres.

4.1 Altered expression of brain cells proliferation/differentiation transcription factors in AGC1 deficiency models of Oli-neu cells and neurospheres

Temporal coordination between cell cycle exit and differentiation requires a mutual antagonism between transcription factors that promote cell cycle entry and those that induce tissue-specific gene expression. The previously obtained results on AGC1 deficiency models of unbalanced regulation of brain cells proliferation and differentiation (Petralla *et al.*, 2019) prompted us to investigate the expression, interaction and sub-cellular localization of transcription factors known to be involved in these biological mechanisms. The proto-oncogene c-Myc, characterized by a leucine-zipper domain responsible for dimerization with several components, acts as transcriptional activator or repressor depending on its binding partners (Blackwell *et al.*, 1990; Pelengaris *et al.*, 2002). Magri and colleagues (2014) reported high levels of c-Myc expression in OPCs, where operates as important modulator of transition between OPCs proliferation and differentiation, by interaction with promoters of genes involved in cell cycle progression and chromatin remodeling. Furthermore, c-Myc regulates acetylation of large chromatin domains through recruitment of acetyltransferases (HATs) or de-acetyltransferases (HDACs) (Guccione *et al.*, 2006; Martinato *et al.*, 2008) and its silencing promotes oligodendrocytes differentiation, although is not sufficient to induce progression into myelinating

phenotype. Given the proliferation defects and early differentiation observed in AGC1 silenced Oli-neu cells (Petralla *et al.,* 2019), Western Blot and immunofluorescence analysis were performed on control (*i.e.,* a stable clone of Oli-Neu cells following transfection with a scramble shRNA) and siAGC1 Oli-neu, to verify variations in c-Myc and the binding partner MAX expression. A significant decrease up to 70% in c-Myc levels was observed, associated with reduction of MAX, confirming a lower expression of these factors involved in OPCs cell cycle progression in AGC1 partially silenced Oli-neu cells (Figure 4.1A). The expected nuclear localization of c-Myc has been confirmed by Western Blot, following subcellular fractionation (Figure 4.1C), as well as through immunofluorescence (Figure 4.1B).
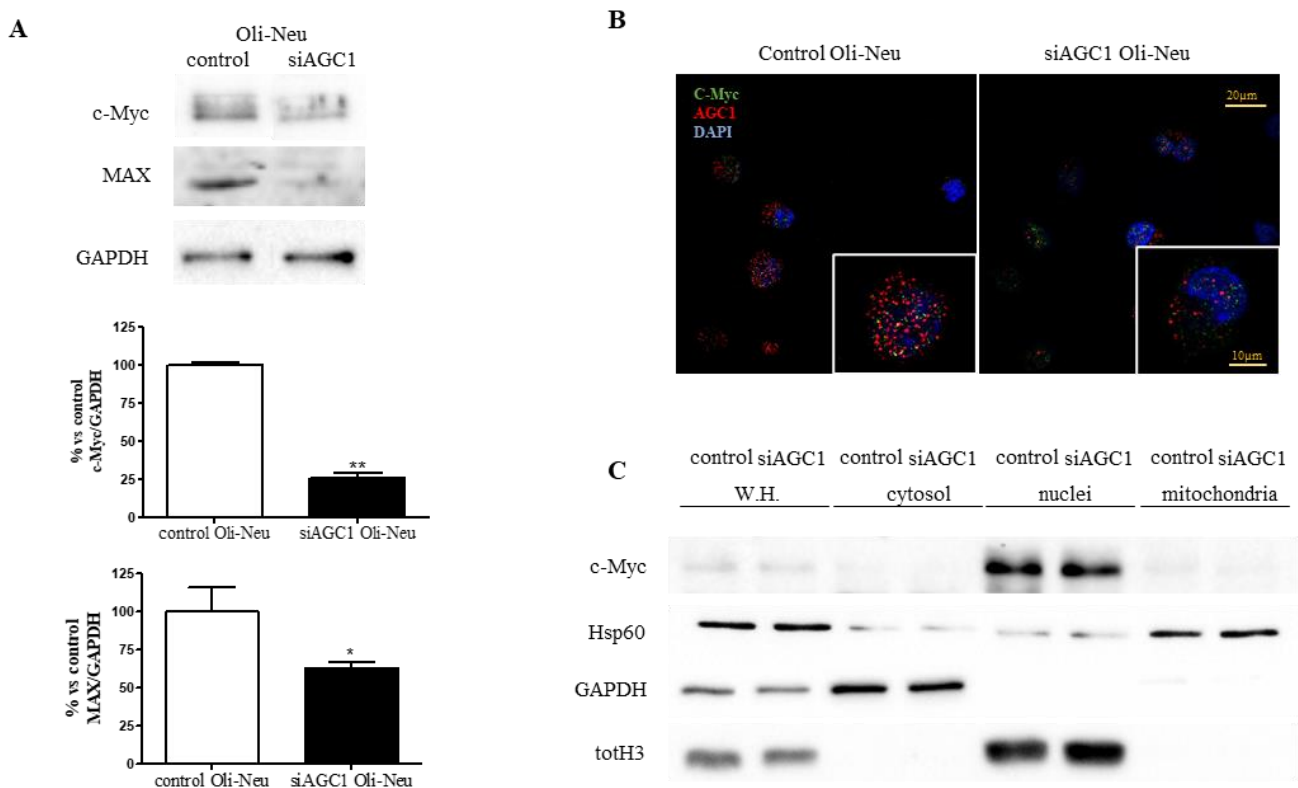

Figure 4.1. Western blot (A), immunostaining (B) and localization analysis through WB following sub-cellular fractionation (C) of c-Myc and MAX expression in siAGC1 and control Oli-Neu cells. (A) Densitometric analysis showed reduction of both c-Myc and its partner MAX expression in siAGC1 Oli-Neu cells compared to control cells. GAPDH was used for endogenous normalization. Values are mean ± SD of 3 independent experiments; ** $P < 0.001$, * $P < 0.05$, compared to control; Student's t-test. (B) Confocal microscopy images (100X) of c-Myc (green) and AGC1 (red); nuclei were labelled with DAPI. Scale bars: 20μm and 10μm. (C) WB analysis of c-Myc expression in whole homogenate, cytosolic, nuclear and mitochondrial fractions from siAGC1 and control Oli-Neu cells; HSP60, GAPDH and totH3 were used as mitochondrial, cytosolic and nuclear specific markers, respectively.

Subsequently, to investigate regulation of Oli-neu cells differentiation, expression of transcription factors Olig2, REST and phosphorylated-CREB, known to be implicated in oligodendrocytes commitment and maturation, was also analysed through Western Blot and immunofluorescence

36

analysis. Olig2 is well recognized as oligodendrocyte-specific marker and its expression is crucial in OPCs specification during early stages of neural development (Zhou and Choi, 2001). It is expressed throughout all maturation processes, with a peak in precursors rather than in postmitotic, mature oligodendrocytes. Western Blot analysis on total protein extracts revealed a significant decrease up to 50% of Olig2 expression in siAGC1 Oli-neu compared to control cells, in line with the early differentiation observed in OPCs following AGC1 partial silencing. Furthermore, the transcriptional repressor REST, which acts via chromatin remodelling to silence neuron-specific genes, thus promoting correct OPCs differentiation (DeWald *et al.*, 2011), increases, although not significantly, compared to Oli-neu control cells. Lastly, during differentiation, oligodendrocytes also express high levels of transcription factor CREB, whose ability to activate transcription is regulated by serine133 phosphorylation (Sato-Bigbee and Yu, 1993; Sato-Bigbee *et al.*, 1994). Several experimental evidences reported CREB to be crucial in different temporal stages of oligodendrocyte development depending on the signal transduction pathways in which it is involved; in maturation phases preceding myelin synthesis, PKA-mediated CREB phosphorylation plays a role in promoting basic myelin protein (MBP) expression and induces OPCs differentiation (Sato-Bigbee and DeVries, 1996). Therefore, Western Blot analysis on control and siAGC1 Oli-neu cells reported a significant increase in pCREB (phosphorylated CREB) expression, with a total pCREB/CREB *ratio* as index of CREB active in promoting OPCs maturation. Results on Olig2, REST and pCREB expression were then confirmed through co-immunostainings with AGC1. Based on fluorescence labelling, reduced expression of Olig2, no significant variations in REST and evident increase in pCREB levels were observed in AGC1 partially silenced Oli-neu compared to control cells. Taken together, these data reveal a different expression of transcription factors involved in cell cycle progression and OPCs differentiation, following partial AGC1 knocking down in Oli-neu cells (Figure 4.2).
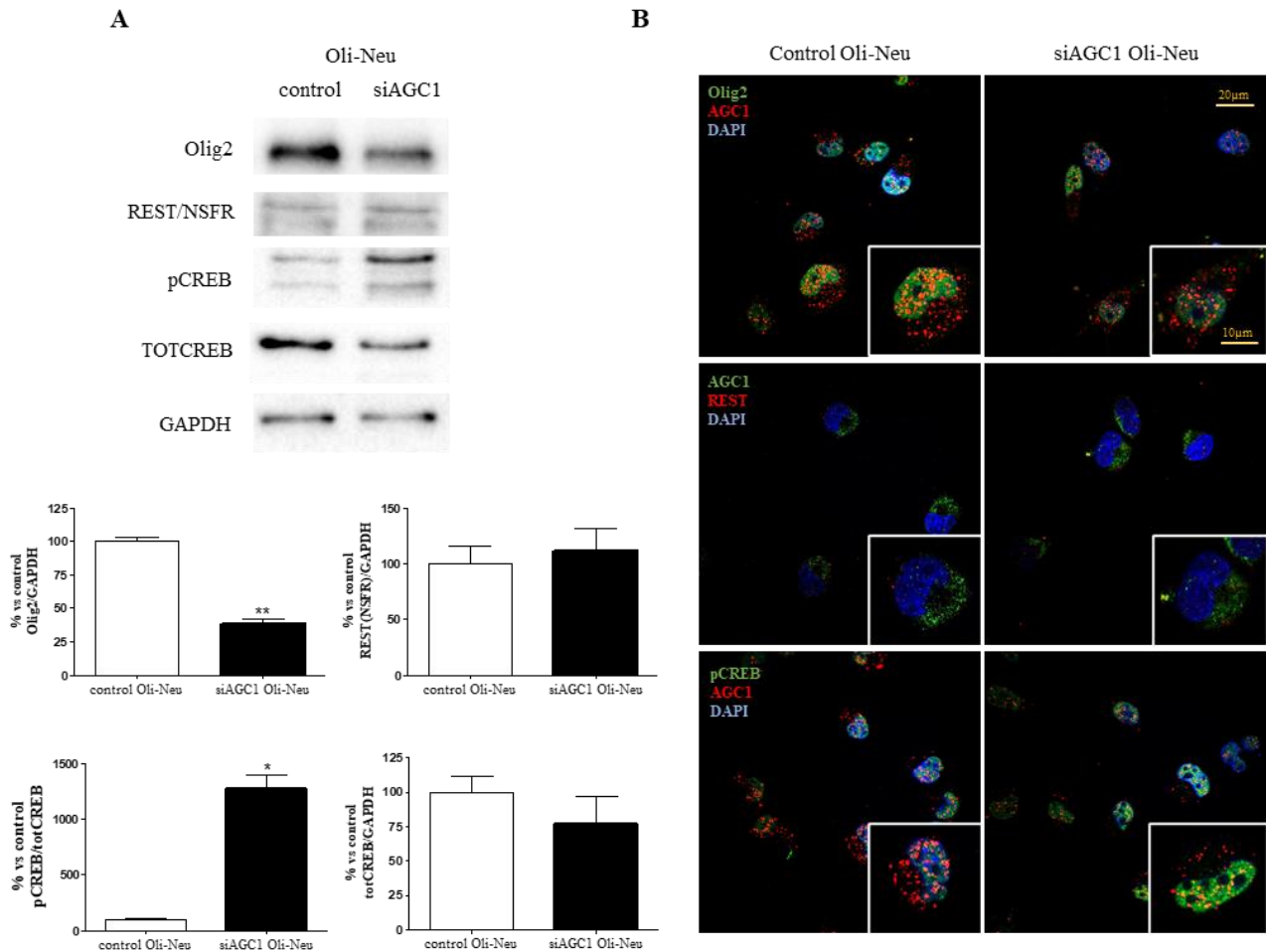
Figure 4.2. Western blot and the relative densitometries (A), as well as immunofluorescence confocal analysis (B) of oligodendrocytes-specific transcription factors Olig2, CREB and of neural repressor REST. Densitometries on western blot analysis of total protein extracts showed reduction of Olig2, significant increase in serine-33 phosphorylated, and thus activated, CREB with a parallel decrease in total CREB and no relevant variations in REST expression in siAGC1 Oli-Neu cells compared to controls; GAPDH was used for endogenous normalization. Values are mean ± SD of 3 independent experiments; ** $P < 0.01$, * $P < 0.05$, compared to controls; Student's t-test. (B) Confocal microscopy images (100X) of Olig2 (green) and AGC1 (red); of AGC1 (green) and REST (red); of pCREB (green) and AGC1 (red); nuclei were always labelled with DAPI. Scale bars: 20µm and 10µm.

In parallel, same analysis were performed on the *in vitro* AGC1 deficiency model of neurospheres, derived from the sub-ventricular zone (SVZ) of both AGC1^{+/+} and AGC1^{+/-} mice, which consist in neurons, astrocytes, and oligodendrocytes progenitors' pool. Western Blot on spontaneously differentiated AGC1^{+/-} neurospheres showed a decrease in c-Myc expression, according to the reduced cell proliferation previously reported compared to WT controls (Petralla *et.al.*, 2019); however, no significant variations were observed in MAX expression. A slight reduction on neural-genes repressor REST was detected, in line with the induction of neuronal commitment during AGC1^{+/-} neurospheres spontaneous differentiation. Therefore, phosphorylated, and total CREB expression, turned out to be remarkably lower, probably due to the least amount of OPCs and mature oligodendrocytes present in the AGC1^{+/-} progenitors' pools (Fig. 4.3).
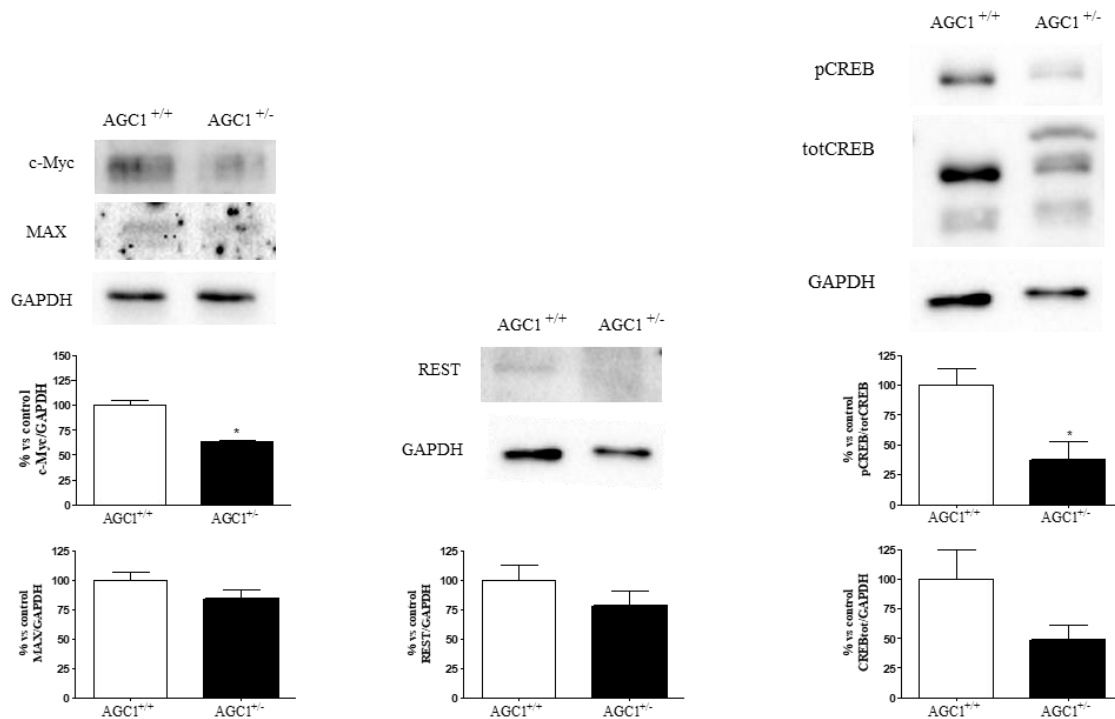
Figure 4.3. Western blot analysis and the relative densitometries of proliferation/differentiation transcription factors in AGC1^{+/-} and WT neurospheres. C-Myc and serine-33 phosphorylated-CREB significantly decrease in AGC1^{+/-} neurospheres compared to control ones, whereas no variations was observed in MAX and REST expression; GAPDH was used for endogenous normalizations. Values are mean ± SD of 3 independent experiments; * P <0.05, compared to control; Student's t-test.

4.2 Altered histone post-translational modifications as well as HATs and HDACs expression and activities in AGC1-silenced Oli-neu cells and AGC1^{+/-} neurospheres

Oligodendrocytes development requires interaction of several molecular factors and intrinsic/extrinsic signals (*i.e.,* epigenetic modulators, microRNA), among which a complex homeostatic balance is needed. Recent studies have reported the contribution of chromatin-regulating complexes to determine transcription factors activity and their temporal regulation (Ruijtenberg *et al.*, 2016). Additionally, a complex transcriptional regulatory network in coordination with epigenetic mechanisms has been identified to regulate the accessibility of transcription factors to their target sequences in the genome (Allis *et al.*, 2016; Chen *et al.*, 2013). Therefore, chromatin remodelling enzymes are crucial elements to allow gene expression. In this sense, the major post-translational histone modifications, acetylation and methylation, and HATs (histone acetyltransferases) and HDACs (histone de-acetylases) expression, sub-cellular localization, and activity, were analysed in both AGC1 deficiency models of Oli-neu cells and neurospheres. Western Blot on purified histones revealed a global decrease in histone H3 pan-acetylation and pan-methylation in siAGC1 Oli-neu cells, whereas no significant differences were observed concerning histone H3 phosphorylation compared to Oli-neu controls (Fig 4.4).
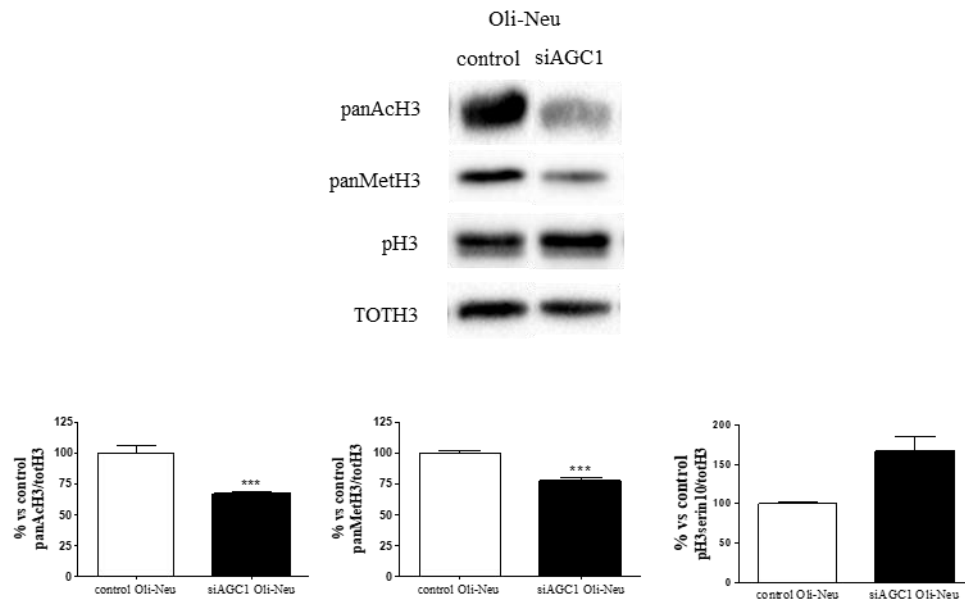
Figure 4.4. Western blot analysis and the relative densitometries of histone H3 post-translational modifications on AGC1 partially silenced Oli-neu compared to control cells. Both H3 pan-acetylation and pan-methylation are reduced in siAGC1 Oli-neu cells compared to controls, whereas H3 phosphorylation levels increased, indicating an altered epigenetic profile affecting AGC1 partially silenced Oli-neu cells. GAPDH was used for endogenous normalizations. Values are mean ± SD of 3 independent experiments; *** P <0.001, compared to control; Student's t-test.

Accordingly, expression of acetyltransferase CREB-binding protein (CBP), which regulates acetylation of cell cycle genes during oligodendrocytes development (Gregath A. and Lu; 2018), is reduced in AGC1 partially silenced Oli-neu compared to control cells, especially in the nuclear subcellular compartment, with a parallel reduced ability to acetylate substrates over time, as shown by the activity assay (Fig. 4.5).
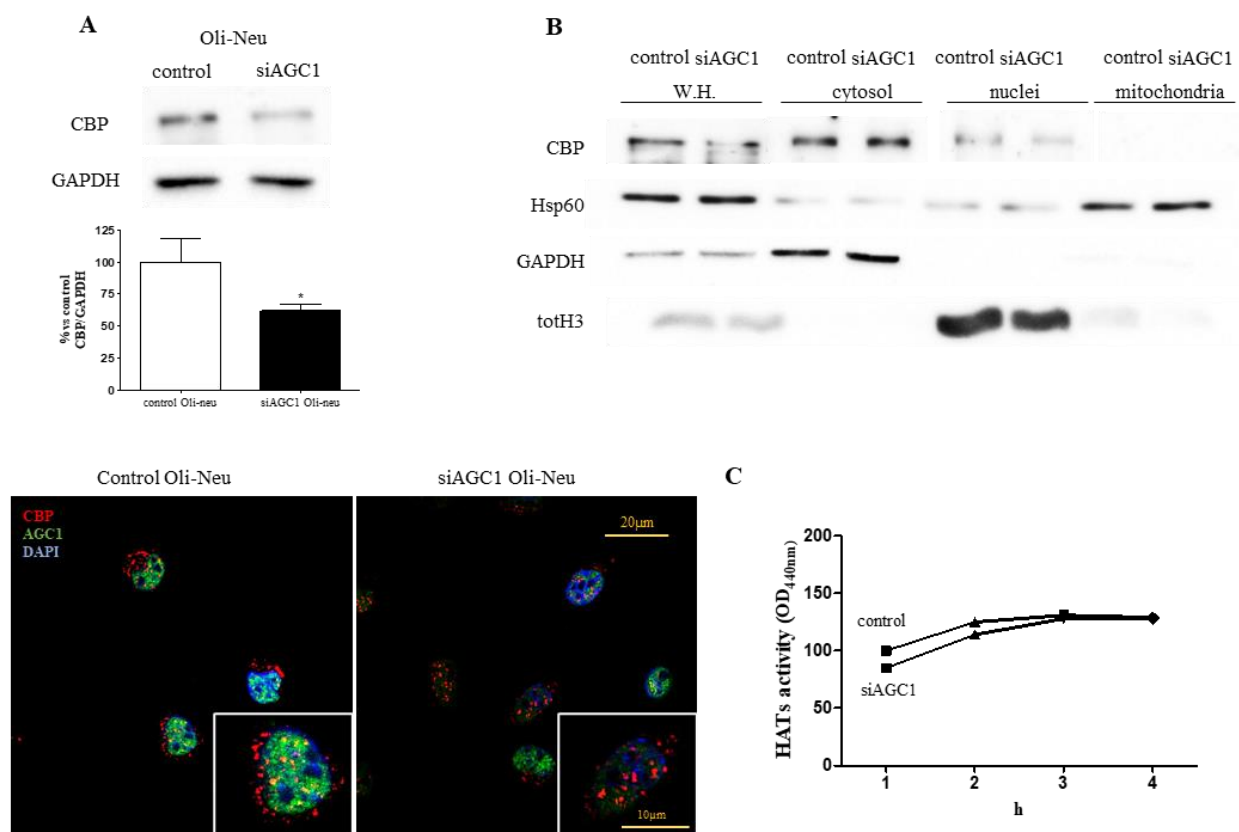
Figure 4.5. Western blot analysis, the relative densitometries and immunostainings (A), sub-cellular localization (B) and activity assay (C) of acetyltransferase in Oli-neu cells. (A) Densitometric analysis showed a reduction in CBP levels in siAGC1 Oli-Neu cells compared to controls; GAPDH was used for endogenous normalization. Values are mean ± SD of 3 independent experiments; * P <0.05, compared to control; t-test Student. Confocal microscopy images (100X) of CBP (green) and AGC1 (red); nuclei were labelled with DAPI. scale bar 20µm and 10µm. (B) CBP sub-cellular localization; HSP60, GAPDH and totH3 were used as mitochondrial, cytosolic and nuclear specific markers, respectively. (C) HAT colorimetric activity assay; acetylated substrates were quantified every hour. N=3.

Regarding histone de-acetylases expression, mixed results emerged from single isoforms analysis. HDACs 2 and 3, essential for repression of genes involved in neuronal and oligodendrocytic maturation (Ye *et al.*, 2009; Castelo-Branco *et al.*, 2014; Samudyata *et al.*, 2020), were significantly less expressed in siAGC1 Oli-neu cells compared to controls, whereas isoform 1 and 4 are only slightly affected by AGC1 silencing (Fig. 4.6A). Furthermore, the ability to produce de-acetylated nuclear extracts substrates turned out to be reduced in time (Fig. 4.6C), in according to the lower HDAC isoforms expression observed in siAGC1 Oli-neu cells. Finally, the sub-cellular localization of statistically significant enzymes was also analysed through Western Blot, however, no clear cytosolic or nuclear compartmental differences were detected (Fig.4.6B). Data on HAT/HDACs expression and localization were then confirmed by AGC1 co-immunostainings, where a reduced expression of CBP and HDAC isoforms 2/3 was observed based on fluorescence labelling (Figures 4.5 and 4.6). Therefore, an altered expression of histone de-acetylases, crucial to repress

transcriptional activators, and acetyltransferase CBP, whose activity is required to cell cycle progression, seems to affect AGC1 partially silenced Oli-neu cells.
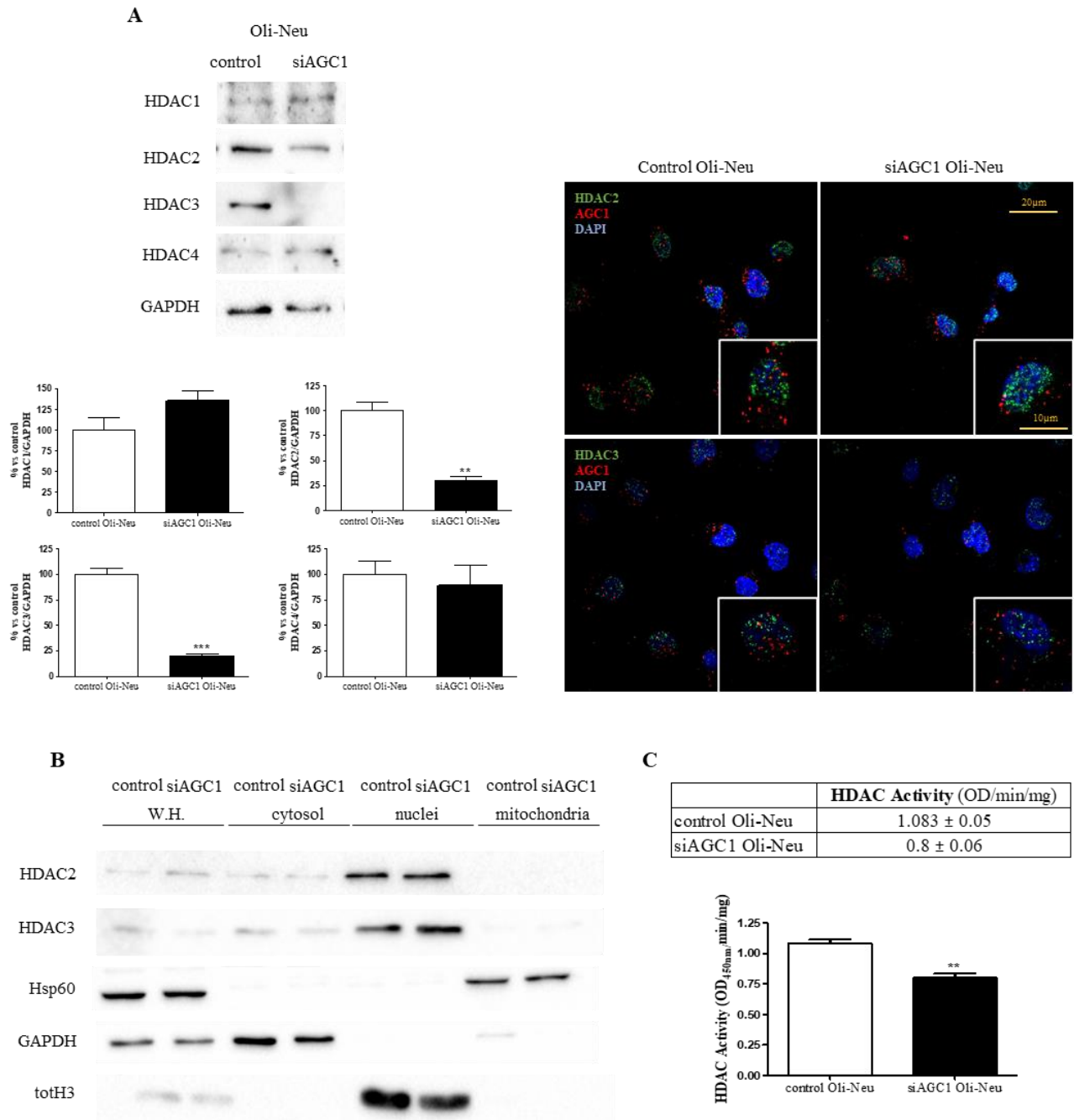

Figure 4.6. Western blot and the relative densitometries, as well as immunostainings (A), sub-cellular localization (B) and activity assay (C) of histone deacetylases on Oli-neu cells. (A) Densitometric analysis following western blot showed significant reduction in HDACs isoform 2 and 3 in siAGC1 Oli-Neu cells compared to controls; GAPDH was used for endogenous normalization. Values are mean ± SD of 3 independent experiments; *** P <0.001, ** P <0.01 compared to control; Student's t-test. Confocal microscopy images (100X) of HDAC2 and HDAC3 (green) and AGC1 (red); nuclei were labelled with DAPI. 20µM and 10µM scale bar. (B) Western blot analysis of HDACs sub-cellular localization after specific fractionation; HSP60, GAPDH and totH3 were used as mitochondrial, cytosolic and nuclear specific markers, respectively. (C) HDACs colorimetric activity assay; deacetylated substrates amount was quantified after one hour. HDACs activity mean ± SEM of control Oli-neu: 1.083±0.0535, Mean ± SEM of siAGC1 Oli-neu: 0.8000±0.0608, N=3. Difference between means 0.2830±0.04676.

Similar observations were made on AGC1$^{+/-}$ neurospheres, in which reduced levels of histone H3 pan-acetylation coinciding with histone H3 pan-methylation enhancement were detected (Fig. 4.7A), thus, suggesting, even in this model, an altered epigenetic profile. Expression of HDAC isoforms and acetyltransferase CBP, strictly involved in determining neural precursors cells (NPCs) commitment, were then analysed through Western Blot on spontaneously differentiated neurospheres. CBP, crucial for OPCs specification from NPCs through the direct binding to glial genes promoters (Wang *et al.*, 2010), significantly decreased in AGC1$^{+/-}$ neurospheres compared to controls (Fig. 4.7B), in line with the drop in OPCs content reported during AGC1$^{+/-}$ neurospheres differentiation. Concerning HDACs expression, as observed in Oli-neu cells, contrasting results were obtained from single isoforms analysis, probably due to the heterogeneity of neurospheres' cells pool and the cell-specific enzymes expression. HDAC 1 and 3 revealed to be significantly more expressed in AGC1$^{+/-}$ neurospheres, whereas isoform 2 and 4 acquired the opposite expression pattern, decreasing than in control ones (fig. 4.7C). Therefore, neurospheres derived from SVZ of AGC1$^{+/-}$ mice show differences in HAT and HDACs expression, which is essential in determining neural precursors cells fate.
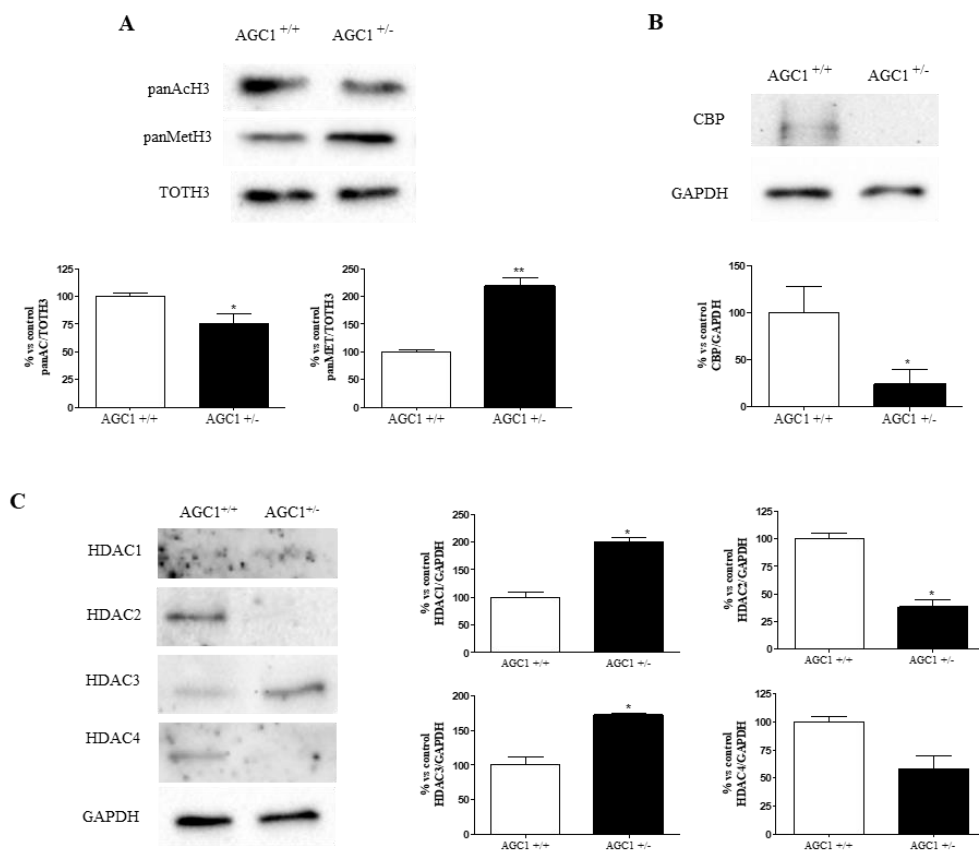

Figure 4.7. Western blot analysis and the relative densitometries of histone H3 post-translational modifications and HAT/HDACs expression on AGC1$^{+/-}$ and AGC1$^{+/+}$ spontaneously differentiated neurospheres. (A) Reduction in histone H3 pan-acetylation coincident with higher pan-methylation levels were detected in AGC1$^{+/-}$ neurospheres compared to AGC1$^{+/+}$ ones. (B-C) Decrease in HAT and HDAC isoforms 2 and 4, parallel to increase in isoform 1 and 3, was observed in AGC1$^{+/-}$ neurospheres compared to AGC1$^{+/+}$ ones indicating an altered epigenetic profile. GAPDH was used for endogenous normalizations. Values are mean ± SD of 3 independent experiments; ** P <0.01, * P <0.05, compared to control; Student's t-test.

4.3 HAT and HDACs inhibition on brain cells proliferation and differentiation

The altered histones acetylation pattern and HAT/HDACs expression profile, combined with the defects in proliferation/differentiation and cell fate acquirement previously reported in AGC1 deficiency models (Petralla *et.al*., 2019), prompted us to further study the biological role of HATs or HDACs enzymes. Therefore, to better understand the possible relation between histone acetylation, transcription factors expression and cells proliferation/differentiation, likewise their alteration in AGC1 deficiency, AGC1 partially silenced Oli-neu cells and AGC1$^{+/-}$ mice-derived neurospheres were treated with different concentrations of specific HATs or HDACs inhibitors. To reduce histone acetyltransferase activity, the natural compound Curcumin, a specific HAT p-300 activity inhibitor (Sunagawa *et al*., 2018) was used; to act on histone deacetylase enzymes, cells were treated with the general HDAC inhibitor Suberanilohydroxamic acid (SAHA; Zhou *et al*., 2011).

4.3.1   Curcumin-mediated HATs inhibition affects Oli-neu cells proliferation

To study whether inhibition of HATs activity, mainly CBP, could affect OPCs proliferation and differentiation, control and AGC1 partially silenced Oli-neu cells were treated with curcumin at different concentrations (10μM or 20μM, based on the toxicity results obtained by preliminary, not shown, MTT assay) for 24h or 48h depending on the analysis; DMSO was used as control. The treatment effect on histone post-translational modifications was verified through Western Blot on histone H3 pan-acetylation, which drastically decreased in control and siAGC1 Oli-neu cells compared to DMSO-treated controls (Fig. 4.10A). Cell count after immunostainings for the proliferation marker Ki67 was carried out to evaluate curcumin effect on Oli-neu cells proliferation. As shown in Figure 4.8, a significant reduction up to 50% of Ki67$^+$ cells was detected after 24h of treatment compared to DMSO-treated controls, with no differences between control and AGC1 partially silenced Oli-neu cells. Similar results were obtained from cell count analysis on optical microscope images; after 24h, reduced cell proliferation was detected in both control and siAGC1 Oli-neu cells, compared to DMSO-treated controls (data not shown) (Fig. 4.8).
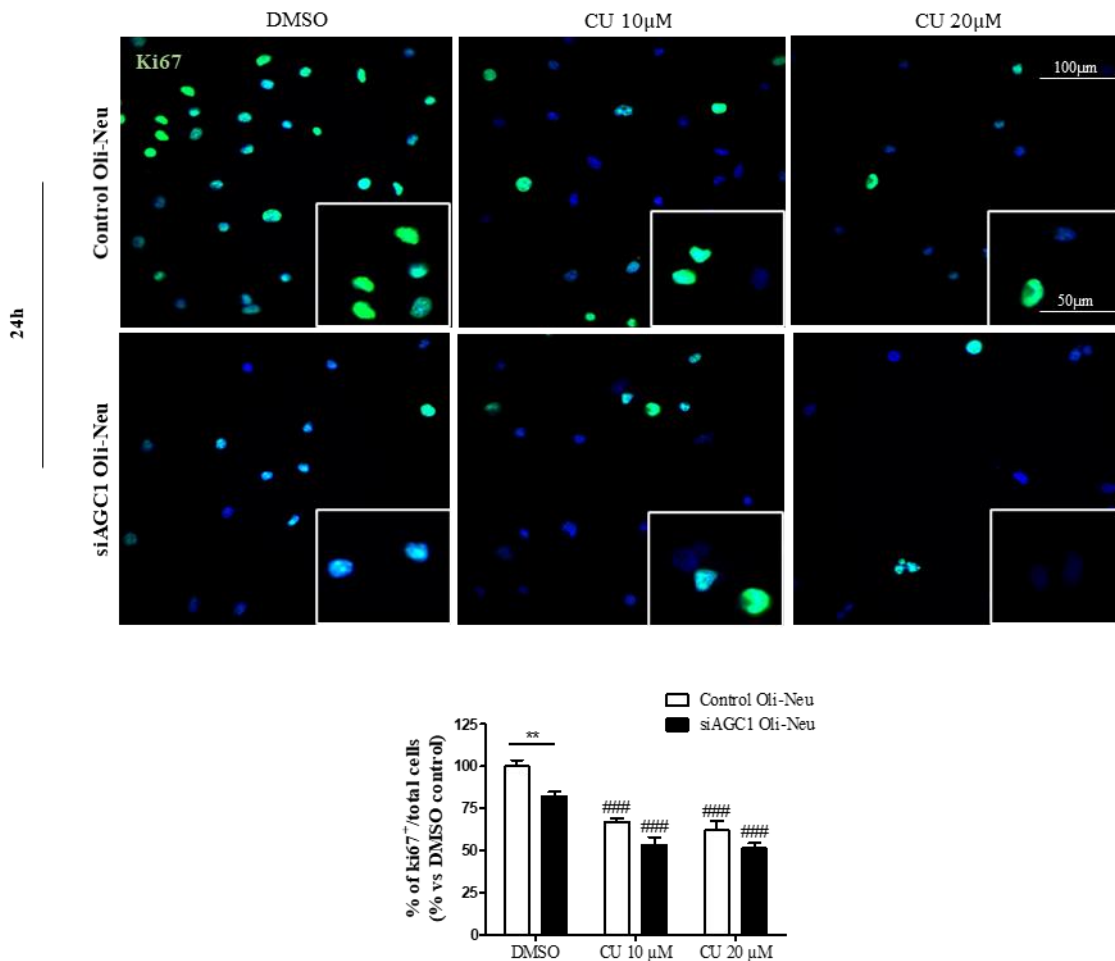
Figure 4.8. Immunostaining for Ki67 proliferation marker and cell counting of Ki67+ cells after 24h of HAT inhibition in control and siAGC1 Oli-neu cells. At 24h, reduction in proliferation was observed in both control and siAGC1 Oli-neu cells in presence of curcumin 10μM-20μM, more evident in control cells. Values are expressed as *ratio* of Ki67+ cells (green)/total cells; nuclei were labelled with DAPI. Values are mean ± SD of 3 independent experiments; 3 different fields were acquired for each condition. 40X objective; 100μm and 50μm bar scale. ### P <0.001, compared to DMSO control, respectively; ** P <0.01, compared to each treated control; two-way ANOVA (Bonferroni's post-hoc comparison test).

Subsequently, effects of CBP inhibition on Oli-neu cells differentiation were evaluated through morphology analysis; in this case, curcumin effect was evaluated not only after 24h of treatment, but also after 48h, as eventual differentiation induction requires a longer time compared to proliferation reduction. Filaments number and lengths, index of oligodendrocytes maturation, were counted and measured, respectively, on control and AGC1-silenced Oli-neu cells previously treated with the HAT inhibitor. From optical microscope images (Fig. 4.9A), after 48h treatment with curcumin 10μM cells appeared more elongated and branched, showing increase in both processes number and average length compared to DMSO-treated controls (Fig. 4.9B). By contrast, Oli-neu cells treated with higher concentration (20μM) showed reduction in cells number and almost total absence of filaments after 48h of culture, suggesting a potential toxicity of the inhibitor at long-time administration. For this

45

reason, statistical analysis and subsequent western blot and immunofluorescence analysis were performed only with the optimal curcumin concentration 10µM.
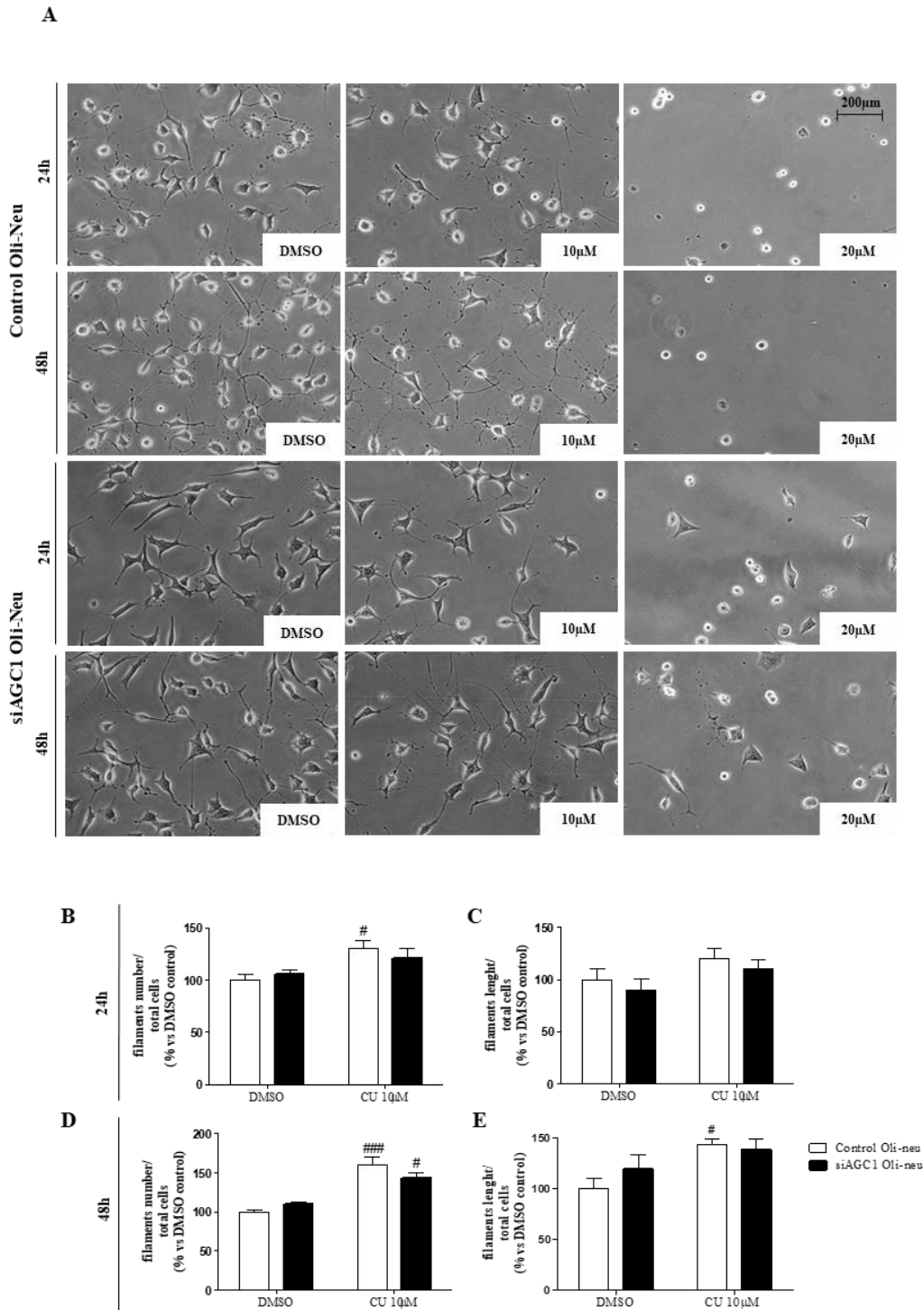

Figure 4.9. Optical microscope proliferation analysis in control and siAGC1 Oli-neu cells following 24h and 48h of treatment with curcumin 10µM and 20µM (A). Given the potential toxicity of curcumin 20µM, statistical analysis were executed only at 10µM (B). After 24h, slight, not significant increase in filaments number and average length was observed compared to DMSO controls, respectively. At 48h, a greater effect was obtained, in both control and siAGC1 Oli-neu cells compared to untreated controls, but more significant in control cells. Analysis were carried out with Fuji Imagej2 software. Values are mean ± SD of 3 independent experiments; 3 different fields were acquired for each condition. 20X objective; 200µm bar scale. ### $P < 0.001$, # $P < 0.05$, compared to DMSO control, respectively; two-way ANOVA (Bonferroni's post-hoc comparison test).

As reported previously, the effect of HATs inhibition on cells differentiation was also investigated through Western Blot. Expressions of OPCs-specific markers NG2 and Olig2, and the OPCs proliferation marker PDGFRα, as well as the mature oligodendrocytes marker CNPase, were analyzed on Oli-neu total protein extracts following DMSO or curcumin treatment. As regards precursors markers NG2, Olig2 and PDGFRα, expression dropped drastically up to 30% following CBP activity inhibition, in both control and siAGC1 Oli-neu compared to DMSO control (P <0.01). Interestingly, expression of differentiation marker CNPase increased after HAT inhibition exclusively in AGC1 silenced Oli-neu cells, already characterized by reduced levels of overall acetylation compared to control. The data were then confirmed by immunostainings, where only increase of CNPase$^+$ siAGC1 cells was observed, suggesting a primary effect on OPCs proliferation rather than differentiation following inhibition of acetyltransferases activity (Fig. 4.10). These data clearly indicate that HATs inhibition stimulates OPCs differentiation by arresting proliferation, and that this effect is more pronounced in the AGC1-deficiency cell model, in which HATs expression and activity are already reduced compared to controls.
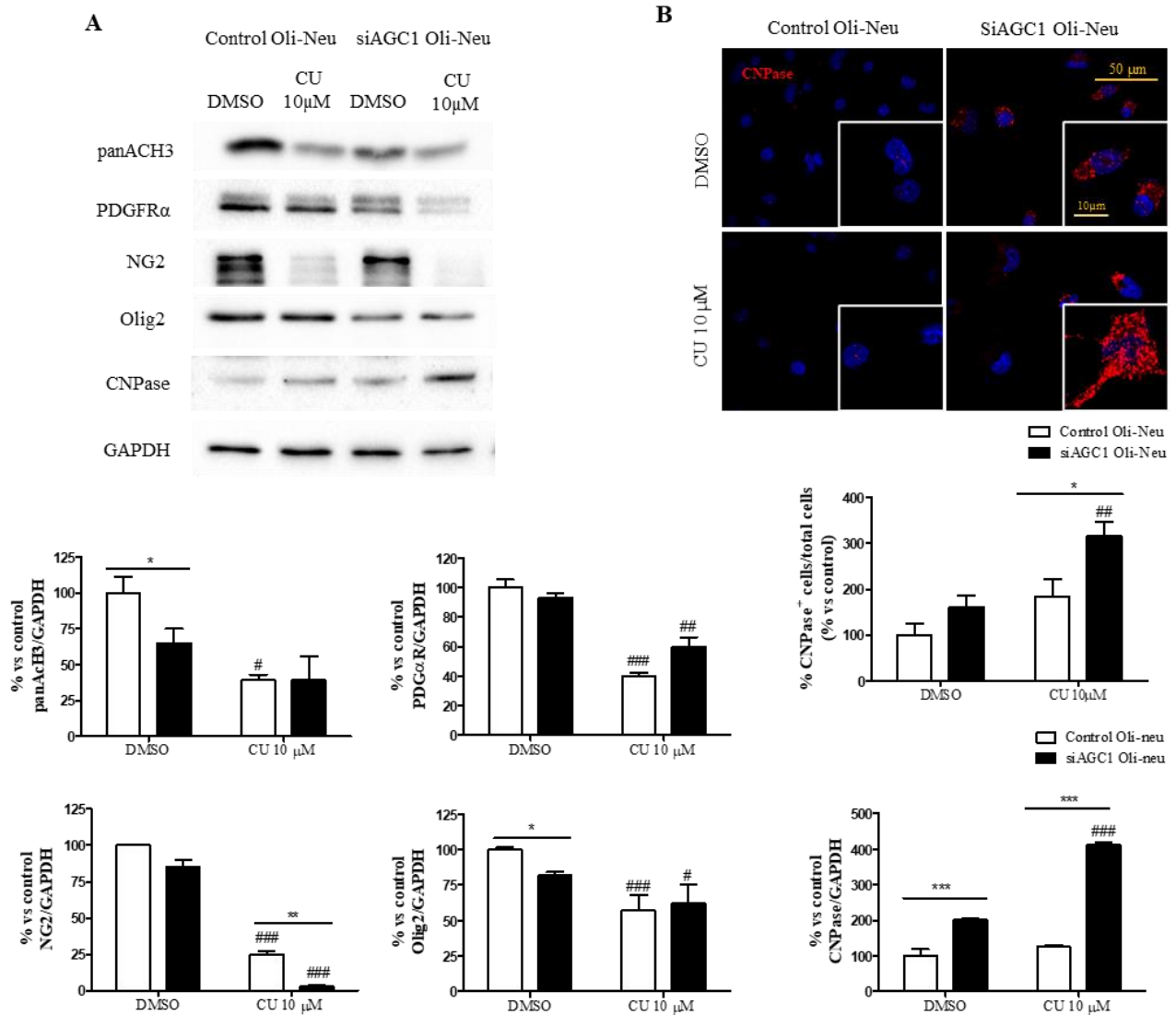
Figure 4.10. Western blot with the relative densitometries (A) and immunofluorescence analysis with cell counting (B) for proliferation/differentiation markers on control and siAGC1 Oli-neu cells following 48h HAT inhibition with curcumin 10µM. (A) Expression of OPCs markers (PDGFRα, NG2, Olig2) turned out drastically reduced in presence of curcumin 10µM in both siAGC1 and control Oli-neu cells, whereas evident increase in CNPase expression was detected only in AGC1 silenced Oli-neu cells. All variations were more evident in siAGC1 than in control cells. (B) Immunostainings and counting for CNPase+ cells; values are expressed as *ratio* of CNPase+ cells (red)/total cells; nuclei were labelled with DAPI. 3 different fields were acquired for each condition. Values are mean ± SD of 3 independent experiments. 40X objective; 50µm and 10µm bar scale. # P <0.05, ## P <0.01, ### P <0.001, compared to DMSO control, respectively; * P <0.05, ** P <0.01, *** P <0.001, compared to each treated control; two-way ANOVA (Bonferroni's post-hoc comparison test).

4.3.2 HDACs inhibition reduces proliferation and promotes differentiation in control and AGC1-silenced Oli-neu cells

To further investigate histone deacetylases role in OPCs proliferation and differentiation, selective inhibition of class 1 HDACs was carried out via SAHA administration (0.5µM or 1µM concentrations were selected for their lack of toxicity based on not published MTT assay) to control and AGC1

partially silenced Oli-neu cells; DMSO was used as control. The effect of SAHA treatment on HDACs activity was verified through Western Blot analysis on global histone H3 acetylation, which increased considerably in SAHA-treated cells compared to DMSO-treated ones (Fig. 4.103A). To evaluate effects of HDACs inhibition on Oli-neu cells proliferation, immunofluorescence analysis were then performed for Ki67 proliferation marker following 24h of SAHA treatment. The amount of Ki67$^+$ cells significantly decreased (P <0.01) in presence of SAHA (0.5μM and 1μM) compared to DMSO controls, with no little differences in proliferation effect between control and AGC1 partially silenced Oli-neu cells, being the latter ones more affected than the control cells (Fig. 4.11).
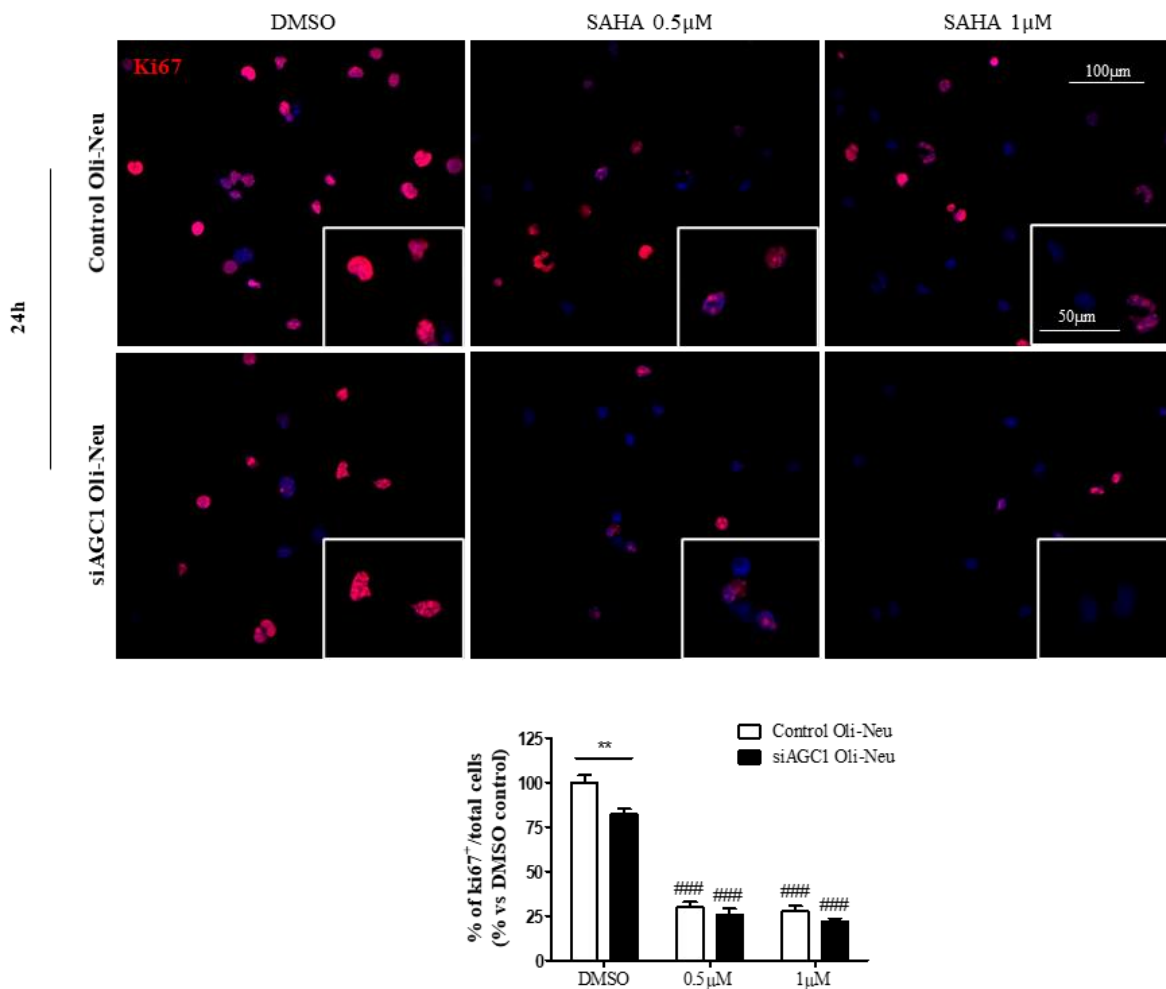
Figure 4.11. Immunostainings for Ki67 proliferation marker and counting of Ki67$^+$ cells in siAGC1 and control Oli-Neu cells after 24h of HDACs inhibition with SAHA 0.5 or 1.0μM. Significant reduction in proliferation was observed in both control and siAGC1 Oli-neu cells in presence of SAHA 0.5μM-1μM. Values are expressed as ratio of Ki67$^+$ cells (red)/total cells; nuclei were labelled with DAPI. Values are mean ± SD of 3 independent experiments; 3 different fields were acquired for each condition. 40X objective; 100μm and 50μm bar scale. ### P <0.001, compared to DMSO control, respectively; ** P <0.01, compared to each treated control; two-way ANOVA (Bonferroni's post-hoc comparison test).

Effect of HDACs inhibition on Oli-neu cells differentiation was then investigated by morphology analysis. After 24h of treatment, a significant difference between AGC1 partially silenced and control Oli-Neu cells was observed only with SAHA 1μM, which decreases filament number and increases their length in siAGC1 cells compared to control ones (Fig. 4.12B). More evident and significant results were obtained after 48h in presence of SAHA at the concentration of 0.5μM, which induces an increase in filament number as well as in filament length compared to DMSO controls. By contrast, no statistically significant differences were carried out between cells treated with DMSO or SAHA, after 24h of treatment (Fig. 4.12).
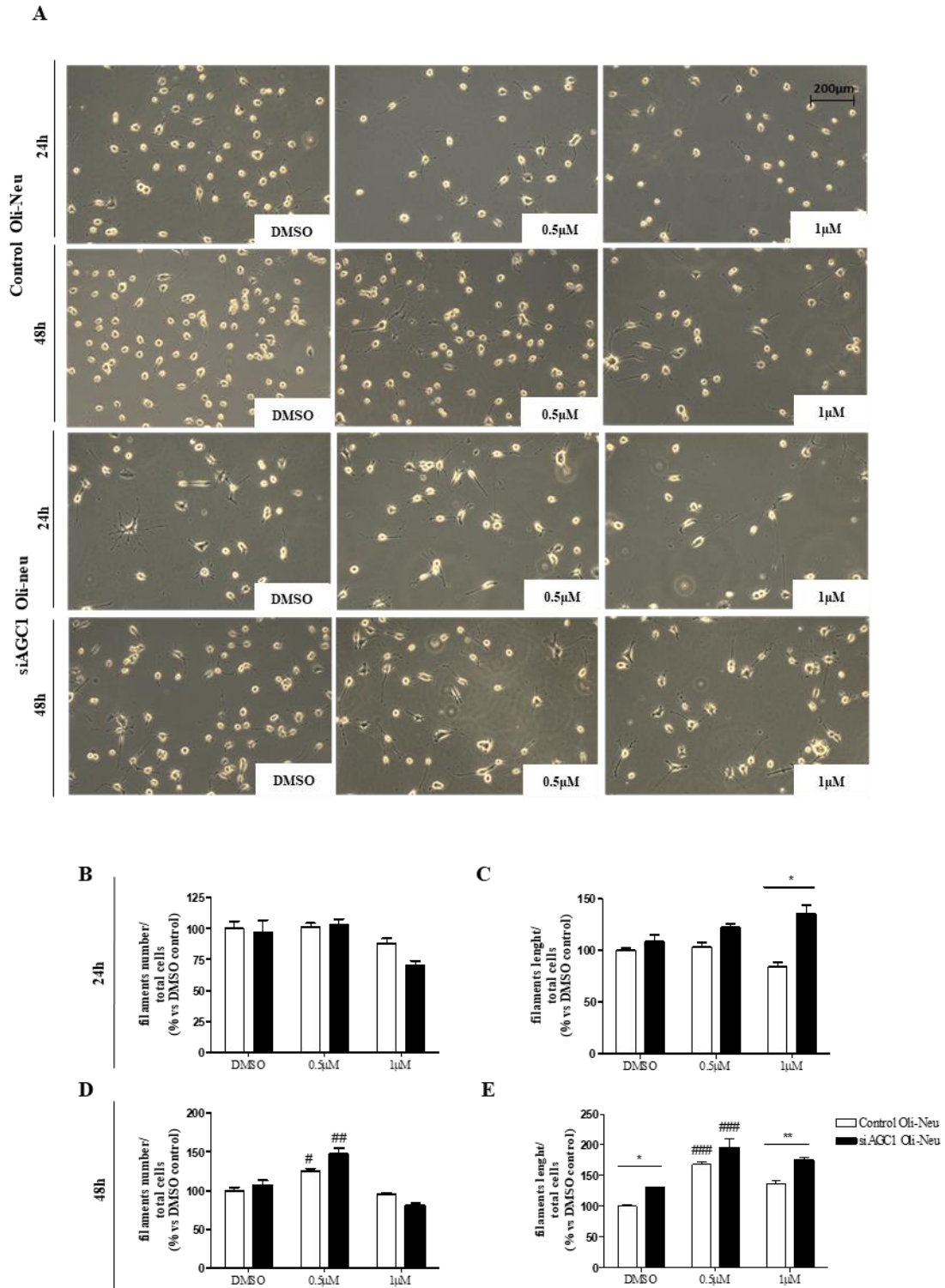
Figure 4.12. Optical microscope proliferation/differentiation analysis in siAGC1 and control Oli-Neu cells following 24h and 48h of SAHA treatment (A). At 48h, a greater increase in filaments number and average length was observed in presence of SAHA 0.5μM, in both control and siAGC1 Oli-neu cells compared to untreated controls. By contrast, no statistically significant differences were carried out after 24h of treatment (B). Analysis were carried out with Fuji Imagej2 software. Values are mean ± SD of 3 independent experiments; 3 different fields were acquired for each condition. 20X objective; 200μm bar scale. # P <0.05, ## P <0.01, ### P <0.001, compared to DMSO control, respectively; * P <0.05, ** P <0.01, compared to each treated control; two-way ANOVA (Bonferroni's post-hoc comparison test).

Oli-neu cells differentiation following HDACs inhibition was also evaluated by Western Blot and immunofluorescence analysis. After 48h of treatment, a significant increase in CNPase expression, as well as in CNPase^{+} cells number was observed, respectively, in both control and siAGC1 Oli-neu cells, suggesting a primary induction of oligodendrocytes maturation, besides decrease in proliferation. Effects of inhibition turned out more evident on AGC1-silenced Oli-neu cells than in control ones, in agreement with the proliferation defects and the early differentiation characterizing AGC1 deficiency *in vitro* models (Petralla *et al*., 2019) (Fig 4.13).
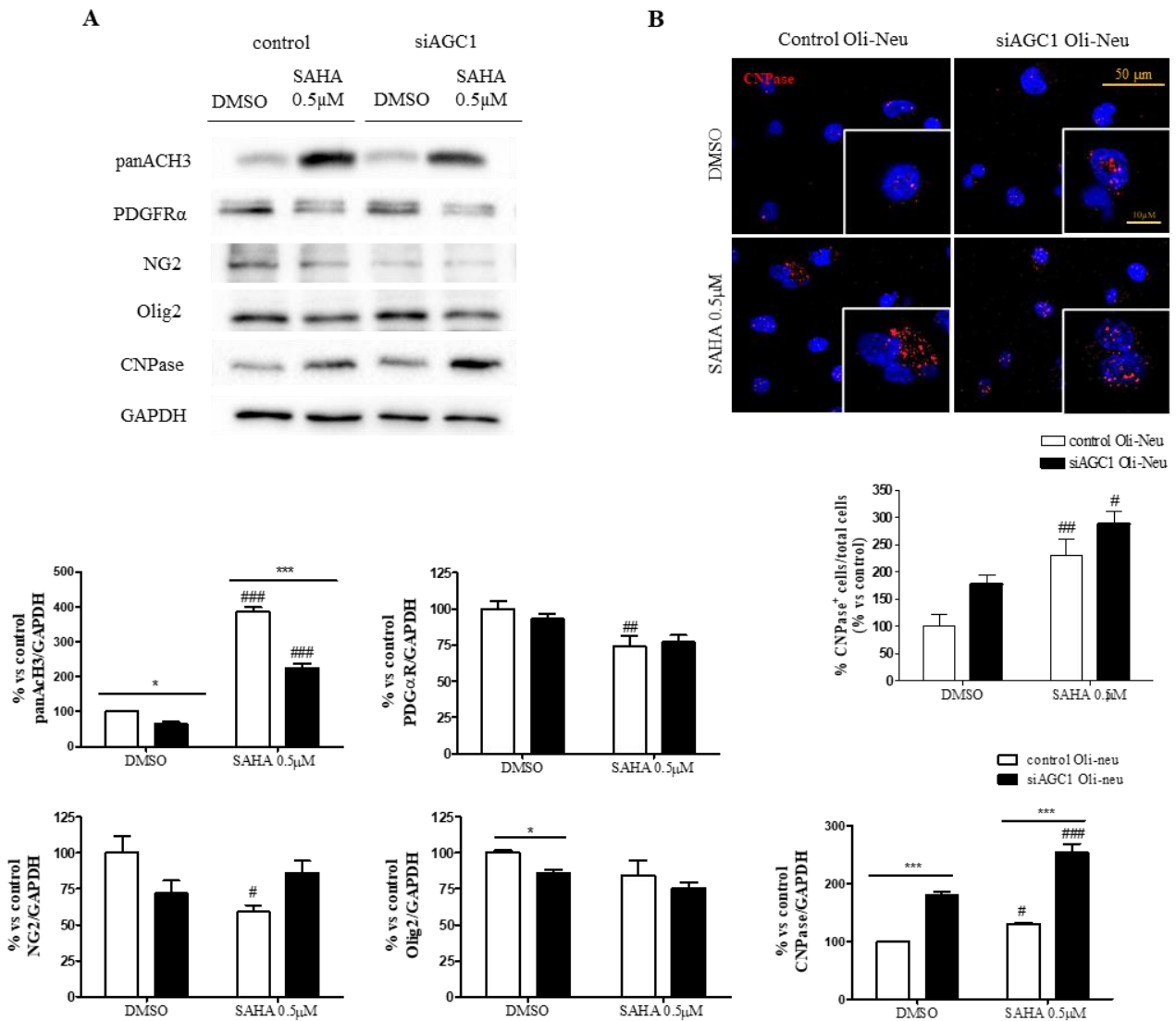

Figure 4.13. Western blot with the relative densitometries (A) and immunofluorescence analysis with cell counting (B) for proliferation/differentiation markers on control and siAGC1 Oli-neu cells following 48h HDACs inhibition with SAHA 0.5μM. (A) Expression of OPCs markers (PDGFRα, NG2, Olig2) decreased in presence of SAHA 0.5μM in control Oli-neu cells, but not in siAGC1 cells, whereas evident variations in CNPase expression were detected in both control and siAGC1 Oli-neu cells. (B) Immunostainings for CNPase and counting of CNPase^{+} cells in control and siAGC1 Oli-Neu cells following 48h treatment with SAHA 0.5μM; values are expressed as ratio of CNPase^{+} cells (red)/total cells; nuclei were labelled with DAPI. 3 different fields were acquired for each condition. 40X objective; 100μM bar scale. Values are mean ± SD of 3 independent experiments. # $P < 0.05$, ## $P < 0.01$, ### $P < 0.001$, compared to DMSO control, respectively; *** $P < 0.001$, compared to each treated control; two-way ANOVA (Bonferroni's post-hoc comparison test).

4.3.3   HATs inhibition on neurospheres proliferation and differentiation

The results obtained on HAT/HDACs inhibition on Oli-neu cells cultures, prompted us to investigate their effect on AGC1$^{+/+}$ and AGC1$^{+/-}$ mice-derived neurospheres too. To this aim, neural precursors cells (NPCs) were grown in suspension or induced to differentiate as cell-monolayer in presence of DMSO, as control, or p300/CBP inhibitor curcumin (5μM or 10μM): the effective decrease in global histone H3 acetylation was then verified by Western Blot analysis, especially at 10μM (Fig 4.15). As proliferation indicators, spheres number and average diameter were evaluated by optical microscope observation after 7 days of spontaneous differentiation in culture. As shown in Fig. 4.14, both AGC1$^{+/+}$ and AGC1$^{+/-}$ curcumin-treated neurospheres appeared significantly smaller compared to DMSO controls. Interestingly, while WT-derived neurospheres presented an increase in spheres number concomitant to reduction in average size, the opposite outcome was observed in AGC1$^{+/-}$ ones, whose number decreased following curcumin administration, suggesting an earlier arrest of proliferation due to acetyltransferases inhibition (Fig 4.14B).
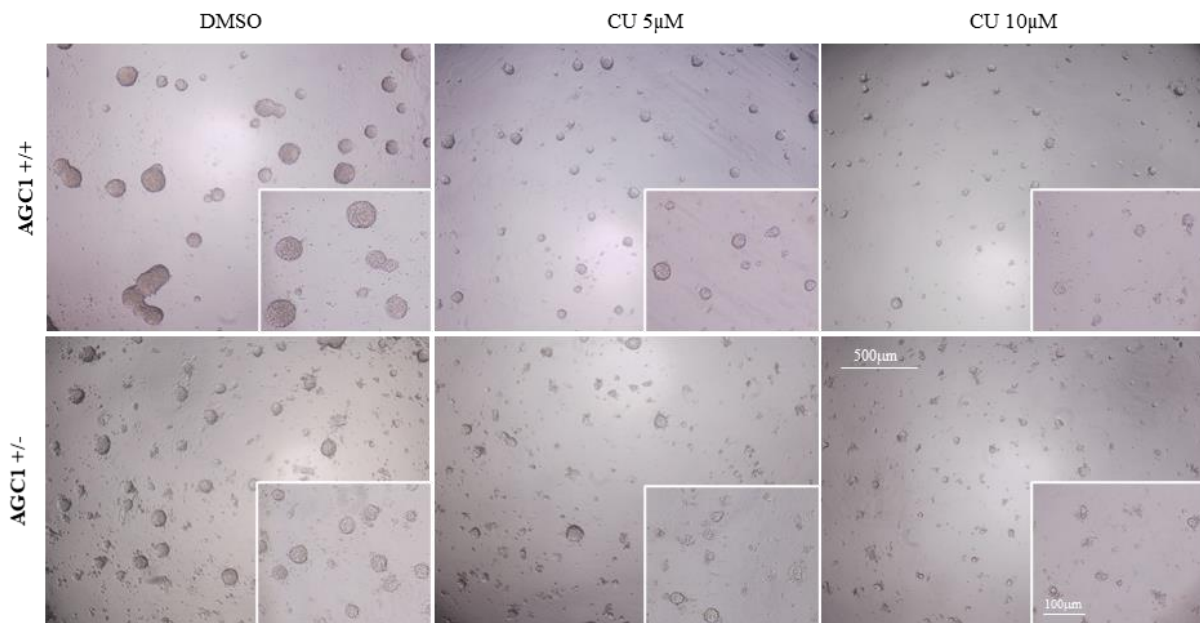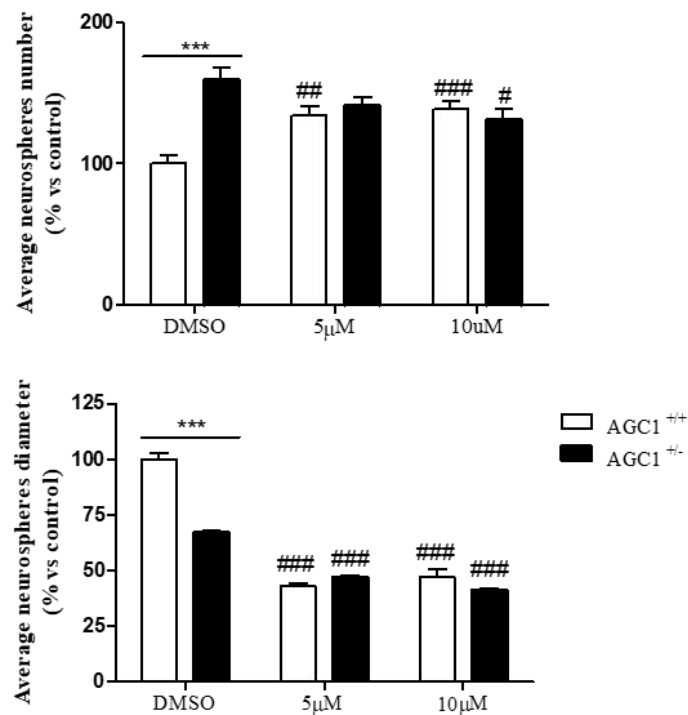
Figure 4.14. Optical microscope images of floating neurospheres after 7 days of culture in presence of curcumin 5 µM and 10 µM (A) and counting of their number and diameter (B) WT-derived neurospheres presented an increase in spheres number concomitant to reduction in average size, the opposite outcome was observed in AGC1+/- ones, whose number decreased following curcumin administration. Average number and size were measured with Fuji Imagej2 software using an automated colony and cell counting method, and only aggregates bigger than 400µm² were considered. Values are mean ± SD of 5 different fields acquired for each condition. 10X objective; 500µM and 100µM bar scale. # P <0.05, ## P <0.01, ### P <0.001, compared to DMSO control, respectively; *** P <0.001, compared to each treated control; two-way ANOVA (Bonferroni's post-hoc comparison test).

Western blot analysis (Fig. 4.15) and immunofluorescence (Fig. 4.16) for specific cell markers were then carried out to understand alterations on neural progenitors' differentiation induced by HATs inhibition. The OPCs marker Olig2, as well as the newly born and immature neurons marker DCX, which are respectively less expressed and more expressed in AGC1$^{+/-}$ neurospheres compared to WT ones, thus indicating a reduction in OPCs and an increase in neuronal progenitors commitment due to the AGC1 reduction, showed no significant alteration following curcumin treatment in both AGC1$^{+/+}$ and AGC1$^{+/-}$ neurospheres. By contrast, both the mature oligodendrocytes marker CNPase and the astrocytes-specific marker GFAP, which are significantly augmented in AGC1$^{+/-}$ neurospheres compared to WT ones, thus indicating that a deficit in the mitochondrial carrier AGC1 determines a switch in NSCs differentiation towards oligodendrocytes and astrocytes, showed a significant decrease following curcumin inhibition compared to DMSO controls. These data indicate an effect of acetyltransferases inhibition on neural progenitors' glial differentiation commitment.
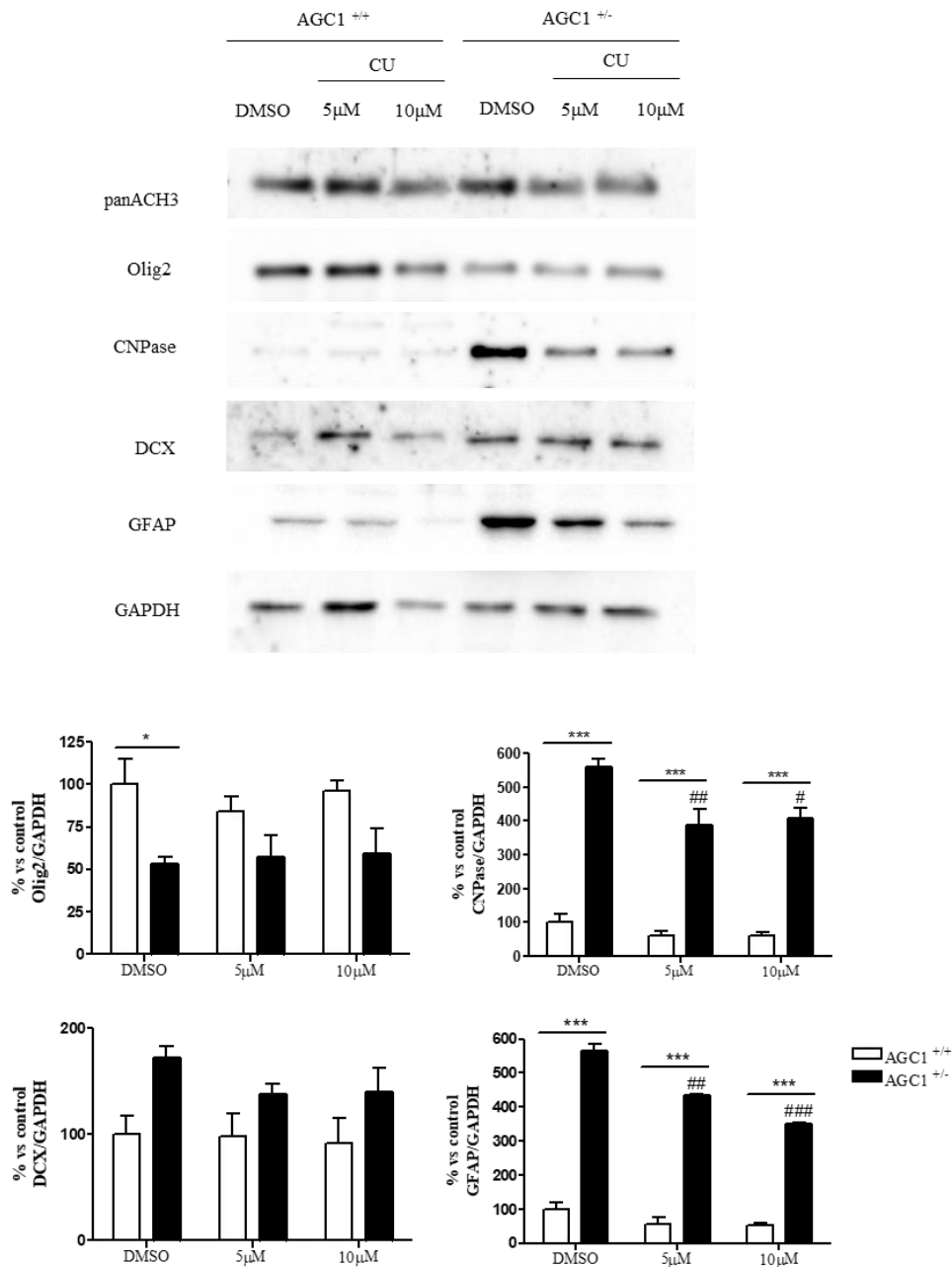
Figure 4.15. Western blot for proliferation/differentiation markers in AGC1^{+/+} and AGC1^{+/-} differentiated neurospheres following HAT inhibition with curcumin 5 and 10μM. Expression of mature oligodendrocytes marker CNPase and astrocytes-specific marker GFAP, both strongly up-regulated in AGC1^{+/-} neurospheres compares to control ones, drastically decreased in presence of curcumin, suggesting inhibition on neural progenitors' glial differentiation commitment. By contrast, Olig2, marker of OPCs, and DCX, marker of neural progenitors, do not show any significant change in both conditions in AGC1^{+/+} and AGC1^{+/-} differentiated neurospheres after curcumin treatment. Values are mean ± SD of 3 independent experiments. # P <0.05, ## P <0.01, ### P <0.001, compared to DMSO control, respectively; * P <0.05, *** P <0.001, compared to each treated control; two-way ANOVA (Bonferroni's post-hoc comparison test).
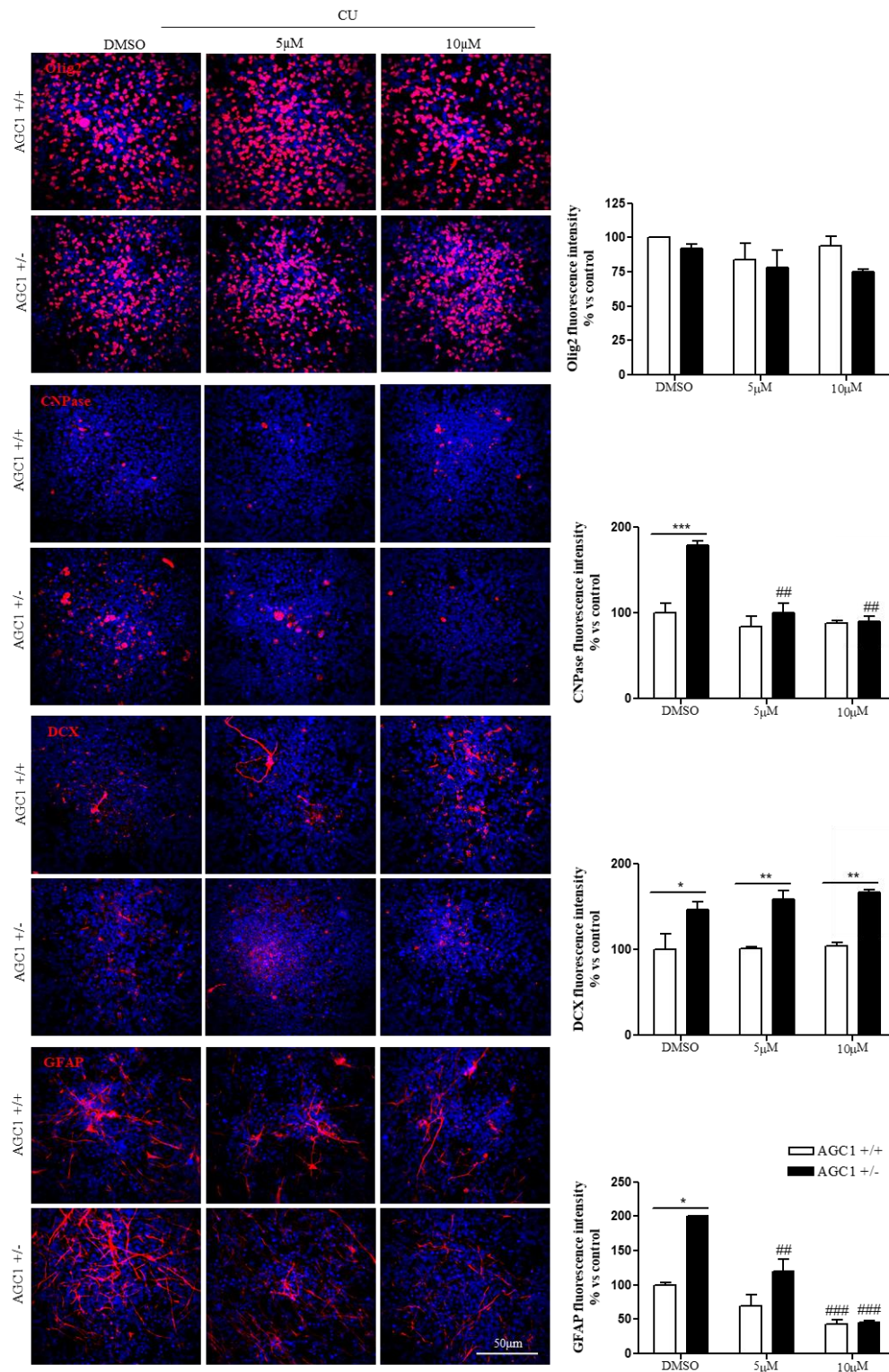
Figure 4.16. Immunofluorescence analysis and cell counting for proliferation/differentiation markers on AGC1$^{+/+}$ and AGC1$^{+/-}$ 7DIV spontaneously differentiated neurospheres following HAT inhibition with curcumin 5 and 10μM. Olig2 does not show any significant difference with treatment, as well as DCX$^+$ cells number, which is significantly higher in AGC1$^{+/-}$ neurospheres compared to controls in all conditions. CNPase$^+$ and GFAP$^+$ cells, both present in higher number in AGC1$^{+/-}$ neurospheres than in control ones, significantly decrease following curcumin treatments. Values are mean ± SD of 3 different fields acquired for each condition. ## P <0.01, ### P <0.001, compared to DMSO control, respectively; * P <0.05, ** P <0.01, *** P <0.001, compared to each treated control; two-way ANOVA (Bonferroni's post-hoc comparison test).

4.3.4 HDACs inhibition on neurospheres proliferation and differentiation

Effects of HDACs inhibition on AGC1$^{+/+}$ and AGC1$^{+/-}$ neurospheres proliferation and differentiation were further investigated by SAHA (Suberanilohydroxamic acid) administration. Firstly, the increase of histone H3 pan-acetylation levels following SAHA treatment were verified through Western blot (Fig. 4.18). By optical microscope images, number and average size of neurospheres were evaluated following 7 day in culture in presence of SAHA (0.5µM or 1µM) or DMSO (negative control). As shown in Fig. 4.17, a significant increase in spheres number and a parallel reduction in their average size were observed in both AGC1$^{+/+}$ and AGC1$^{+/-}$ proliferating progenitors following HDACs inhibition, thus suggesting that HDACs inhibition induces a general decrease in proliferation, with consequent loss of ability to acquire the typical shape of sphere, with a parallel increase in differentiation. The SAHA effect is less evident in AGC1$^{+/-}$ neurospheres, which already show a decrease in proliferation and a pronounced spontaneous differentiation compared to control ones, probably related to the decrease in HDACs expression due to the reduction of AGC1.

A
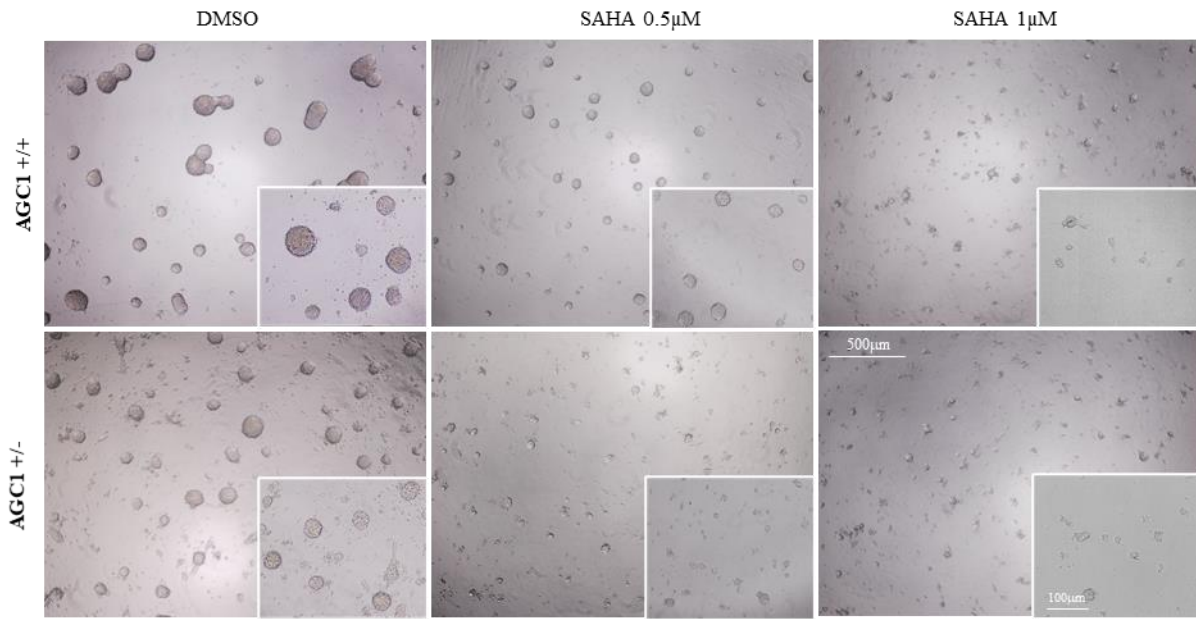
B
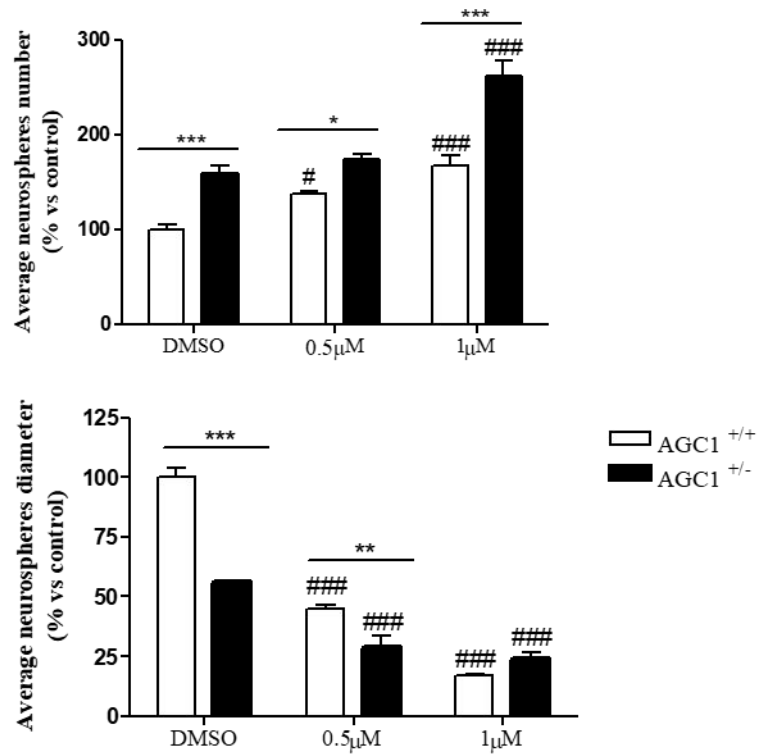
Figure 4.17. Optical microscope images of floating neurospheres after 7 days of culture in presence of SAHA 0.5 µM and 1 µM (A) and counting of their number and diameter (B) Both WT and AGC1^{+/-} derived neurospheres presented an increase in spheres number concomitant to reduction in average size following SAHA administration. Average number and size were measured with Fuji Imagej2 software using an automated colony and cell counting method, and only aggregates bigger than 400µm^2 were considered. Values are mean ± SD of 5 different fields acquired for each condition. 10X objective; 500µM and 100µM bar scale. # P <0.05, ### P <0.001, compared to DMSO control, respectively; * P <0.05, ** P <0.01, *** P <0.001, compared to each treated control; two-way ANOVA (Bonferroni's post-hoc comparison test).

59

HDACs inhibition on brain precursor cells' differentiation was then investigated by Western Blot (Fig. 4.18) and immunofluorescence analysis (Fig. 4.19). Olig2, marker of OPCs, and DCX, neuronal progenitors' marker, which are respectively less expressed and more expressed in AGC1$^{+/-}$ neurospheres compared to WT ones, thus indicating a reduction in OPCs and an increase in neuronal progenitors commitment due to the AGC1 reduction, showed no relevant differences following SAHA administration, in both AGC1$^{+/+}$ and AGC1$^{+/-}$ neurospheres compared to DMSO controls, similarly to what previously observed with the curcumin treatment. Differently, both CNPase, marker of mature oligodendrocytes, and GFAP, astrocytes marker, which are both strongly up-regulated in AGC1$^{+/-}$ neurospheres compared to control ones, thus indicating a switch of brain cells progenitors towards mature glial cells sue to AGC1 reduction, showed a significant reduction their levels in SAHA-treated AGC1$^{+/-}$ neurospheres only. These data therefore suggest an arrest in oligodendrocytes and astrocytes spontaneous differentiation following histone de-acetylases activity inhibition. Interestingly, the greater effect was observed concerning GFAP (astrocytes marker) expression, which dropped drastically in AGC1$^{+/-}$ neurospheres with SAHA at low concentrations (0.5µM), suggesting a significant impairment in astrocytes differentiation commitment.
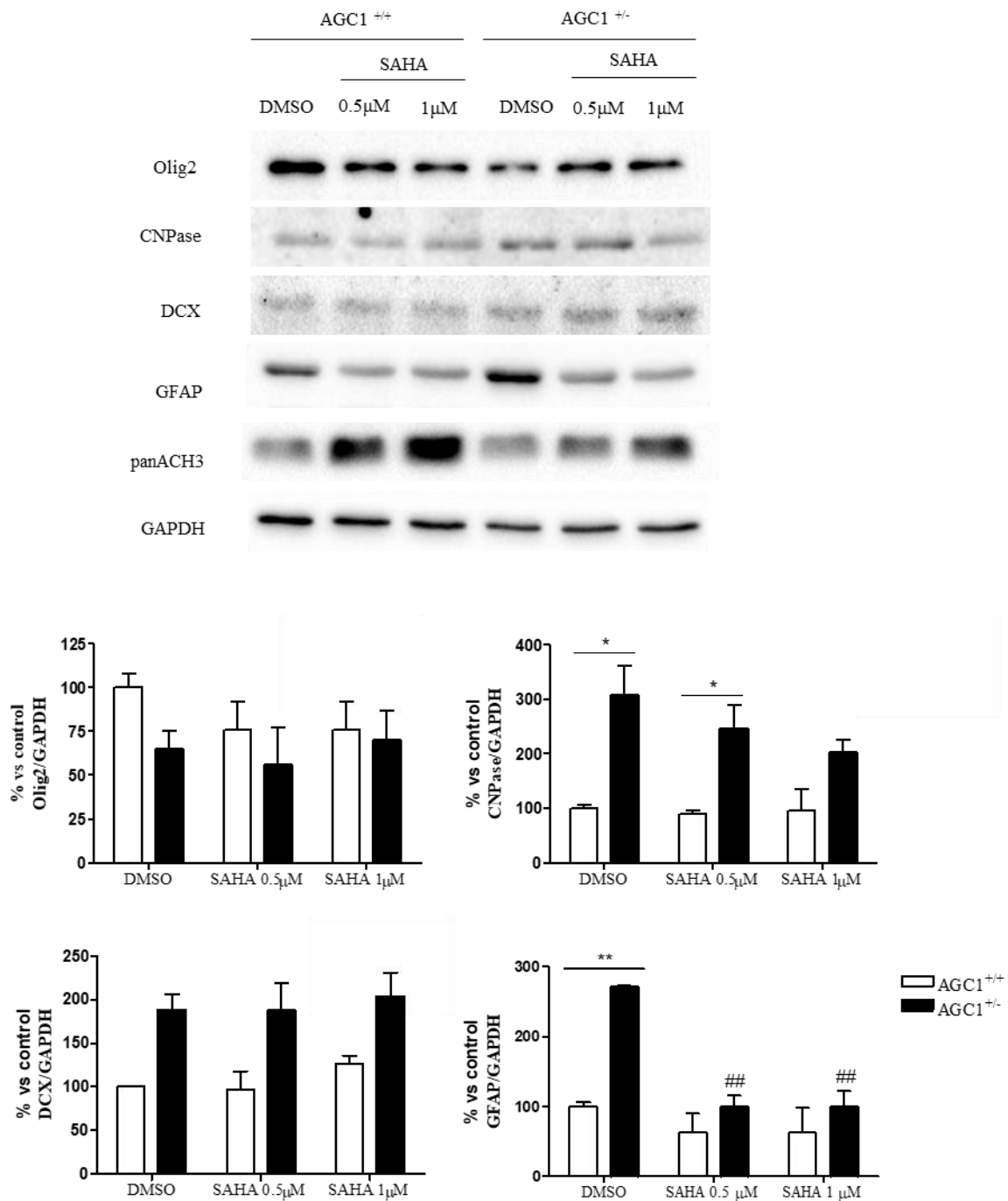
Figure 4.18. Western blot for proliferation/differentiation markers in AGC1^{+/+} and AGC1^{+/-} differentiated neurospheres following HDACs inhibition with SAHA 0.5 and 1μM. Expression of astrocytes-specific marker GFAP, strongly up-regulated in AGC1^{+/-} neurospheres compares to control ones, drastically decreased in presence of SAHA, suggesting inhibition on neural progenitors astrocytic differentiation commitment. By contrast, Olig2, marker of OPCs, and DCX, marker of neural progenitors, do not show any significant change in both conditions after curcumin treatment. Values are mean ± SD of 3 independent experiments. ## P <0.01, compared to DMSO control, respectively; * P <0.05, ** P <0.01, compared to each treated control; two-way ANOVA (Bonferroni's post-hoc comparison test).
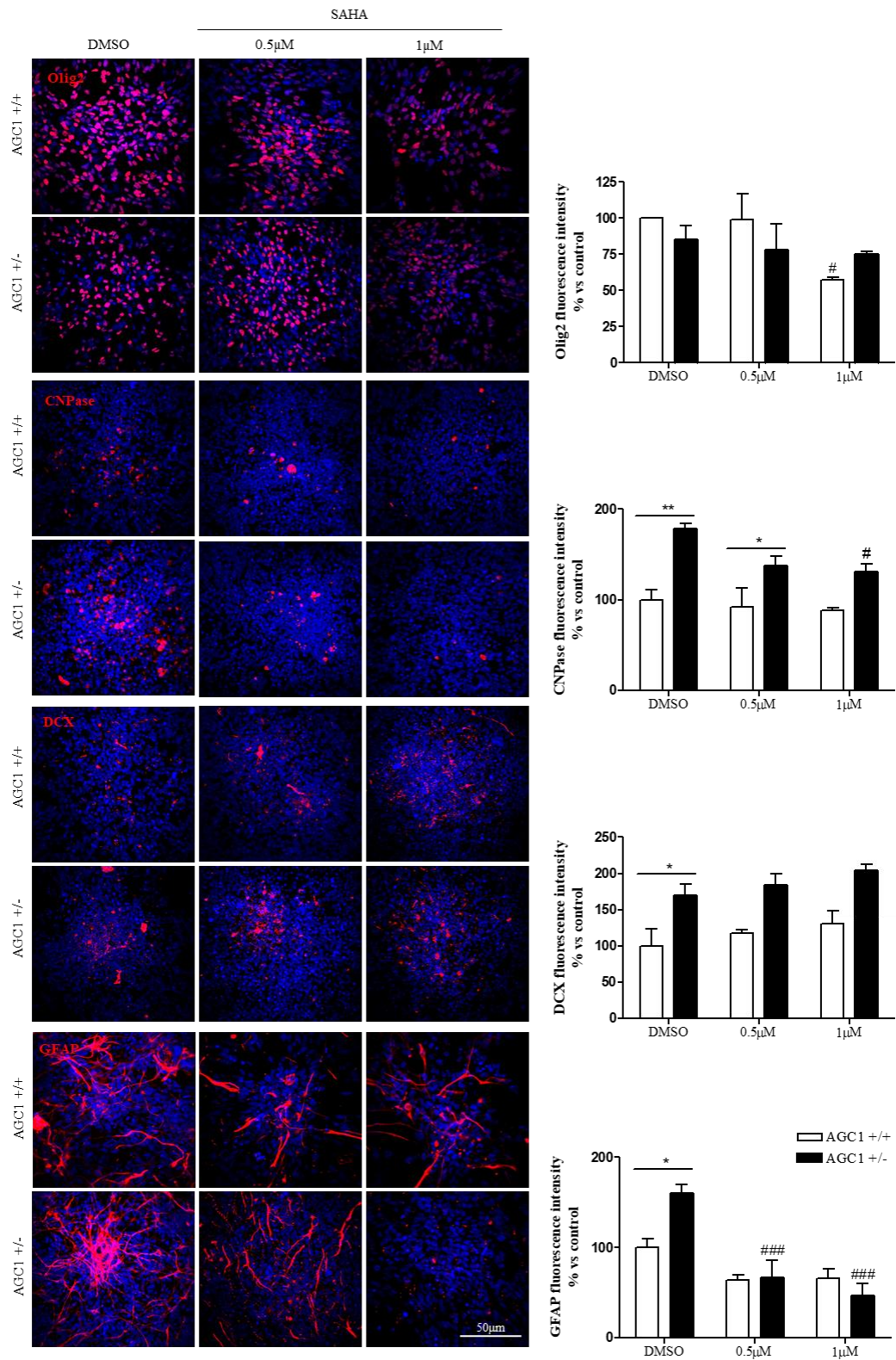
Figure 4.19. Immunofluorescence analysis and cell counting for proliferation/differentiation markers on AGC1^{+/+} and AGC1^{+/-} 7DIV spontaneously differentiated neurospheres following HDACs inhibition with SAHA 0.5 and 1μM. Olig2 does not show consistent expression variations with treatment, as well as DCX^{+} cells number, which is significantly higher in AGC1^{+/-} neurospheres compared to controls in all conditions. CNPase[+] and GFAP^{+} cells, both present in higher number in AGC1^{+/-} neurospheres than in control ones, significantly decrease following SAHA treatments, with greater effect on expression of the astrocytes-specific marker. Values are mean ± SD of 3 different fields acquired for each condition. # P <0.5, ### P <0.001, compared to DMSO control, respectively; * P <0.05, ** P <0.01, compared to each treated control; two-way ANOVA (Bonferroni's post-hoc comparison test).

4.4 Transcription factors and HDACs interactions: preliminary results in the AGC1 deficiency Oli-Neu cell model

To better understand the altered regulation of cells proliferation and differentiation, we subsequently investigate the possible interaction between transcription factors and HDACs in order to observe whether their alteration could play a role in AGC1 deficiency. Given the significant decrease (about 70%) in c-Myc levels and the reduction of the binding partner MAX previously observed in siAGC1 Oli-neu cells compared to controls, we first verified in Oli-Neu cells their well-known interaction. Immunoprecipitation experiments were conducted on total cell lysates, followed by proteins resolution on SDS-page and immunoblot (fig. 4.20). As expected, co-immunoprecipitation of c-Myc/MAX turned out evident, proving their effective interaction in both control and AGC1 partially silenced Oli-Neu cells. Subsequently, since recent evidences reported a functional significant interplay between c-Myc and HDAC isoform 2, which acts as c-Myc cofactor to define its transcriptional profile (Northcott *et al.*, 2017), co-immunoprecipitations were also performed to verify their interaction. Their interaction was confirmed by co-immunoprecipitations c-Myc/HDAC2 and HDAC2/c-Myc, respectively, in both control and siAGC1 Oli-neu cells (Fig. 4.20). Interestingly, c-Myc/HDAC2 complex has been reported to be found in correspondence of most c-Myc binding sites, and only a small amount of c-Myc without HDAC2 to DNA has been detected. Moreover, inhibition of class I HDAC leads to the stabilization and reduced c-Myc DNA binding, inducing a downregulation of c-Myc dependent genes and activation of those repressed (Ecker *et al.*, 2020).
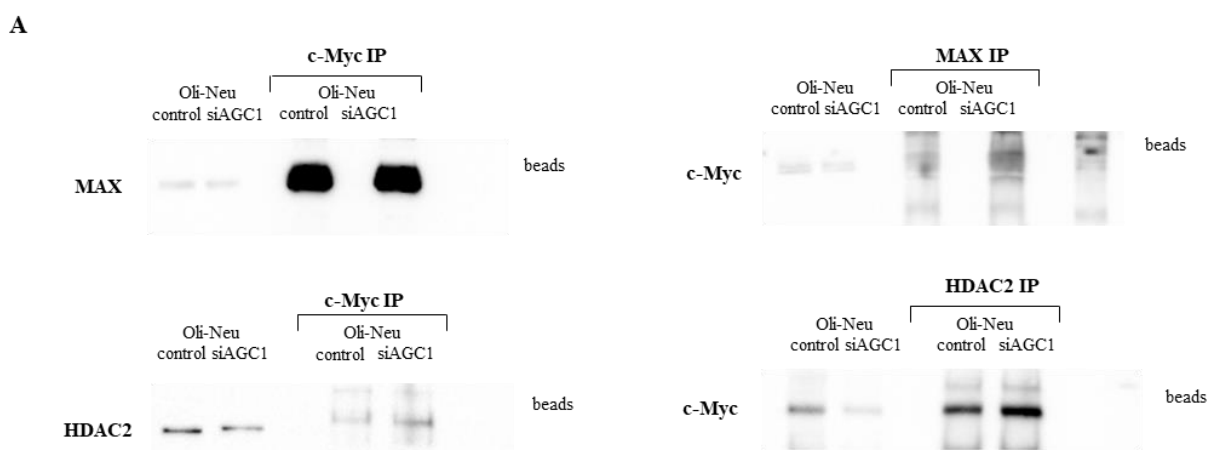

Figure 4.20. Immunoprecipitation experiments performed on total extracts from control and siAGC1 Oli-Neu. c-Myc, co-factor MAX and HDAC isoform 2 interactions were analyzed through immunoprecipitation followed by reciprocal Western Blot analysis. Non-immunoprecipitated samples were used as positive control, agarose beads and normal IgG (not shown) were loaded as negative control.

Prior data from our group surprisingly reported localization of mitochondrial carrier AGC1 also in nuclear compartment (data not published); in this sense, fractionation experiments were then carried out aimed to verify the sub-cellular localization of AGC1 in control and AGC1-partially silenced Oli-Neu cells. Cytosolic, mitochondrial fractions and nuclear extracts were resolved in SDS-page and analysed by immunoblot; total protein lysates were used as control. As shown by Western Blot (Fig. 4.21A), AGC1 expression was detected not only in mitochondria, but also in nuclei, then confirmed through immunostainings (Fig. 4.21B). Subsequently, to better understand the functional role of AGC1 nuclear localization, eventual interplays with transcription factors were further investigated. Immunoprecipitation experiments were conducted to clarify whether AGC1 may be part of cMyc-HDAC2-AGC1 or cMyc-MAX-AGC1 complexes. While a possible AGC1-Myc and AGC1-MAX interaction was found in both control and siAGC1 Oli-Neu (Fig. 4.21C), no AGC1-HDAC2 interactions were detected (data not shown). However, these results are preliminary and need further confirmations. At the moment, bioinformatics cross analyzes using publicly accessible tools (iLoc Animal, SCLpredT, Euk-mPLoc 2.0) predict AGC1 localization not only in the mitochondrial compartment, but also in the nuclear and cytosolic one. Indeed, immunostainings on A-431 (skin cells), U-2 OS (osteosarcoma) and U-251 MG (glioblastoma) for both AGC isoforms highlighted AGC1 localization also in nucleus and cytosol, unlike AGC2, which confirmed an exclusively mitochondrial localization (in collaboration with Prof. Giorgi F., Dott. Balboni N., University of Bologna, Italy) (Fig. 4.21D).
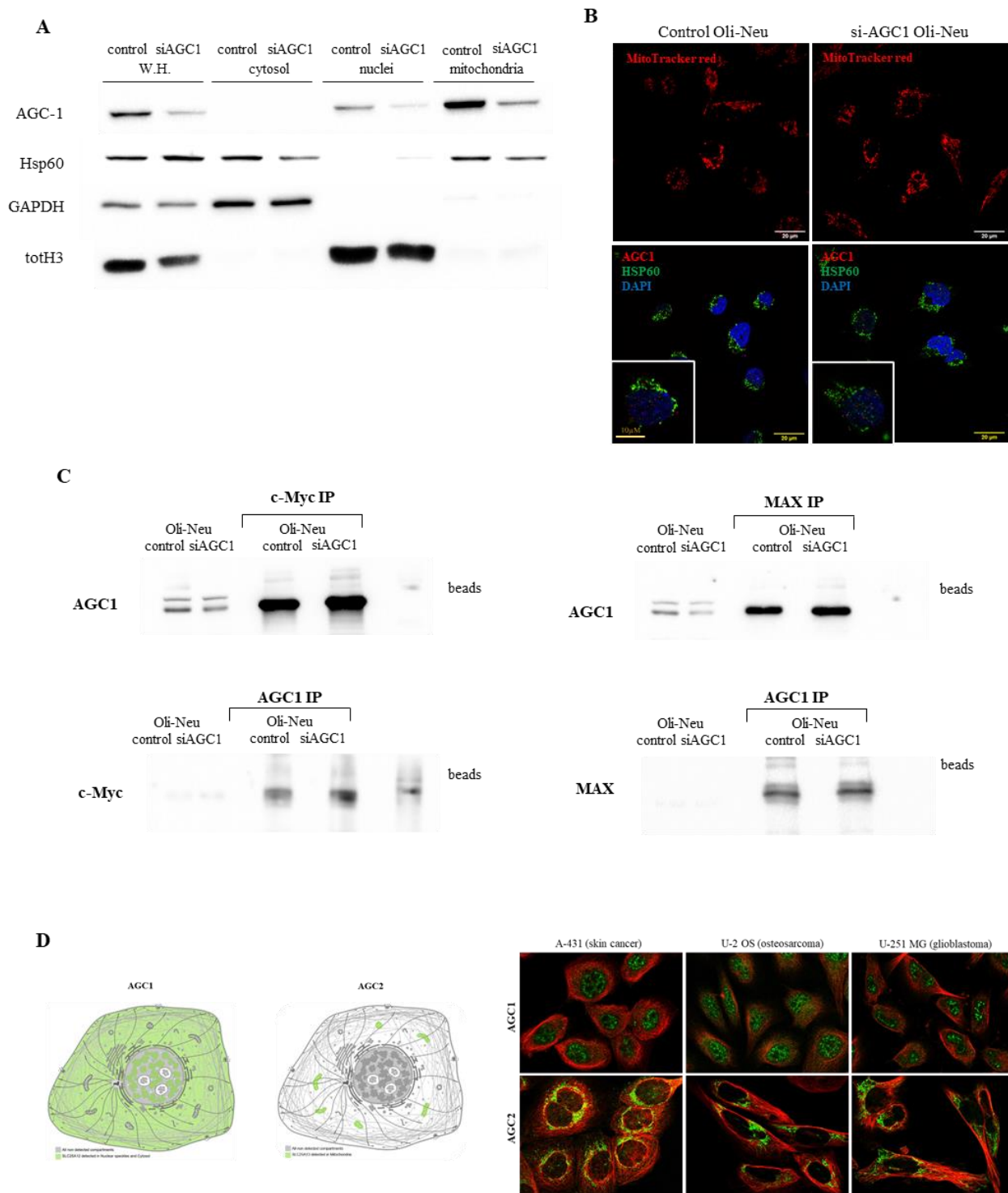
Figure 4.21. Sub-cellular localization (A), immunofluorescence analysis (B) and immunoprecipitations (C) of AGC1 in control and siAGC1 Oli-neu cells. Hsp60, GAPDH, and total histone H3 markers were used as mitochondrial, cytosolic and nuclear specific markers, respectively. Immunoprecipitation experiments were followed by reciprocal Western Blot analysis; pre-clarified and non-immunoprecipitated samples were used as positive control, agarose beads and normal IgG were loaded as negative control. (D) Predicted AGC1 localization by bioinformatics cross analyzes using publicly accessible tools (iLoc Animal, SCLpredT, Euk-mPLoc 2.0) and immunostainings on A-431 (skin cells), U-2 OS (osteosarcoma) and U-251 MG (glioblastoma) for both AGC isoforms (in collaboration with Prof. Giorgi F., Dott. Balboni N., University of Bologna, Italy) (Fig. 4.21D).

4.4.1 Chromatin immunoprecipitations' preliminary experiments

Given the unexpected interplay between AGC1 and c-Myc, further chromatin immunoprecipitation (ChIP) will be performed on control and siAGC1 Oli-Neu to verify c-Myc binding, by itself or through the multi-protein complexes, to promoters of genes involved with OPCs proliferation/differentiation. However, due to the peculiar lipid composition of OPCs cell membranes (Aggarwal *et al.*, 2011; Schmitt *et al.*, 2011), sonication tests are still ongoing in order to obtain the optimal DNA fragments of 300-500kb (Fig. 4.22). Once optimal sonication times will be established, promoters of transcription factors involved in OPCs proliferation and differentiation will be analysed to further clarify the altered regulation of biological mechanisms affecting AGC1 silenced Oli-neu cells.
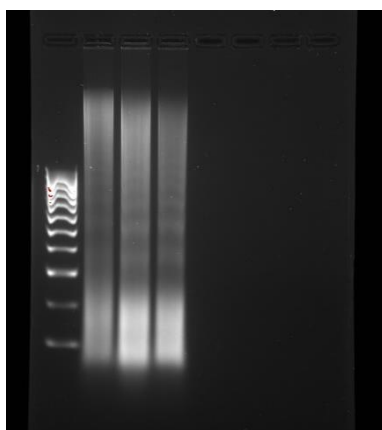
Figure 4.22 Chromatin sonication tests on control Oli-neu cells. Different times and intensities were performed; at 60high/20low combination, ideal fragments (100kb-300kb) were obtained.

4.4.2 HAT and HDACs silencing or overexpression on AGC1 partially silenced and control Oli-Neu cells

In order to better clarify the epigenetic regulation underlying OPCs proliferation and differentiation and their alteration in AGC1-deficiency OPCs model, transfections with overexpressing plasmids or shRNAs for histone de-acetylase isoform 2 and 3 (HDAC2; HDAC3) or for acetyltransferase CBP, whose expression was significantly altered following AGC1 partial silencing, have been executed on control and siAGC1 Oli-neu cells, respectively. These experiments are still ongoing, to identify plasmids able to induce comparable silencing or overexpression to the ones observed in AGC1 silenced and control Oli-neu cells. Subsequently, analysis will be performed, to further investigate effects on oligodendrocytes precursors proliferation and differentiation.

5.

DISCUSSION

AGC1 deficiency is a rare genetic and demyelinating disease caused by recessive autosomal mutations in SLC25A12 gene, which encodes for the mitochondrial Aspartate Glutamate Carrier 1 (AGC1)/Aralar. AGC1 is a member of MAS (malate-aspartate shuttle), where it carries aspartate in cytosol in exchange to glutamate into the mitochondrial matrix. N-acetyl aspartate (NAA) is then produced through acetylation of aspartate mediated by aspartate-N-acetyltransferase, and it is transported by trans-axonal transport from neurons to oligodendrocytes, where it acts as a store of acetyl groups essential for synthesis of myelin lipids and therefore myelination (Wibom *et al.,* 2009). Main features of AGC1 deficiency are cerebral atrophy, general arrest of psychomotor development and CNS hypomyelination within first years of age (Wibom *et al.,* 2009; Falk *et al.,* 2014); all symptoms are associated with significant reduction in NAA content due to impairment in AGC1 activity (Jalil *et al.,* 2005; Sakurai *et al.,* 2010). Profilo and colleagues (2017) reported decrease in proliferation and neuronal metabolic disturbances with limited NAA production in murine neuroblastoma cells (N2A cell line) following AGC1 silencing, as consequence of reduced levels of both aspartate and acetyl-CoA, substrates required for N-acetyl aspartate synthesis. However, no metabolic defects were noticed in oligodendrocytes precursors cultures derived from AGC1$^{-/-}$ KO mice, where a lack of myelination associated with reduced OPCs maturation was observed. This leaded to consider alterations in OPCs maturation, strictly related to deficit in neuronal NAA synthesis due to AGC1 downregulation. Subsequent studies conducted by our group, reported proliferation deficit and early differentiation in a stable clone of immortalized murine oligodendrocytes precursors (Oli-neu cells) transfected with a shRNA for SLC25A12 gene, which leaded to 30-40% reduction in AGC1 activity; however, no consequences on OPCs ability to differentiate into mature oligodendrocytes were detected. In addition, AGC1 partially silenced Oli-neu cells showed relevant alterations in pathways involved in OPCs proliferation and differentiation, including low levels of growth factor PDGFα (which favours OPCs proliferation) and significant increase in TGFβ1/2 expression (required for OPCs maturation). Same observations were made on brain sections of heterozygous mice for AGC1 knock-out (AGC1$^{+/-}$ C57BL6/N background) and neural stem cells derived from their subventricular zone, where a global decrease in cells proliferation and a specific reduction in oligodendrocytes progenitors pool were observed. Altogether, the results obtained suggest an improper OPCs proliferation and differentiation characterizing AGC1 deficiency, which leads to subsequent defects in myelin synthesis and hypomyelination (Petralla *et al.*, 2019).

5.1 Altered expression of brain cells' transcription factors could underlie the proliferation/differentiation dysregulation in AGC1 deficiency models

Since it is well known that temporal coordination between cell cycle exit and differentiation strictly depends on interactions between specific transcription factors, the first aim of this work was understanding the transcriptional mechanisms underlying the unbalanced OPCs proliferation and differentiation observed in both AGC1 deficiency *in vitro* models of Oli-neu cells and SVZ-derived neurospheres. Magri and colleagues (2014) reported high levels of transcription factor c-Myc in active proliferating OPCs, where it acts on promoters of genes involved in cell cycle progression and chromatin remodeling. Conversely, its down-regulation is correlated to cell cycle exit and onset of OPCs differentiation, although is not sufficient to induce progression into myelinating phenotype (Magri *et al.,* 2014). Western blot and immunofluorescence analysis on both AGC1 partially silenced Oli-neu cells and neurospheres derived from AGC1$^{+/-}$ mice, showed significant decrease in c-Myc expression compared to controls (*i.e.,* a stable clone of Oli-Neu cells following transfection with a scramble shRNA, and neurospheres derived from WT mice, respectively), according to the lower proliferation rate previously reported (Petralla *et al.,* 2019). Subsequently, to investigate regulation of OPCs specification and maturation, transcription factors Olig2, REST and serine133phosphorylated-CREB, known to be implicated in oligodendrocytes commitment and development, were also analyzed on Oli-neu cells and neurospheres. Olig2, well recognized as oligodendrocyte-specific marker, is crucial in OPCs specification during early stages of neural development (Zhou and Choi, 2001); its expression occurs throughout all maturation processes, with a peak in precursors rather than in postmitotic, mature oligodendrocytes. In AGC1 partially silenced Oli-Neu cells, a consistent reduction in Olig2 levels was detected, in line with the early differentiation into mature oligodendrocytes observed following AGC1 down-regulation. Similarly, decreased in Olig2 expression was obtained also on AGC1$^{+/-}$ neurospheres, due to the low amount of oligodendrocytes precursors present in the AGC1$^{+/-}$ mice-derived progenitors pools (Petralla *et al.,* 2019). Then, expression of the transcriptional repressor REST was investigated, which acts via chromatin remodeling to silence neuron-specific genes and promotes correct OPCs differentiation (DeWald *et al*., 2011). In siAGC1 Oli-neu cells REST levels increased, although not significantly, compared to control, in line with their premature differentiation. Conversely, a slight reduction in REST expression was detected on AGC1$^{+/-}$ neurospheres, in agreement with the switch from oligodendrocytic to neuronal and astrocytic NSCs commitment previously reported during neurospheres spontaneous differentiation (Petralla *et al.,* 2019). Lastly, expression of serine133-phosphorylated, and thus activated, transcription factor CREB was analyzed. Several experimental

evidences reported CREB to be crucial in different temporal stages of oligodendrocyte development; in maturation phases preceding myelin synthesis, PKA-mediated phosphorylated CREB promotes basic myelin protein (MBP) expression, thus inducing OPCs differentiation (Sato-Bigbee and DeVries, 1996). As expected, Western blot analysis and immunostainings on siAGC1 Oli-neu cells reported a significant increase in phosphorylated CREB expression, which justifies rise in OPCs maturation. However, opposite results were obtained on AGC1$^{+/-}$ neurospheres, where pCREB and total pCREB/CREB *ratio* (as index of CREB active in promoting OPCs maturation), turned out less expressed compared to WT, result of the low number of OPCs, and consequently mature oligodendrocytes, present in spontaneously differentiated AGC1$^{+/-}$ neurospheres. Taken together, all these data revealed an altered transcriptional regulation of cell cycle progression, as well as OPCs and NPCs specification and differentiation, which could underlie the proliferation and differentiation defects that characterize both AGC1 deficiency models of Oli-neu cells and SVZ-derived neurospheres.

5.2 An aberrant epigenetic regulation in NSCs and OPCs maturation could explain the early arrest proliferation and premature differentiation observed in AGC1 deficiency models

Nevertheless, contribution of chromatin-regulating complexes is known to be required to determine transcription factors activity and temporal regulation (Ruijtenberg *et al*., 2016). Additionally, a complex transcriptional regulatory network together with epigenetic mechanisms has been identified to regulate accessibility of transcription factors to their target sequences in the genome (Allis *et al*., 2016; Chen *et al*., 2013). Therefore, chromatin remodelling enzymes and post-translational histone modifications are crucial elements to regulate gene expression. As examples, lysine-acetylation on histones N-terminal tails stretches chromatin conformation by neutralizing positive charges, enhancing transcriptional activation; by contrast, tri-methylation on histoneH3 lysine residues leads to heterochromatin formation and transcriptional repression. During oligodendrocytes development, an elaborate interaction between several molecular factors and intrinsic/extrinsic signals (i.e., epigenetic modulators, microRNA) is needed, and OPCs go through considerable changes in transcriptional regulation during transition into myelinating oligodendrocytes. They stay in a proliferating active and undifferentiated state thanks to transcriptional repressors (*i.e.,* Hes5, Id2/4 and Sox6), which prevent late myelin gene expression, meanwhile genes involved in cell cycle progression are highly expressed (Emery B., 2010). Then, differentiation requires inhibition of these transcriptional repressors, with subsequent activation of myelin genes expression and onset of OPCs maturation. Hernandez and Casaccia (2015), proposed a model in which HATs (histone

acetyltransferases) and HDACs (histone de-acetylases) act, with different roles, in specific temporal windows during oligodendrocytes development. Initially, highly proliferative progenitors are characterized by a transcriptionally active chromatin conformation thanks to abundant deposition of acetyl groups by HATs to promoters of genes regulating proliferation, while myelin genes expression are inhibited. Therefore, genes promoting cell cycle and those encoding for differentiation repressors, which act together with histone de-acetylases to form repressive complexes, turn out highly expressed in OPCs thanks to HATs activity. At the onset of differentiation, however, the functional role of HDACs changes. They are recruited with transcription factors (*i.e.,* E2F4, YY1) into repressive complexes, targeted to promoters of genes expressing myelin genes transcriptional inhibitors, as well as modulators of cell proliferation and neuronal lineage. Lastly, transition from pre-myelinating to myelinating oligodendrocyte requires HDACs inhibition, to set up the expression of transcriptional activators (*i.e.,* MYRF and Sox10), which act by recruiting HATs on late myelin genes promoters. Therefore, given the large functional role of HATs and HDACs in oligodendrocyte lineage development, we then investigated if premature OPCs maturation and transcriptional dysregulation affecting our AGC1 deficiency models could be consequences of an altered epigenetic regulation. In this sense, the major post-translational histone modifications (*i.e.* acetylation and methylation) and HATs and HDACs expression, sub-cellular localization and activity were analyzed in both Oli-neu cells and neurospheres. Western blot on purified histones revealed a global decrease in histone H3 pan-acetylation and pan-methylation in AGC1 partially silenced Oli-neu cells. Similar studies were made on AGC1$^{+/-}$ neurospheres, in which reduced levels of histone H3 pan-acetylation coinciding with histone H3 pan-methylation enhancement were detected, suggesting an altered epigenetic profile affecting both models. As expected, also expression of acetyltransferase CBP, which regulates acetylation of cell cycle promoting genes during oligodendrocytes development (Gregath, A. and Lu; 2018), significantly decreased in both siAGC1 Oli-neu and AGC1$^{+/-}$ neurospheres compared to controls, in line with the low proliferation rate and premature differentiation observed. Additionally, since CBP activity is crucial for NSCs commitment to OPCs through its direct binding to glial genes promoters, and its knockdown prevents glial precursors specification *in vivo* (Wang *et al.*, 2010), CBP reduced expression and activity could explain the drop in OPCs content reported during AGC1$^{+/-}$ neurospheres spontaneous differentiation. Nevertheless, regarding histone de-acetylases expression, contrasting results were obtained in both models, probably due to the cell-specific expression and functional role of each single isoform. HDACs 2 and 3, which act to repress genes involved in neuronal and oligodendrocytic maturation, whose silencing is associated with increased expression of activators of late myelin genes (Ye *et al.*, 2009; Castelo-Branco *et al.*, 2014; Samudyata *et al.*, 2020), decreased in siAGC1 Oli-neu cells compared to control, while isoform 1 and 4 turned out

slightly affected. Conversely, in AGC1$^{+/-}$neurospheres HDAC 1 and 3 revealed to be significantly more expressed compared to isoform 2 and 4, which acquired the opposite pattern decreasing than in control ones. Therefore, altered expression of both HDAC isoforms, which act to repress myelin genes transcriptional activators, and CBP, whose HAT activity is required to promote cell-cycle progression (Hernandez and Casaccia, 2015), could lead to the arrest in proliferation and premature differentiation observed in AGC1 partially silenced Oli-neu cells. On the other hand, the different HAT and HDACs expression pattern observed in AGC1$^{+/-}$ mice-derived neurospheres, which is essential in determining neural precursors cells fate, could explain the altered neural precursors commitment previously published during neurospheres spontaneous differentiation (Petralla et al., 2019). For instance, HDAC isoform 1 and 2 has been reported to be crucial for OPCs specification by suppressing the canonical Wnt/β-catenin signalling pathway (Ye et al., 2009), whereas HDAC isoform 3, through its direct binding to promoter regions, represses neuronal genes in neural stem cells (Castelo-Branco et al., 2014). Subsequently, given the wide role of acetylation in regulating OPCs specification, cell-cycle progression, and maturation (Hernandez and Casaccia; 2015), as well as its alterations in both AGC1 deficiency in vitro models, to better clarify HATs and HDACs implication in the unbalance regulation of brain cells proliferation and differentiation, Oli-neu cells and neurospheres were treated with specific HAT or HDACs inhibitors (curcumin and SAHA, respectively). Several evidences reported that HDACs inhibition by Trichostatin A (TSA) and sodium butyrate, decrease cell proliferation on primary OPCs cultures (Conway et al., 2012), whereas Valproic Acid (VPA) injection in mice with induced-cuprizone demyelinating damages, prevents remyelination, as consequence of reduced OPC differentiation (Shen et al., 2008). In the present work, to act on histone deacetylase enzymes, the general specific class I and II HDACs inhibitor Suberanilohydroxamic acid (SAHA) was used (Abdel-Ghany et al., 2020). Zhou and colleagues (2011), reported reduced proliferation rate in neurospheres following SAHA treatment, suggesting an arrest in cell-cycle progression, together with suppression on glial commitment. On the other hand, to act on histone acetyltransferases, Oli-neu cells and neurospheres were treated with the natural compound curcumin, which specifically affects CBP activity, the most relevant HAT enzyme in oligodendrocyte lineage (Sunagawa et al., 2018). In vivo, curcumin administration leaded to increase in myelinating oligodendrocytes markers expression (Yavarpour-Bali et al., 2019), whereas adult curcumin-treated NSCs showed neuronal rather than glial differentiation commitment (Kang et al., 2006). Effects of CBP and HDACs inhibition on Oli-neu cells proliferation/differentiation were evaluated through immunostainings and morphology analysis, followed by Western Blot for OPCs-specific markers NG2/Olig2, OPCs proliferation marker PDGFRα, as well as the mature oligodendrocytes marker CNPase. Following both curcumin and SAHA treatment, a worsening of

AGC1 silenced Oli-neu phenotype was obtained, with reduction in proliferation and induction towards OPCs differentiation. In parallel, HDACs inhibition on AGC1$^{+/-}$ neurospheres leaded to decrease in proliferation rate, as indicated by increased spheres number concomitant to smaller average diameter. SAHA-treated control neurospheres acquired a similar phenotype to AGC1$^{+/-}$ ones, confirming HDACs implication in the altered proliferation and differentiation, characterizing AGC1 deficiency models. Differently, effects of curcumin administration resulted in reduction of both AGC1$^{+/-}$ neurospheres size and number, indicating an earlier arrest of proliferation in neural progenitors cells following HATs activity inhibition in line with the proposed role of histone acetyltransferases of activating transcription of cell-cycle genes during oligodendrocytes development (Hernandez and Casaccia, 2015). As previously reported, AGC1 knocking down results in shift of NSCs commitment, with impairment in OPCs specification in favour of neuronal and astrocytic cell fate. To better clarify HATs and HDACs functional role in alterations on neural progenitors' differentiation, effects of their pharmacological inhibition were also tested on differentiated neurospheres. While no evident variations were detected on neuronal and oligodendrocytic commitment, as indicated by Doublecortin (DCX) and mature oligodendrocytes marker CNPase, impairment in astrocytic fate acquirement was observed in SAHA-treated AGC1$^{+/-}$ neurospheres, with significant reduction in GFAP expression. By contrast, both GFAP and CNPase levels decrease in differentiated AGC1$^{+/-}$ neurospheres following curcumin administration, indicating an effect on neural progenitors' glial fate acquirement. Altogether, the alterations observed on neurospheres proliferation and differentiation following SAHA and curcumin administration, confirm the involvement of HATs and HDACs in specific temporal stages during neural stem cells specification. CBP activity could be required on early phases of NSCs development when the glial fate has yet to be acquired. Subsequently, HDACs act to regulate glial progenitors (GPs) maturation into astrocytes or oligodendrocytes.

Therefore, a proper OPCs development strictly depends on interaction of several molecular factors and intrinsic/extrinsic signals (*i.e.,* epigenetic modulators, microRNA), among which a complex homeostatic balance is required. The premature differentiation that prevents proliferation, which affects both *in vitro* AGC1 deficiency models of Oli-Neu cells and SVZ-derived neurospheres, is thus related to the alterations previously observed in the expression of transcription factors and epigenetic modulators involved in regulating these biological mechanisms. From our finding, changes in the epigenetic profile, as well as expression and activity of key enzymes, *i.e.,* histone acetyltransferase CBP and histone deacetyl transferases, could result in the transcriptional dysregulation that lead improper control on brain cells proliferation and differentiation, concerning not only OPCs transition

to myelinating oligodendrocyte, but also OPCs specification from NSCs. In AGC1 deficiency context, the energy imbalance caused by AGC1 impairment activity, could directly contribute to the lack of acetyl groups by acetyl-CoA compromised production, leading to alterations in histones acetylation pattern. In neurons, AGC1 reduced activity leads to MAS (malate-aspartate shuttle) failure, forcing cells to shift from aerobic to anaerobic metabolism, in which pyruvate is reduced to lactate, instead of entering the TCA cycle to produce acetyl-CoA (Profilo *et al.*, 2017). The same could happen in OPCs and NSCs, leading to deficiency of acetyl groups that affect the correct regulatory activity on histones. This could explain why the ketogenic diet, based on carbohydrate restriction and high-fat and protein rate, in which ketone bodies are provided as a direct source of acetyl-CoA, and, consequently, of acetyl-groups for energetic and biosynthetic processes, improves symptoms and restores myelination in AGC1 deficiency patients (Dahlin *et al.,* 2015).

6.

CONCLUSIONS

In AGC1 deficiency, the reduced activity of the mitochondrial carrier AGC1 prevents in neurons generation of N-acetyl-aspartate (NAA), substrate required for myelin synthesis, leading to CNS developmental delay and hypomyelination (Profilo *et al.,* 2017). Previous studies correlated lack of myelination affecting AGC1 deficiency to defects in OPCs proliferation and premature maturation, and thus, non-sufficient oligodendrocytes progenitors pool to sustain remyelination (Petralla *et al.,* 2019). Here, we demonstrated that altered transcriptional and epigenetic mechanisms underlie the improper regulation of brain cells proliferation and differentiation in *in vitro* AGC1 deficiency models of Oli-neu cells and neurospheres. Transcription factors known to be involved in these biological processes, *i.e.,* c-Myc, Olig2, phosphorylated-CREB and REST (Magri *et al.*, 2014; Sato and De Vries, 1996; Bruce *et al.*, 2004), showed different expression profile, in accordance with defects in cell proliferation and maturation previously reported. Additionally, histone post-translational modifications, as well as histone acetyltransferases (HATs) and histone deacetylases (HDACs) expression, whose role in controlling the timing of oligodendrocyte lineage development has been widely demonstrated (Hernandez and Casaccia 2015; Samudyata *et al.*, 2020), turned out to be altered, as expected, in both AGC1 deficiency models. HDACs/HATs involvement in brain cells proliferation and differentiation impairment has been further clarified by treatment with specific pharmacological inhibitors, which leaded to worsening of phenotype in both AGC1 partially silenced Oli-neu cells and AGC1$^{+/-}$ mice-derived neurospheres, inducing similar alterations in their respective control. Altogether, these data confirm our hypothesis that an altered transcriptional and epigenetic regulation could lead to an improper OPCs specification and proliferation, together with a different NSCs commitment, characterizing our *in vitro* AGC1 deficiency models. However, further analysis are required. In this sense, to investigate the relation between transcription factors and epigenetic modulators, co-immunoprecipitations and chromatin immunoprecipitations (ChIP) are now conducted to understand whether their interactions, and thus modification, could play a role in the onset of AGC1 deficiency.

Once clarified the interplay between the transcriptional changes and the altered epigenetic regulation of NSCs and OPCs proliferation/differentiation, our aim will be to carry out the same analyses on human iPS from AGC1 deficiency patients and iPS-derived hNSC, respectively, in order to confirm

also in the human model of AGC1 deficiency the proliferation and differentiation alterations previously observed in mouse siAGC1 Oli-neu cells and AGC1$^{+/-}$ neurospheres. Furthermore, being NAA a source of acetate for histone acetylation (Long *et al.*, 2013; Bogner-Strauss, 2017), it will be investigated a possible link between the metabolic/mitochondrial and the epigenetic/transcriptional dysfunctions, which has never been evaluated in AGC1-deficiency. In fact, the energy imbalance caused by AGC1 impairment activity could directly contribute to the lack of acetyl groups by acetyl-CoA compromised production, leading to alterations in histones acetylation pattern in both NSCs and OPCs. Together with epigenetic alterations, reduced acetyl-CoA levels may affect a high number of biological activities, including fatty acids synthesis which represent the main components of myelin sheath, thus bringing to hypomyelination. In fact, the RNA-seq analysis on OPCs confirmed this metabolic impairment, showing altered expression of transcriptional factors and enzymes involved in the fatty acids synthesis pathway, such as SREBP (Sterol Regulatory Element Binding Protein) and FASN (Fatty Acids Synthase N). In this sense, we will verify the in silico data from RNA-seq analysis, to assess the potential of this bioinformatic tool and prove the metabolic alteration also in our models. Specifically, starting from preliminary experiments on cells viability and mitochondrial activity, we will move towards morphological and biochemical analysis to identify the main compounds responsible for a potential recovery of differentiation/proliferation defects. Based on these observation, the supplementation of amino acids and vitamins directly involved in NAA synthesis for compensating the metabolic impairment and the lack of acetyl-CoA, could lead to a recover in phenotype solving the imbalance proliferation and differentiation in our *in vitro* AGC1 deficiency models. This, could explain why the ketogenic diet, in which ketone bodies are provided as a direct source of acetyl-CoA, and, consequently, of acetyl-groups for energetic and biosynthetic processes, improves symptoms and restores myelination in AGC1 deficiency patients (Dahlin *et al.*, 2015).

REFERENCES

1. Abrajano JJ, Qureshi IA, Gokhan S, Zheng D, Bergman A, Mehler MF. (2009), "REST and CoREST modulate neuronal subtype specification, maturation and maintenance", *PLoS One*, 4(12):e7936

2. Agostini M., Romeo F., Inoue S., Niklison-Chirou M.V., Elia A.J., Dinsdale D., Morone N., Knight R.A., Mak T.W., Melino G. (2016), "Metabolic reprogramming durin g neuronal differentiation", *Cell Death and Differentiation*, 23, 1502-1514

3. Allis CD, Jenuwein T. (2016), "The molecular hallmarks of epigenetic control", *Nat Rev Genet.*, 17(8):487-500

4. Amoedo ND, Punzi G, Obre E, et al., (2016), "AGC1/2, the mitochondrial aspartate-glutamate carriers", *Biochim Biophys Acta*, 1863(10):2394-2412

5. Barateiro A., Fernandes A. (2014), "Temporal oligodendrocyte lineage progression: In vitro models of proliferation, differentiation and myelination", *Biochimica et Biophysica Acta*, 1843, 1917-1929

6. Baron W., Metz B., Bansal R., Hoekstra D., De Vries H. (2000), "PDGF and FGF-2 signaling in oligodendrocyte progenitor cells: regulation of proliferation and differentiation by multiple intracellular signaling pathways", *Molecular and Cellular Neuroscience*, 15, 314-329

7. Batiz LF, Castro MA, Burgos PV, et al. (2015), "Exosomes as Novel Regulators of Adult Neurogenic Niches", *Front Cell Neuroscience*, 9:501

8. Belyaev ND, Wood IC, Bruce AW, Street M, Trinh JB, Buckley NJ. (2004), "Distinct RE-1 silencing transcription factor-containing complexes interact with different target genes", *J Biol Chem.,* 279(1):556-61

9. Bez A, Corsini E, Curti D, et al. (2003), "Neurosphere and neurosphere-forming cells: morphological and ultrastructural characterization", *Brain Res.*, 993(1-2):18-29

10. Blackwell TK, Kretzner L, Blackwood EM, Eisenman RN, Weintraub H. (1990), "Sequence-specific DNA binding by the c-Myc protein", *Science*, 250(4984):1149-51

11. Bogner-Strauss JG. N-Acetylaspartate Metabolism Outside the Brain: Lipogenesis, Histone Acetylation, and Cancer. Front Endocrinol (Lausanne). 2017 Sep 20;8:240. doi: 10.3389/fendo.2017.00240

12. Campbell K, Götz M. (2002), "Radial glia: multi-purpose cells for vertebrate brain development", *Trends Neuroscience*, 25(5):235-8

13. Castelo-Branco G., Lilja T., Wallenborg K., Falcao A.M., Marques S.C., Gracias S.C., Solum D., Paap R., Walfridsson J., Teixeira A.I., Rosenfeld M.G., Jepsen K., Hermanson O. (2014), "Neural

stem cell differentiation is dictated by distinct actions of nuclear receptor corepressors and histone deacetylases", *Stem Cell Reports*, 3, 502-515

14. Cavero S, Vozza A, del Arco A, et al. (2003), "Identification and metabolic role of the mitochondrial aspartate-glutamate transporter in Saccharomyces cerevisiae", *Molecular Microbiology*, 50(4):1257-1269

15. Chen QW, Zhu XY, Li YY, Meng ZQ. (2013), "Epigenetic regulation and cancer (review)", *Oncol Rep.*, 31(2):523-32

16. Conway G.D., O'Bara M.A., Vedia B.H., Pol S.U. (2012), "Histone deacetylase activity is required for human oligodendrocyte progenitor differentiation", *Glia*, 60, 1944-1953

17. Dahlin M., Martin D.A., Hedlund Z., Jonsson M., Von Dobeln U., Wedell A. (2015), "The ketogenic diet compensates for AGC1 deficiency and improves myelination", *Epilepsia*, 56 (11), 176-181

18. Del Arco A., Satrùstegui J. (1998), "Molecular cloning of aralar, a new member of the mitochondria carrier superfamily that binds calcium and is present in human muscle and brain", *The Journal of Biological Chemistry*, vol. 273, 36, 23327-23334

19. Del Arco A., Morcillo J., Martìnez-Morales J.R., Galiàn C., Martos V., Bovolenta P., Satrùstegui J. (2002), "Expression of the aspartate/glutamate mitochondrial carriers aralar1 and citrin during development and in adult rat tissues", *Eur. J. Biochem.*, 269, 3313-3320

20. Del Bene F, Wehman AM, Link BA, Baier H. (2008), "Regulation of neurogenesis by interkinetic nuclear migration through an apical-basal notch gradient", Cell, 134(6):1055-65

21. Dessaud E., Ribes V., Balaskas N., Yang L.L., Pierani A., Kicheva A., Novitch B.G., Briscoe J., Sasai N. (2010), "Dynamic assignment and maintenance of positional identity in the ventral neural tube by the morphogen sonic hedgehog", *PLoS Biology*, 8 (6)

22. Dewald LE, Rodriguez JP, Levine JM. (2011), "The RE1 binding protein REST regulates oligodendrocyte differentiation", *J Neuroscience*, 31(9):3470-83

23. Dugas J.C., Cuellar T.L., Scholze A., Ason B., Ibrahim A., Emery B., Zamanian J.L., Foo L.C., McManus M.T., Barres B.A. (2010), "Dicer1 and miR-219 are required for normal oligodendrocyte differentiation and myelination", *Neuron*, 65 (5), 597-611

24. Emery B. (2010), "Regulation of oligodendrocyte differentiation and myelination", *Science*, 330, 779-782

25. Erecinska M., Silver I.A. (1990), "Metabolism and role of glutamate in mammalian brain", *Progress in Neurobiology*, 35 (4), 245-296

26. Falk M.J., Li D., Gai X., McCormick E., Place E., Lasorsa F.M., Otieno F.G., Hou C., Kim C.E., Abdel-Magid N., Vazquez L., Mentch F.D., Chaivacci R., Liang J., Liu X., Jiang H., Giannuzzi

G., Marsh E.D., Yiran G., Tian L., Palmieri F., Hakonarson H. (2014), "AGC1 deficiency causes infantile epilepsy, abnormal myelination, and reduced N-acetylaspartate", *JIMD reports*, 14, 77-85

27. Fancy S.P.J., Zhao C., Franklin R.J.M. (2004), "Increased expression of Nkx2.2 and Olig2 identifies reactive oligodendrocyte progenitor cells responding to demyelination in the adult CNS", *Molecular and Cellular Neuroscience*, 27, 247-254

28. Fancy S.P.J., Baranzini S.E., Zhao C., Yuk D., Irvine K., Kaing S., Sanai N., Franklin R.J.M., Rowitch D.H. (2009), "Dysregulation of the Wnt pathway inhibits timely myelination and remyelination in the mammalian CNS", *Genes & Development*, 23, 1571-1585

29. Fiermonte G., Palmieri L., Todisco S., Agrimi G., Palmieri F., Walker J.E. (2002), "Identification of the mitochondrial glutamate transporter. Bacterial expression, reconstitution, functional characterization, and tissue distribution of two human isoforms" *The Journal of Biological Chemistry*, 277 (22), 19289-19294

30. Gil-Perotín S, Duran-Moreno M, Cebrián-Silla A, Ramírez M, García-Belda P, García-Verdugo JM. (2013), "Adult neural stem cells from the subventricular zone: a review of the neurosphere assay", Anat Rec (Hoboken), 296(9):1435-52

31. Ginhoux F., Prinz M. (2015), "Origin of microglia: current concepts and past controversies", *Cold Spring Harb Perspect Biol*, 7(8): a020537

32. Gregath A, Lu QR. (2018), "Epigenetic modifications-insight into oligodendrocyte lineage progression, regeneration, and disease", *FEBS Lett*., 592(7):1063-1078

33. Grove BD, Bruchey AK. (2001), "Intracellular distribution of gravin, a PKA and PKC binding protein, in vascular endothelial cells", *J Vasc Res.,* 38(2):163-175

34. kGuccione E, Martinato F, Finocchiaro G, Luzi L, Tizzoni L, Dall' Olio V, Zardo G, Nervi C, Bernard L, Amati B. (2006), "Myc-binding-site recognition in the human genome is determined by chromatin context", *Nat Cell Biol*., 8(7):764-70

35. Hernandez M., Casaccia P. (2015), "Interplay between transcriptional control and chromatin regulation in the oligodendrocyte lineage", *Glia*, 63 (8), 1357-1375

36. Hertz L., Peng L., Dienel G.A. (2007), "Energy metabolism in astrocytes: high rate of oxidative metabolism and spatiotemporal dependence on glycolysis/glycogenolysis", *Journal of Cerebral Blood Flow & Metabolism*, 27, 219-249

37. Hertz L. (2011), "Brain glutamine synthesis requires neuronal aspartate: a commentary", *Journal of Cerebral Blood Flow & Metabolism*, 31, 384-387

38. Hochstim C, Deneen B, Lukaszewicz A, Zhou Q, Anderson DJ. (2008), "Identification of positionally distinct astrocyte subtypes whose identities are specified by a homeodomain code", Cell, 133(3):510-522

39. Hsieh J., Nakashima K., Kuwabara T., Meija E., Gage F.H. (2004), "Histone deacetylase inhibition-mediated neuronal differentiation of multipotent adult neural progenitor cells", *Proc Natl Acad Sci U.S.A.*, 101 (47), 16659-16664

40. Huu NT, Yoshida H, Umegawachi T, Miyata S, Yamaguchi M. (2014), "Structural characterization and subcellular localization of Drosophila organic solute carrier partner 1", *BMC Biochemistry,* 15:11. doi: 10.1186/1471-2091-15-11

41. Jalil A., Begum L., Contreras L., Pardo B., Iijima M., Li M.X., Ramos M., Marmol P., Horiuchi M., Shimotsu K., Nakagawa S., Okubo A., Sameshima M., Isashiki Y., Del Arco A., Kobayashi K., Satrùstegui J., Saheki T. (2005), "Reduced N-acetylaspartate levels in mice lacking aralar, a brain- and muscle-type mitochondrial aspartate-glutamate carrier", *The Journal of Biological Chemistry*, vol. 280, 35, 31333-31339

42. Jeong W., Ro E.J., Choi K. (2018), "Interaction between Wnt/β-catenin and RAS-ERK pathways and an anti-cancer strategy via degradations of β-catenin and RAS by targeting the Wnt/β-catenin pathway", *npj Precision Oncology*, 2 (1), 5

43. Kessaris N., Fogarty M., Iannarelli P., Grist M., Wegner M., Richardson W.D. (2006), "Competing waves of oligodendrocytes in the forebrain and postnatal elimination of an embryonic lineage", *Nature Neuroscience*, 9 (2), 173-179

44. Kouzarides T. (2007), "Chromatin modifications and their function", *Cell*, 128 (4), 693-705

45. Kriegstein A., Alvarez-Buylla A. (2009), "The glial nature of embryonic and adult neural stem cells", *Annual Review Neuroscience*, 32, 149-184

46. Levine J.M., Reynolds R., Fawcett J.W. (2001), "The oligodendrocyte precursor cell in health and disease", *Trends in Neurosciences*, 24 (1), 39-47

47. Lim D.A., Alvarez-Buylla A. (2016), "The adult ventricular –subventricular zone (V-SVZ) and olfactory bulb (OB) neurogenesis", *Cold Spring Harb Perspect Biol*, 8:a018820

48. Liu A., Li J., Marin-Husstege M., Kageyama R., Fan Y., Gelinas C., Casaccia-Bonnefil P. (2006), "A molecular insight of Hes5-dependent inhibition of myelin gene expression: old partners and new players", *The EMBO Journal*, 25, 4833-4842

49. Liu J., Casaccia P. (2010), "Epigenetic regulation of oligodendrocyte identity", *Trends Neuroscience*, 33 (4), 193-201

50. Liu J., Sandoval J., Doh S.T., Cai L., Lòpez-Rodas G., Casaccia P. (2010), "Epigenetic modifiers are necessary but not sufficient for reprogramming non-myelinating cells into myelin gene-expressing cells", *PLoS One*, 5 (9)

51. Liu J., Magri L., Zhang F., Marsh N.O., Albrecht S., Huynh J.L., Kaur J., Kuhlmann T., Zhang W., Slesinger P.A., Casaccia P. (2015), "Chromatin landscape defined by repressive histone methylation during oligodendrocyte differentiation", *The Journal of neuroscience*, 35 (1), 352-65

52. Long PM, Moffett JR, Namboodiri AMA, Viapiano MS, Lawler SE, Jaworski DM. N-acetylaspartate (NAA) and N-acetylaspartylglutamate (NAAG) promote growth and inhibit differentiation of glioma stem-like cells. J Biol Chem. 2013 Sep 6;288(36):26188-26200. doi: 10.1074/jbc.M113.487553.

53. Lonze B.E., Ginty D.D. (2002), "Function and regulation of CREB family transcription factors in the nervous system", *Neuron*, 35, 605-623

54. Lowry OH, Rosebrough NJ, Farr AL, Randall RJ. (1951), "Protein measurement with the Folin phenol reagent", *J Biol Chem.*, 193(1):265-275

55. Magri L., Gacias M., Wu M., Swiss W.A., Janssen W.J., Casaccia P. (2014), "c-Myc-dependent transcriptional regulation of cell cycle and nucleosomal histones during oligodendrocyte differentiation", *Neuroscience*, 276, 72-86

56. Martinato F, Cesaroni M, Amati B, Guccione E. (2008), "Analysis of Myc-induced histone modifications on target chromatin", *PLoS One*, 3(11):e3650

57. McKenna M.C., Waagepetersen H.S., Schousboe A., Sonnewald U. (2006), "Neuronal and astrocytic shuttle mechanisms for cytosolic-mitochondrial transfer of reducing equivalents: Current evidence and pharmacological tools", *Biochemical Pharmacology*, 2006, 399-407

58. McMorris F.A. (1983), "Cyclic AMP induction of the myelin enzyme 2',3'-cyclic nucleotide 3'-phosphohydrolase in rat oligodendrocytes", *Journal of Neurochemistry*, 41, 506-515

59. Menn B., Garcia-Verdugo J.M., Yaschine C., Gonzalez-Perez O., Rowitch D., Alvarez-Buylla A. (2006), "Origin of oligodendrocytes in the subventricular zone of the adult brain", *The Journal of Neuroscience*, 26 (30), 7907-7918

60. Mergenthaler P., Lindauer U., Dienel G.A., Meisel A. (2013), "Sugar for the brain: the role of glucose in physiological and pathological brain function", *Trends Neuroscience*, 36 (10), 587-597

61. Merkle F.T., Alvarez-Buylla A. (2006), "Neural stem cells in mammalian development", *Current Opinion in Cell Biology*, 18, 704-709

62. Nait-Oumesmar B., Decker L., Lachapelle F., Avellana-Adalid V., Bachelin C., Van Evercooren A.B. (1999), "Progenitor cells of the adult mouse subventricular zone proliferate, migrate and

differentiate into oligodendrocytes after demyelination", *European Journal of Neuroscience*, 11, 4357-4366

63. Noctor SC, Martinez-Cerdeno V, Ivic L, Kriegstein AR, (2004), "Cortical neurons arise in symmetric and asymmetric division zones and migrate through specific phases", Nat Neurosci., 7(2):136-144

64. Northcott, P., Buchhalter, I., Morrissy, A. et al. (2017), "The whole-genome landscape of medulloblastoma subtypes", *Nature 547*, 311–317

65. Nowakowski TJ, Pollen AA, Sandoval-Espinosa C, Kriegstein AR. (2016), "Transformation of the Radial Glia Scaffold Demarcates Two Stages of Human Cerebral Cortex Development", *Neuron*, 91(6):1219-1227

66. Palazuelos J., Klingener M., Aguirre A. (2014), "TGFβ signaling regulates the timing of CNS myelination by modulating oligodendrocyte progenitor cell cycle exit through SMAD3/4/FoxO1/Sp1" *The Journal of Neuroscience*, 34 (23), 7917-7930

67. Palmieri F. (2013), "The mitochondrial transporter family SLC25: Identification, properties and physiopathology", *Molecular Aspects of Medicine*, 34, 465-484

68. Palmieri L., Pardo B., Lasorsa F.M., Del Arco A., Kobayashi K., Iijima M., Runswick M.J., Walker J.E., Saheki T., Satrùstegui J., Palmieri F. (2001), "Citrin and aralar1 are Ca^{2+}-stimulated aspartate/glutamate transporters in mitochondria", *The EMBO journal*, 20, 5060-5069

69. Pebay-Peyroula E., Brandolin G. (2004), "Nucleotide exchange in mitochondria: insight at a molecular level", *Current Opinion in Structural Biology*, 14, 420-425

70. Pelengaris S, Khan M, Evan G. (2002), "c-MYC: more than just a matter of life and death", *Nat Rev Cancer*, 2(10):764-76

71. Petralla S, Peña-Altamira LE, Poeta E, Massenzio F, Virgili M, Barile SN, Sbano L, Profilo E, Corricelli M, Danese A, Giorgi C, Ostan R, Capri M, Pinton P, Palmieri F, Lasorsa FM, Monti B. (2019), "Deficiency of Mitochondrial Aspartate-Glutamate Carrier 1 Leads to Oligodendrocyte Precursor Cell Proliferation Defects Both In Vitro and In Vivo", *Int J Mol Sci.,* 20(18):4486

72. Pfeiffer B., Sen K., Kaur S., Pappas K. (2019), "Expanding phenotypic spectrum of cerebral aspartate–glutamate carrier isoform 1 (AGC1) deficiency", *Neuropediatrics*, DOI: 10.1055/s-0039-3400976

73. Picard-Riera N., Decker L., Delarasse C., Goude K., Nait-Oumesmar B., Liblau R., Pham-Dinh D., Evercooren A.B. (2002), "Experimental autoimmune encephalomyelitis mobilizes neural progenitors from the subventricular zone to undergo oligodendrogenesis in adult mice", *Proc Natl Acad Sci*, 99, 13211-13216

74. Profilo E., Peña-Altamira L.E., Corricelli M., Castegna A., Danese A., Agrimi G., Petralla S., Giannuzzi G., Porcelli V., Sbano G., Viscomi C., Massenzio F., Palmieri E.M., Giorgi C., Fiermonte G., Virgili M., Palmieri L., Zeviani M., Pinton P., Monti B., Palmieri F., Lasorsa F.M. (2017), "Down-regulation of the mitochondrial aspartate-glutamate carrier isoform 1 AGC1 inhibits proliferation and N-acetylaspartate synthesis in Neuro2A cells", *Biochimica et Biophysica Acta*, 1863, 1422-1435

75. Ramos M., Del Arco A., Pardo B., Martìnez-Serrano A., Martìnez-Morales J.R., Kobayashi K., Yasuda T., Bogònez E., Bovolenta P., Saheki T., Satrùstegui J. (2003), "Developmental changes in the Ca -regulated mitochondrial aspartate–glutamate carrier aralar1 in brain and prominent expression in the spinal cord", *Developmental brain research*, 143, 33-46

76. Sakurai T., Ramoz N., Barreto M., Gazdoiu M., Takahashi N., Gertner M., Dorr N., Gama Sosa M.A., De Gasperi R., Perez G., Schmeidler J., Mitropoulou V., Le H.C., Lupu M., Hof P.R., Elder G.A., Buxbaum J.D. (2010), "Slc25a12 disruption alters myelination and neurofilaments: A model for a hypomyelination syndrome and childhood neurodevelopmental disorders", *Biol Psichiatry*, 67 (9), 887-894

77. Samudyata, Castelo-Branco G, Liu J. (2020), "Epigenetic regulation of oligodendrocyte differentiation: From development to demyelinating disorders", *Glia*, 68(8):1619-1630

78. Sanz R, del Arco A, Ayuso C, Ramos C, Satrustegui J., (2000), "Assignment of the calcium-binding mitochondrial carrier Aralar1 gene (SLC25A12) to human chromosome band 2q31 by in situ hybridization", Cytogenet Cell Genet., 89(3-4):143-144

79. Sato-Bigbee C, Yu RK. (1993), "Presence of cyclic AMP response element-binding protein in oligodendrocytes", *J Neurochem.,* 60(6):2106-10

80. Sato-Bigbee, C., Chan, E.L.P. and Yu, R.K. (1994), "Oligodendroglial cyclic AMP response element-binding protein: A member of the CREB family of transcription factors", *J. Neurosci. Res.*, 38: 621-628

81. Sato-Bigbee C., DeVries G.H. (1996), "Treatment of oligodendrocytes with antisense deoxyoligonucleotide directed against CREB mRNA: effect on the cyclic AMP-dependent induction of myelin basic protein expression", *Journal of Neuroscience*, 46, 98-107

82. Satrustegui J, Pardo B, Del Arco A. (2007), "Mitochondrial transporters as novel targets for intracellular calcium signaling", Physiol Rev., 87(1):29-67

83. Scardigli R, Bäumer N, Gruss P, Guillemot F, Le Roux I. (2003), "Direct and concentration-dependent regulation of the proneural gene Neurogenin2 by Pax6", *Development*, 130(14):3269-81

84. Shechter D, Dormann HL, Allis CD, Hake SB. (2007), "Extraction, purification and analysis of histones", *Nat Prot.*, 2(6):1445-57

85. Shen S., Sandoval J., Swiss V.A., Li J., Dupree J., Franklin R.J.M., Casaccia-Bonnefil P. (2008), "Age-dependent epigenetic control of differentiation inhibitors is critical for remyelination efficiency", *Nature Neuroscience*, 11 (9), 1024-1034

86. Sher F., Rössler R., Brouwer N., Balasubramaniyan V., Boddeke E., Copray S. (2008), "Differentiation of neural stem cells into oligodendrocytes: involvement of the polycomb group protein Ezh2", *Stem Cells*, 26 (11), 2875-83

87. Siddiq M.M., Hannila S.S. (2015), "Looking downstream: the role of cyclic AMP-regulated genes in axonal regeneration", *Frontiers in Molecular Neuroscience*, 8 (26)

88. Siegel P.M., Massagué J. (2003), "Cytostatic and apoptotic actions of TGF-beta in homeostasis and cancer", *Nature Reviews Cancer*, 3 (11), 807-821

89. Siegenthaler JA, Ashique AM, Zarbalis K, Patterson KP, Hecht JH, Kane MA, Folias AE, Choe Y, May SR, Kume T, Napoli JL, Peterson AS, Pleasure SJ. (2009), "Retinoic acid from the meninges regulates cortical neuron generation", Cell, 139(3):597-609. Erratum in: Cell. 2011 Aug 5;146(3):486

90. Sinasac DS, Crackower MA, Lee JR, et al., (1999), "Genomic structure of the adult-onset type II citrullinemia gene, SLC25A13, and cloning and expression of its mouse homologue" Genomics, 62(2):289-292

91. Sunagawa Y, Funamoto M, Sono S, Shimizu K, Shimizu S, Genpei M, Miyazaki Y, Katanasaka Y, Morimoto E, Ueno M, Komiyama M, Kakeya H, Wada H, Hasegawa K, Morimoto T. (2018), "Curcumin and its demethoxy derivatives possess p300 HAT inhibitory activity and suppress hypertrophic responses in cardiomyocytes", *J Pharmacol Sci.*, 136(4):212-217

92. Timsit S., Martinez S., Allinquant B., Peyron F., Puelles L., Zalc B. (1995), "Oligodendrocytes originate in a restricted zone of the embryonic ventral neural tube defined by DM-20 mRNA expression", *The Journal of Neuroscience*, 15 (2), 1012-024

93. Tropepe V, Sibilia M, Ciruna BG, Rossant J, Wagner EF, van der Kooy D. (1999) "Distinct neural stem cells proliferate in response to EGF and FGF in the developing mouse telencephalon", *Developmental Biology*, 208(1):166-188

94. Urenjak J., Williams S.R., Gadian D.G., Noble M. (1993), "Proton nuclear magnetic resonance spectroscopy unambiguously identifies different neural cell types", *The Journal of Neuroscience*, vol. 13, 3, 981-989

95. Ye W., Chen Y., Hoang T., Montgomery R.L., Zhao X., Bu H., Hu T., Taketo M.M., Van Es J.H., Clevers H., Hsieh J., Duby-Bassel R., Olson E.N., Lu Q.R. (2009), "HDAC1 and HDAC2 regulate

oligodendrocyte differentiation by disrupting β-catenin-TCF interaction", *Nature Neuroscience*, 12 (7), 829-838

96. Walker TL, Kempermann G. (2014), "One mouse, two cultures: isolation and culture of adult neural stem cells from the two neurogenic zones of individual mice", *J Vis Exp.*, (84):e51225. Erratum in: J Vis Exp. 2014;(93)

97. Wang J, Weaver IC, Gauthier-Fisher A, Wang H, He L, Yeomans J, Wondisford F, Kaplan DR, Miller FD. (2010), "CBP histone acetyltransferase activity regulates embryonic neural differentiation in the normal and Rubinstein-Taybi syndrome brain", *Dev Cell.*, 18(1):114-25

98. Wegner M. (2007), "A matter of identity: transcriptional control in oligodendrocytes", *Journal of Molecular Neuroscience*, 35, 3-12

99. Weiss S., Dunne C., Hewson J., Wohl C., Wheatley M., Peterson A.C., Reynolds B.A. (1996), "Multipotent CNS stem cells are present in the adult mammalian spinal cord and ventricular neuroaxis", *The Journal of Neuroscience*, 16 (23), 7599-7609

100. Wiame E, Tyteca D, Pierrot N. et al., (2009), "Molecular identification of aspartate N-acetyltransferase and its mutation in hypoacetylaspartia" Biochem J., 425(1):127-136.

101. Wibom R., Lasorsa F.M., Töhönen V., Barbaro M., Sterky F.H., Kucinski T., Naess K., Jonsson M., Pierri C.L., Palmieri F., Wedell A. (2009), "AGC1 deficiency associated with global cerebral hypomyelination", *The New England Journal of Medicine*, 361, 489-495

102. Zhou Q, Choi G, Anderson DJ. (2001), "The bHLH transcription factor Olig2 promotes oligodendrocyte differentiation in collaboration with Nkx2.2", *Neuron*, 31(5):791807

103. Zhou Q, Dalgard CL, Wynder C, Doughty ML. (2011), "Histone deacetylase inhibitors SAHA and sodium butyrate block G1-to-S cell cycle progression in neurosphere formation by adult subventricular cells", *BMC Neurosci.*, 12:50

Acknowledgements